



University of Bergen

Research Proposal

**Master of Global Health Submitted to
Center for International Health (CIH)**

Tsering Yangzom

Title: Stem Cell-based Study on Defining Toxic Astrocytes in Neurodegeneration

Main Supervisor:

Kristina Xiao Liang, DDS, PhD
Senior Researcher,
Department of Clinical Medicine (K1)
University of Bergen.
Neuro-SysMed, Department of Neurology,
Haukeland University Hospital, Bergen.

Co-supervisor:

Laurence Albert Bindoff, MD, PhD
Emeritus Professor,
Department of Clinical Medicine (K1)
University of Bergen.
Neuro-SysMed, Department of Neurology,
Haukeland University Hospital, Bergen.

Co-supervisor:

Sonia Gavasso, PhD
Senior Researcher,
Department of Clinical Medicine (K1)
University of Bergen.
Neuro-SysMed, Department of Neurology, Haukeland
University Hospital, Bergen.

TABLE OF CONTENT

SCIENTIFIC ENVIRONMENT	4
ACKNOWLEDGEMENT	5
LIST OF ABBREVIATIONS	6
SUMMARY	9
CHAPTER 1: INTRODUCTION	11
1.1 Neurodegenerative Diseases (NDs) and their Epidemiology	11
1.1.1 NDs.....	11
1.1.2 Epidemiology of NDs.....	12
1.2. Mitochondria.....	15
1.2.2 Mitochondrial DNA (mtDNA).....	16
1.2.3 Mitochondrial Dysfunction and NDs	18
1.3 Mitochondrial DNA Polymerase Gamma (POLG) and POLG-related Diseases	19
1.3.4 POLG-Related Disorders.....	26
1.4 Stem Cell Models for NDs	27
1.4.1 Disease Model of NDs	27
1.4.2 Human Pluripotent Stem Cells (hPSCs).....	28
1.4.3 Induced Pluripotent Stem Cells (iPSCs).....	29
1.4.4 Astrocyte Differentiation from iPSCs	30
1.4.5 Brain Organoids	31
1.5 Astrocytes in NDs	33
1.5.1 Astrocytes and Their Normal Function	33
1.5.2 Progression of resting (A0) astrocytes to reactive (A1 and A2) astrocytes	34
1.5.3 Reactive astrocytes in NDs.....	36
1.5.3 Reactive Astrocytes in POLG-Related Disorders	38
CHAPTER 2: RATIONAL AND AIMS	41
2.1 Rational.....	41
2.2 Aim.....	41
CHAPTER 3: MATERIALS AND METHOD.....	42
3.1 Equipment and Consumables	42
3.2 Chemical Reagent	44
3.3 iPSC Cell Culture and Differentiation	46
3.3.5 Astrocyte Differentiation	47
3.3.8 Differentiation of DA Neurons from iPSCs.....	49
3.3.9 Cortical Organoid Generation.....	51
3.4 Nicotinamide Riboside (NR) Treatment.....	51
3.5 Immunofluorescence	51
3.6 Flow cytometry.....	53
3.7 Indirect Astrocyte Neuron Co-Culture System.....	55
3.8 Human Cytokines Array	56
3.9 Statistical analysis	56
CHAPTER 4: RESULT	57

4.1 POLG Patient Astrocytes Exhibited Lower Levels of A2 markers compared to Controls.....	57
4.2 Patient Astrocytes Showed a Loss of Complex 1, Complex IV and TFAM Compared to Controls.	59
4.3 Differentiation and Characterization of Cortical Organoid from Patient and Control iPSCs. ...	60
4.4 Patient Cortical Organoids Showed Higher Expression of the A1 Marker and Lower Level of A2 Maker than Control Organoids.	61
4.5 POLG Astrocytes Secreted High Levels of Pro-inflammatory Cytokines and Chemokines.	63
4.6 DA Neurons Displayed Morphological and Mitochondrial Damage When Cultured with POLG Astrocyte.	65
CHAPTER 5: DISCUSSION	68
CHAPTER 6: CONCLUSIONS AND FUTURE PERSPECTIVES	74
CHAPTER 7: REFERENCES	77
CHAPTER 8: APPENDICES	83

SCIENTIFIC ENVIRONMENT

The work presented in this thesis was carried out at Neuro-SysMed, Department of Clinical Medicine (K1), Faculty of Medicine, University of Bergen and Department of Neurology, Haukeland University Hospital, Berge, Norway. The study was performed under the supervision of Principal Investigator/ Senior Researcher Kristina Xiao Liang as the main supervisor, Emeritus Professor Laurence A Bindoff and Senior Researcher Sonia Gavasso as co-supervisors at Department of Clinical Medicine (K1), Faculty of Medicine, University of Bergen and Department of Neurology, Haukeland University Hospital, Bergen, Norway.

ACKNOWLEDGEMENT

I would like to extend my heartfelt gratitude and appreciation to my main supervisor, Kristina Xiao Liang, for her invaluable guidance, support, and expertise throughout the completion of my master's thesis. Your profound knowledge, critical insights, and continuous encouragement have been a source of inspiration for me. Your guidance and constructive feedback have refined my thesis and enhanced my overall research skills. I am truly grateful for your countless hours in guiding me through this thesis, sharing your knowledge, and challenging me to think critically.

I would also like to express my gratitude to my co-supervisors, Laurence Bindoff and Sonia Gavasso for their valuable contributions to my thesis. Their expertise and perspective have provided me with a well-rounded understanding of my research topic. I appreciate their input and guidance, which have enriched the quality of my work.

I am also immensely grateful to Cecilie Kristiansen for her extensive knowledge and impactful feedback that improved the quality of my work. Her constructive feedback and thoughtful suggestions helped me refine my ideas and improve the overall structure of my thesis.

I extend sincere gratitude to Linda Karin Forshaw and Sven Gudmund Hinderaker from Central for International Health, UiB and Kamal Babikeir Elnour Mustafa from the Department of Clinical Dentistry, UiB for their invaluable support and guidance throughout the completion of my thesis.

I am also grateful to my colleagues Sharika Maharjan, Bjørn Christian Lundberg, and others for creating a supportive research environment that made this journey fulfilling.

Lastly, I would like to thank my family and friends for their unwavering support and encouragement throughout this journey. Their belief in me has been a constant motivation to overcome challenges and achieve my goals.

Thank You!

LIST OF ABBREVIATIONS

AD	Alzheimer's disease
adPEO	Autosomal dominant Progressive External Ophthalmoplegia
ALS	Amyotrophic lateral sclerosis
arPEO	Autosomal recessive Progressive External Ophthalmoplegia
ATP	Adenosine triphosphate
BBB	Blood brain barrier
BDNF	Brain-derived neurotrophic factor
C1	Complement system 1
CCL2	Chemokines like β -chemokine 2
CCL20	β -chemokine 20
CDM	Chemically differentiated medium
CNS	Central nervous system
CXCL10	α -chemokine 12
DA	Dopaminergic neuron
DALYs	Disability adjusted life-years
DNA	Deoxy ribonucleic acid
DPBS	Dulbecco's phosphate-buffered saline
EB	Embryonic body
ESC	Embryonic stem cells
ETC	Electron transport chain
ETC	Electron transport chain
GDNF	Glial-derived neurotrophic factor
GFAP	Glial fibrillary acidic proteins
HD	Huntington's disease
hPSCs	Human pluripotent stem cells
IL-6	Interleukin-1

IL-8	Interleukin-8
ipSCs	Induced pluripotent stem cells
LMIC	Low-income and middle-income countries
MAP2	Microtubules associated protein 2
MCHS	Childhood Myocerebrohepatopathy Spectrum
MFI	Median fluorescence intensity
MMP	Mitochondrial membrane potential
MNGIE	mitochondrial neuro gastrointestinal encephalomyopathy
MS	Multiple sclerosis
mtDNA	Mitochondrial DNA
NDs	Neurodegenerative diseases
NR	Nicotinamide riboside
NSCs	Neuronal stem cells
OXPPOS	Oxidative phosphorylation
PD	Parkinson disease
POLG	DNA Polymerase gamma
POLG2	DNA polymerase gamma 2, accessory subunit
PSCs	Pluripotent stem cells
ROS	Reactive oxygen species
rRNA	Ribosomal ribonucleic acid
RT	Room temperature
S100A10	S100 calcium binding protien A10
SANDO	sensory ataxic neuropathy with dysarthria and ophthalmoplegia
SCG2	Secretogranin 2
SERPING1	Serine protease inhibitor 1
SSBP	Single strand binding proteins
TFAM	Mitochondrial transcription factor A

TH	Tyrosine hydroxylase
TNF- α	Tumor necrosis factor- α
tRNA	Transfer ribonucleic acid
VDAC	Voltage dependent anionic channel
VEGF	Vascular endothelial growth factor
WHO	World health organization

SUMMARY

Defects in the *POLG* gene, which encodes polymerase gamma, are implicated in severe mitochondrial dysfunction and neurodegeneration. As a critical enzyme in the replication and repair of mitochondrial DNA, aberrations in *POLG* present a complex clinical challenge with currently no existing therapies. The unpredictable onset of *POLG*-related disease symptoms can span a wide age range, from infancy to old age, affecting multiple tissues. Upon manifestation, these symptoms trigger significantly elevated rates of morbidity and mortality. Our research focused on establishing a *POLG* disease model using induced pluripotent stem cells (iPSCs), exploring the role of reactive astrocytes within the disease mechanism.

We embarked on a mission to identify markers for *POLG*-reactive astrocytes, revealing a potential indicator in the overexpression of GFAP and C3 alongside the downregulation of S100A10. Our co-culture experiments confirmed that astrocytes derived from patients posed a toxic threat to neurons. Interestingly, we observed a higher secretion of pro-inflammatory cytokines and chemokines by *POLG* astrocytes, indicating that neuroinflammation may contribute to neuronal dysfunction. A notable breakthrough came when we discovered that treating patient samples with the NAD⁺ precursor NR led to a reduction in both astrocyte reactivity and toxic cytokine secretion, hinting at a promising therapeutic strategy. The incorporation of 3D brain organoids offered an authentic simulation of in vivo conditions and thus, an invaluable tool for studying disease mechanisms.

Despite our encouraging findings, further validation and expansion with larger sample sizes is essential. Collectively, our research illuminates the detrimental role of reactive astrocytes in *POLG* disease, emphasizing their crucial role in associated neurodegenerative conditions. This highlights the necessity to target these cells in future therapeutic strategies aimed at mitigating the devastating effects of *POLG*-related diseases.

These findings and methodologies may prove beneficial beyond the scope of *POLG*-related diseases. For instance, they could be applicable to other neurodegenerative diseases such as Parkinson's, characterized by the death of dopamine-producing neurons, often linked to mitochondrial dysfunction and neuroinflammation. Potential markers for reactive astrocytes could assist researchers in understanding their role within Parkinson's, possibly leading to strategies for controlling their reactivity. Additionally, the strategy of curbing astrocyte reactivity and toxic cytokine secretion with the NAD⁺ precursor NR might also hold therapeutic potential in Parkinson's. Moreover, the use of iPSCs and 3D brain organoids could provide invaluable models to study Parkinson's disease

mechanisms and evaluate potential therapies. While additional research is necessary to tailor these insights to the unique context of Parkinson's, the potential for cross-application is undeniable.

CHAPTER 1: INTRODUCTION

1.1 Neurodegenerative Diseases (NDs) and their Epidemiology

1.1.1 NDs

The term "neurodegenerative" refers to diseases resulting in or characterized by degeneration of the nervous system, especially the neurons in the brain. The common symptoms of NDs include loss of motor control, emotional abnormalities, and cognitive deficiencies. The disorders are characterized by neuronal degeneration. Neurons are non-replicating nerve cells in the brain and spinal cord. Damaged neurons are unable to repair themselves, resulting in brain malfunction and irreversible illnesses. These diseases can be genetic or sporadic and can affect people of all ages, although the risk of developing NDs increases with age. The most common types of NDs include Alzheimer's disease (AD) as the most common type of ND and is characterized by the progressive loss of memory and cognitive function; Parkinson's disease (PD) characterized by the progressive loss of motor function, including tremors, rigidity, and bradykinesia and caused by the death of dopamine-producing neurons in the brain; Huntington's disease (HD) as a genetic ND that causes the progressive loss of cognitive and motor function and caused by a mutation in the huntingtin gene; Amyotrophic lateral sclerosis (ALS) as is a progressive ND that affects the neurons responsible for controlling voluntary muscle movement and Multiple sclerosis (MS) as a chronic autoimmune ND that affects the central nervous system and caused by the destruction of myelin, which is the protective covering around nerve fibers.

NDs are strongly associated with ageing, as the risk of developing these disorders increases significantly with age. Many NDs are considered age-related disorders, as they become more prevalent as people get older. The ageing process itself is thought to play a key role in the development of NDs. As the body ages, it undergoes various changes, including increased oxidative stress, inflammation, and cellular and mitochondrial damage (1). These changes can lead to the accumulation of protein aggregates and other toxic substances in the brain, which can contribute to the development of NDs (2). Furthermore, genetic and environmental factors that increase the risk of NDs can also accumulate over time, increasing the likelihood of developing these disorders as people age. Some NDs, such as AD and PD, are particularly strongly associated with the ageing (2). For example, the prevalence of AD doubles every 5 years after the age of 65, and by the age of 85, nearly 50% of people have AD. While the link between NDs and ageing is clear, researchers are still working to understand the underlying mechanisms and to develop new therapies that can delay or prevent the onset of these devastating disorders.

During the last decade, researchers have identified several key pathways and processes that contribute to the degeneration and death of neurons in the brain and nervous system (1). For example, many NDs are characterized by the abnormal folding and aggregation of specific proteins in the brain, such as amyloid-beta in AD and alpha-synuclein in PD (3). These protein aggregates can disrupt cellular function and lead to inflammation and cell death (3). Chronic inflammation is another hallmark of NDs and can contribute to the progression of neurodegeneration (4). Inflammation can be triggered by the presence of protein aggregates or by other factors and can lead to further damage to neurons and surrounding tissues. Furthermore, oxidative stress and mitochondrial dysfunction contribute to the NDs (5). NDs can also lead to increased levels of oxidative stress, which occurs when the body produces more free radicals than it can neutralize (6). This can damage cells and tissues, including the mitochondria, which are the energy-producing organelles within cells (4). Mitochondrial dysfunction can further exacerbate oxidative stress and lead to cellular death (7). However, the disease mechanisms of NDs and neural death are still yet fully understood. Currently, there is no cure for ND, and treatment options are limited to controlling symptoms and slowing disease progression, partly due to the complexity of the disease and lack of good disease models.

1.1.2 Epidemiology of NDs

The prevalence of neurodegenerative diseases increases with age, and most cases are diagnosed in people over the age of 65. AD is the most common neurodegenerative disease, affecting an estimated 50 million people worldwide. Parkinson's disease affects approximately 1% of the population over the age of 60, and Huntington's disease is much rarer, affecting about 1 in 10,000 people worldwide.

The epidemiology of NDs in Norway is similar to other developed countries. The prevalence of NDs in Norway is estimated to be around 2-3% of the population over the age of 65. AD is the most common neurodegenerative disease, accounting for approximately 60-70% of cases. PD is the second most common, followed by other less common NDs such as multiple system atrophy and frontotemporal dementia. Although the incidence of NDs in Norway is difficult to estimate accurately, it is believed to be increasing due to the ageing population. A study published in 2018 found that the incidence of PD in Norway had increased by 27% over a period of 15 years (8). NDs are a leading cause of death in Norway, accounting for approximately 10% of all deaths. AD is the fourth leading cause of death in Norway, after cardiovascular disease, cancer, and respiratory disease. Overall, the epidemiology of ND in Norway underscores the need for continued research and investment in prevention, diagnosis, and treatment.

NDs have a significant impact on individuals, families, and society as a whole. These diseases are a major cause of disability and can place a significant burden on caregivers. They also have economic implications, as the cost of care for people with NDs can be high. In developed countries, the life expectancy of patients with NDs is now significantly over 80 years (9). On the other hand, a longer life expectancy increases the risk of developing ageing related NDs, such as AD, PD, or dementia. As these diseases worsen, they become increasingly debilitating until full-time care is required. Currently, around €130 billion is spent annually in Europe to care for people who have dementia due to NDs. As the elderly population grows, the number of people affected, and the cost will increase dramatically. In addition, developing new treatments and therapies for NDs is expensive and time-consuming. This can lead to a lack of investment in research and development, which in turn can limit the availability of effective treatments. Overall, the societal burden of NDs highlights the need for increased awareness and investment in research and development.

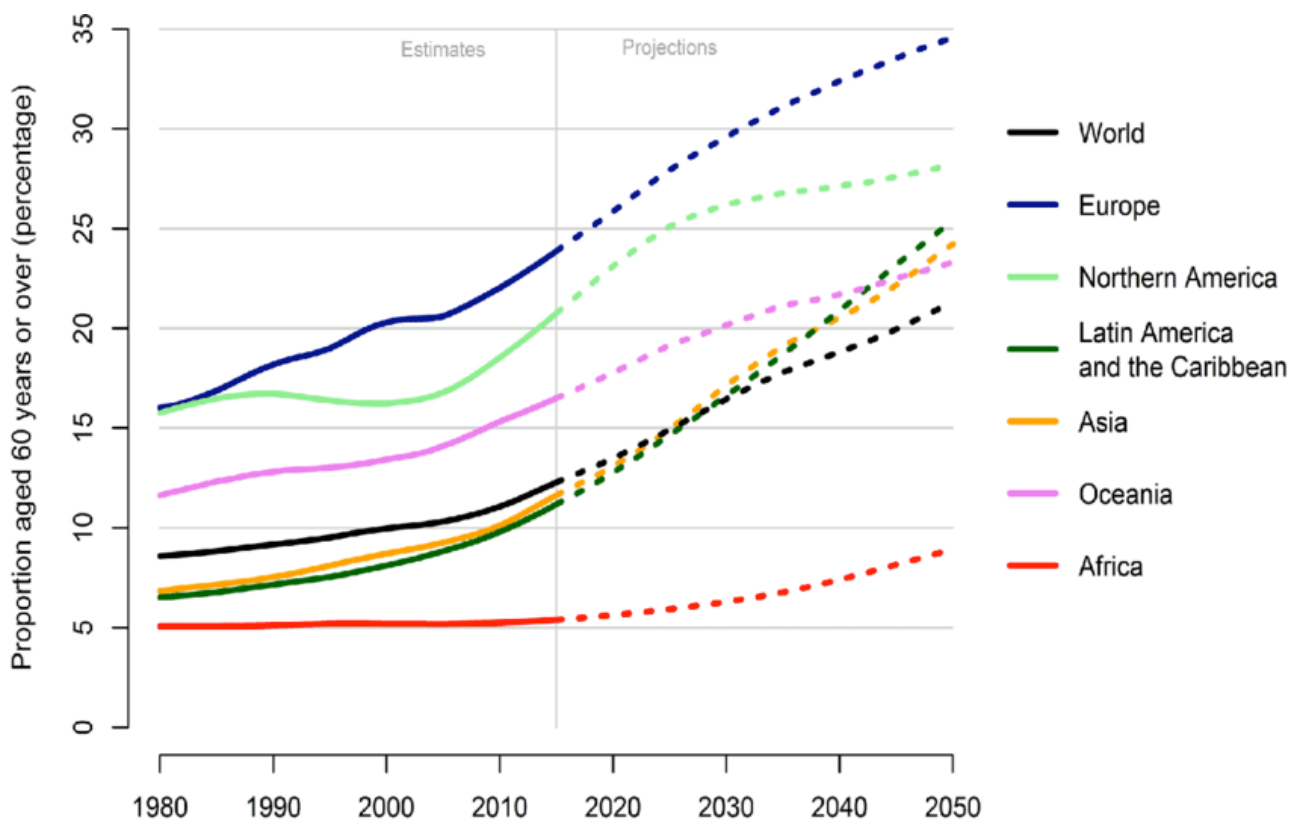


Figure 1: Percentage of population aged 60 years and older (10). This graph shows that the proportion of the world's population over 60 years will see a high increase in all World health organization (WHO) regions, especially from low and middle-income countries by 2050. WHO 2022 reported that in 2050, 80% of older people will be living in low and middle-income countries. In 2020. The number of people aged 60 years and older outnumbered children younger than 5 years (Source: <https://www.who.int/news-room/fact-sheets/detail/ageing-and-health>).

NDs are the leading cause of disability and the second leading cause of death worldwide. It is recognized as a global public health challenge. This burden will increase in the coming decades due to the increase in ageing populations and this burden is highest in low-income and middle-income countries (LMICs). In the past 30 years, the absolute number of deaths has increased by 39% and Disability-Adjusted Life-years (DALYs) have increased by 15%. Symptoms of neurological disorders include slowness of movement, memory loss, mood swings, and difficulty speaking, among others. These dysfunctions do not significantly affect patients at the early stage, and they can continue to live a self-sufficient existence. However, as the diseases progress, the patient's quality of life deteriorates rapidly, eventually requiring full-time care. So, as the disease progresses, social and economic difficulties can also arise. To date, there are limited treatments for NDs, and most of which only address the symptoms. Therefore, effective therapies that delay or minimize the symptoms of these chronic disorders are essential to limit the negative impact on individuals, families, society, and economies (11).

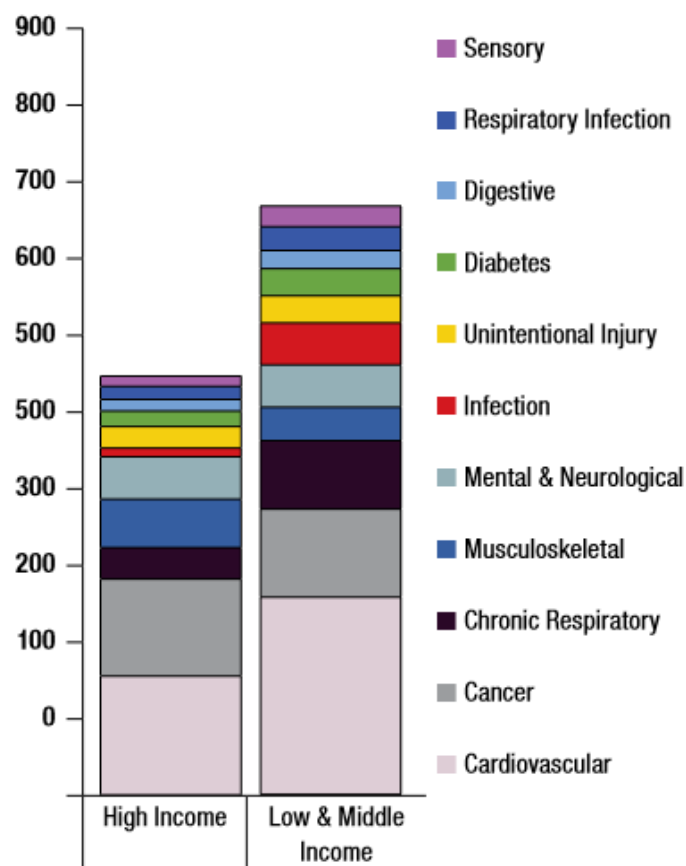


Figure 2: Burden of diseases in high and low-and middle-income countries. This graph shows the Leading contributors to the burden of disease among people aged 60 years and over - DALYs (per 1000 population) among people aged 60 and over, by cause and income region (12).

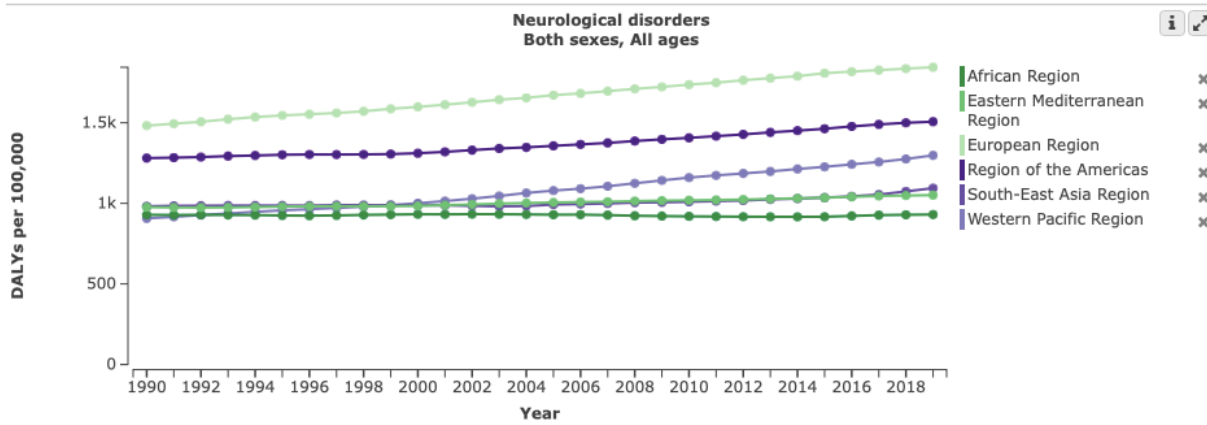


Figure 3: DALYs of neurological disorders in WHO regions. The figure shows that the European region has the highest DALYs rate with 1,844.58 DALYs per 100,000 (1,123.36-2,288.8) as compared to the African region which has the lowest DALYs rate with 930.57 DALYs per 100,000 (528.14-1522.52) according to GBD2019 (13).

1.2. Mitochondria

A mitochondrion is the double-membrane cell organelle found in every cell in our body, except for the red blood cells. The main function is to generate energy in the form of ATP, so it is called the powerhouse of the cell. In addition to their primary role, they are also involved in a wide range of cellular processes such as apoptosis, calcium signalling and stem cell fate and differentiation. Evolutionary biologists believe mitochondria evolved as aerobic bacteria that were engulfed by pro-eukaryotic cells and essentially domesticated and eventually entered a symbiotic relationship that facilitated ATP production and oxygen detoxification by the host (14, 15). This theory is supported by the discovery that mitochondria share many characteristics with bacteria. For example, they both have their own DNA, which is round and similar in size. The mitochondrial translation machinery is also very similar to that of prokaryotes. Mitochondrial numbers and morphology vary by cell type and energy requirements. For example, muscles, the brain, and the heart require high energy to function, so they have higher mitochondria numbers.

1.2.1 Structure and Function of Mitochondria

Mitochondria possess an inner and outer membrane, which differ in structure, composition, and function. While the outer membrane wraps the organelle and regulates transport between the cytosol and the mitochondrial intermembrane space (Figure 4), the inner membrane is invaginated to form a baffle-like structure called cristae. Cristae are composed of many different proteins involved in ATP production such as electron transport chain (ETC) complexes (complex I - IV) and ATP synthase (complex V), as well as proteins involved in the transport of specific proteins and metabolites between

the mitochondrial intermembrane space and matrix. It was also found that cristae undergo structural modification such as tightness, length, and width, in response to changes in substrate availability, bioenergetic state and metabolic stresses, glucose consumption, and high reactive oxygen species (ROS), or increased toxicity (16). Stem cell studies have shown that mitochondrial architecture can switch between elongated and interconnected networks to the fragmented state during reprogramming and cell differentiation to meet metabolic demands (17, 18).

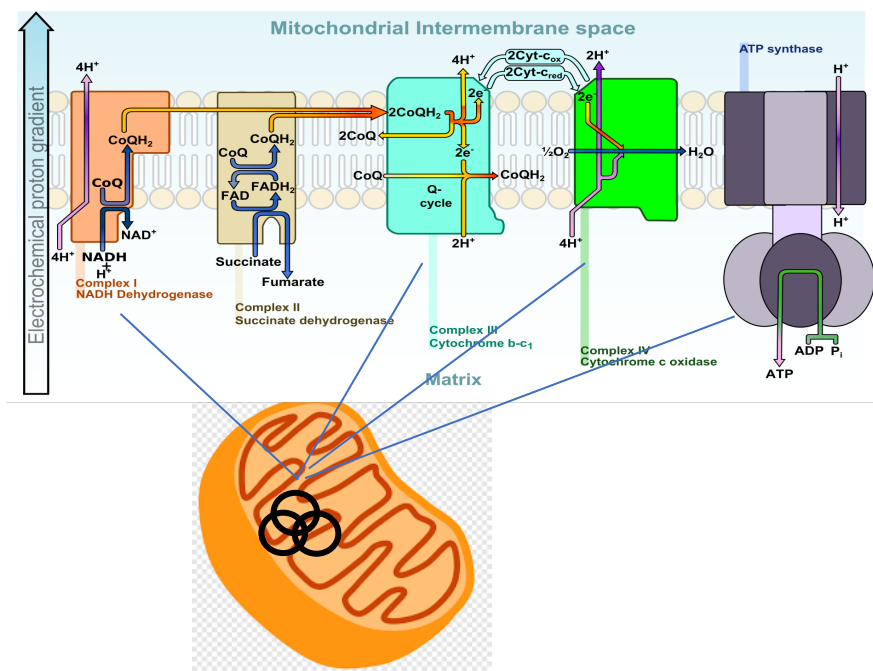


Figure 4: ETC and intermembrane space of a mitochondrion (Source from: https://www.wikiwand.com/en/Intermembrane_space_of_mitochondria).

1.2.2 Mitochondrial DNA (mtDNA)

The mitochondrial genome, called mtDNA, is a circular, double-stranded DNA molecule of 16,569 base pairs long (Figure 5). Chromosomes of mtDNA are tightly packed with genes. Unlike nuclear chromosomes which have large intergenic regions of non-coding DNA between genes, most mitochondrial genes lack introns. Human mtDNA contains 37 genes, 13 of which are involved in the process of oxidative phosphorylation, 22 genes encode transfer RNAs (tRNA) for specific amino acids, and 2 genes encode 2 subunits of ribosomal RNA (rRNA). The control region contains the signals that control RNA and DNA synthesis in mitochondria. As our fastest evolving DNA sequence, this hypervariable control region accumulates mutations at about ten times the rate of nuclear DNA. This region, also known as the D-loop (Figure 5), is involved in the formation of mtDNA during replication. MtDNA is replicated by the DNA polymerase gamma complex which is composed of a 140 kDa catalytic DNA polymerase encoded by the *POLG* gene and two 55 kDa accessory subunits

encoded by the *POLG2* gene. The replisome machinery is formed by DNA polymerase, mitochondrial helicase (Twinkle), and mitochondrial single-strand binding protein (SSBP). TWINKLE is a helicase, which unwinds short stretches of dsDNA in the 5' to 3' direction. All these polypeptides are encoded in the nuclear genome. In addition, mitochondrial transcription factor A (TFAM), a 24 kDa protein that binds mtDNA through two DNA-binding domains. The amount of bound TFAM is proportional to the mtDNA copy number (19).

Human mtDNA is inherited through the female germline. The genetic composition is identical to the mother. Each cell type has its own mtDNA copy number threshold, and failure to maintain mtDNA copy number or its integrity can lead to both impaired mitochondrial function and diseases. To maintain mitochondrial function and metabolic homeostasis, mtDNA integrity and copy number play critical roles. MtDNA copy number is highly regulated in a tissue-specific manner. Tissues or organs with higher energy requirement have higher mtDNA copy number, suggesting that copy number and energy distribution are associated with mitochondrial function and diseases.

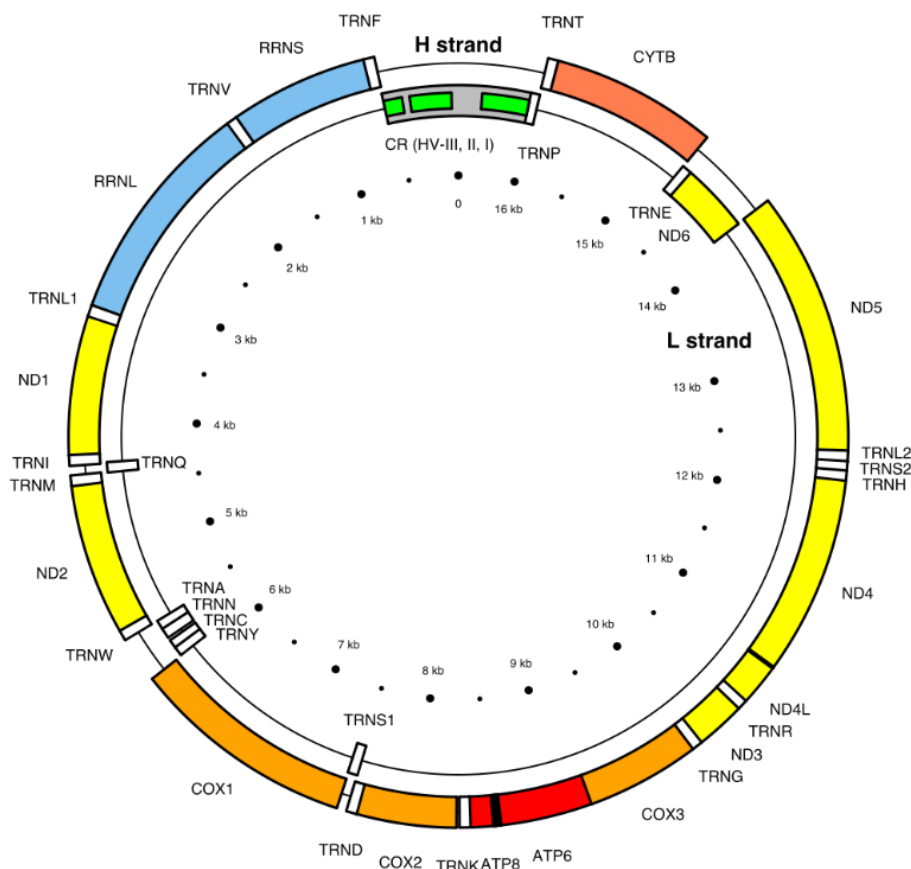


Figure 5: Human mtDNA with the 37 genes on their respective H- and L-strands (Source from: https://en.wikipedia.org/wiki/Mitochondrial_DNA)

1.2.3 Mitochondrial Dysfunction and NDs

Mitochondrial dysfunction has been implicated in the pathogenesis of many NDs, such as PD, AD, MS, and other diseases including diabetes etc. (Figure 6). Mitochondria are critical for energy production in the brain, and mitochondrial dysfunction can lead to reduced energy production and increased oxidative stress, which can damage neurons and contribute to the development of NDs. In PD, pathogenic mutations in several key genes such as *PARK7* (encoding DJ-1), *α-synuclein*, *parkin*, *PINK1*, or *LRRK2* lead to abnormal mitochondrial dynamics and function (3). In AD, mitochondria are more prone to create ROS, which results in increased levels of cellular and mitochondrial oxidative stress and further impairs the functioning of the ETC as the disease worsens (5). In addition, functional impairments in the ETC cause a decrease in MMP and ATP production, which affects mitochondria's capacity to meet the active demands of the cell. In ALS, mitochondria exhibit increased amounts of reactive oxygen species, depolarized mitochondria, impaired oxidative phosphorylation, ATP loss, and damaged mitochondrial proteins (20).

MtDNA homeostasis is important for the proper functioning of mitochondria, the organelles responsible for energy production within cells. Mitochondrial dysfunction resulting from mtDNA abnormalities has been implicated in the pathogenesis of several NDs, including AD, PD, HD and ALS. Researchers have found some ways in which mtDNA homeostasis may be linked to NDs: MtDNA is more susceptible to mutations than nuclear DNA due to its proximity to the reactive oxygen species (ROS) generated during oxidative phosphorylation. Mutations in mtDNA can lead to impaired mitochondrial function and contribute to the pathogenesis of NDs (5, 21). On the other hand, the mtDNA copy number is tightly regulated, and both low and high mtDNA copy number have been associated with NDs (22). For example, reduced mtDNA copy number has been observed in the brains of Alzheimer's disease patients, while increased mtDNA copy number has been observed in the blood of Parkinson's disease patients. Furthermore, mtDNA damage can occur as a result of oxidative stress, which can lead to mitochondrial dysfunction and contribute to the pathogenesis of NDs (21). In addition, given the removal of damaged mitochondria via mitophagy is an important process for maintaining mitochondrial homeostasis, the dysregulation of mitophagy has been linked to the pathogenesis of NDs (23). MtDNA encodes for several proteins involved in oxidative phosphorylation, thus the abnormalities in these proteins can lead to mitochondrial dysfunction and contribute to the pathogenesis of NDs (24). Overall, the link between mitochondrial dysfunction, mtDNA homeostasis and NDs highlights the need for further research into the mechanisms underlying these diseases and the development of new treatments targeting mitochondrial dysfunction.

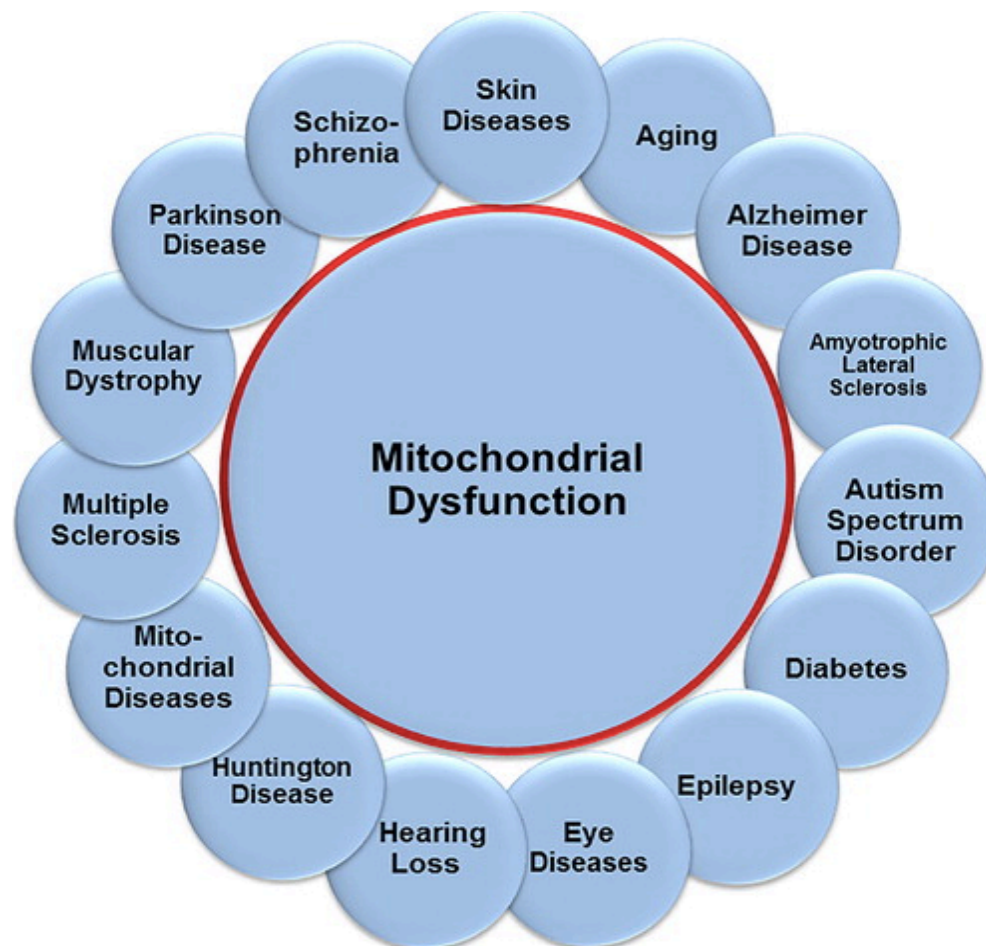


Figure 6: In the pathophysiology of neurological diseases and illnesses, mitochondrial dysfunction is a well-established enabling factor (1).

1.3 Mitochondrial DNA Polymerase Gamma (POLG) and POLG-related Diseases

1.3.1 POLG: History, Cloning and Expression

The identification of DNA Polymerase Gamma (POLG) dates to the 1970s when researchers discovered DNA polymerase activity in isolated mitochondria (25). This discovery led to the hypothesis that a specific mtDNA polymerase was responsible for the replication and repair of mtDNA. In the following decades, biochemical and genetic studies were conducted to uncover the details of this enzyme. The human *POLG* gene was first cloned in the late 1990s, and its protein product, the POLG, was subsequently characterized. This breakthrough allowed for a greater understanding of the enzyme's structure, function, and role in maintaining mtDNA integrity.

In 1987, the first proof of the function of POLG in mtDNA replication was presented (25). The DNA polymerase is known to function in mammalian mitochondria, POLG, is crucial for embryonic

development (26). This enzyme occurs in human cells as a heterotrimer, consisting of one large catalytic subunit and two smaller accessory subunits. POLG is a nuclear-encoded enzyme that plays a crucial role in the replication and repair of mtDNA. As the sole DNA polymerase responsible for mtDNA maintenance, it is essential for proper cellular function and energy production. This essay will explore the history, cloning, and expression of POLG, highlighting its importance in understanding mitochondrial diseases and developing potential therapies.

The gene *POLG*, which has 23 exons and is found on chromosome 15q25, encodes the catalytic subunit (27). *POLG2*, a gene with 8 exons that are found on chromosome 17q23, encodes the accessory subunits (28). In 1996, Ropp and Copeland successfully cloned a human *POLG*. There are 1,239 amino acids in the human *POLG* sequence, and its molecular weight is 139.5 kDa. In *Drosophila*, *S. Cerevisiae*, and *G. gallus*, the amino acid sequence of human POLG is 49%, 43%, and 78% respectively (29). The human *POLG* gene is located on chromosome 15 and comprises 23 exons. The gene encodes a protein of 1239 amino acids with a molecular weight of approximately 140 kDa. The cloning of POLG involved several key steps, including the isolation of its complementary DNA (cDNA), the creation of recombinant DNA constructs, and the expression of the protein in a suitable host organism. Once the POLG cDNA was isolated, researchers utilized recombinant DNA technology to generate constructs that contained the coding sequence for the enzyme. These constructs were then inserted into appropriate host organisms, such as bacteria, yeast, or mammalian cells, to facilitate the expression of the recombinant POLG enzyme. By studying the recombinant enzyme, researchers gained insights into its structure, function, and role in maintaining mtDNA stability.

Expression of POLG is tightly regulated to ensure proper mtDNA replication and repair. In the nucleus, *POLG* gene is transcribed and translated in the cytosol and transported into the IMM where it combines with other proteins to generate the machinery needed for mtDNA replication and nucleoids (30). Studies have shown that POLG expression is influenced by various factors, including developmental stage, tissue type, and cellular stress. POLG is expressed in most human tissues, with the highest levels observed in tissues with high energy demands, such as the heart, brain, and skeletal muscles. This pattern of expression reflects the essential role of POLG in maintaining mtDNA and energy production in these tissues. Research has also revealed that the expression of POLG can be modulated in response to cellular stress (31).

Overall, the discovery, cloning, and expression of POLG have significantly advanced our understanding of mtDNA maintenance and its role in cellular energy production. The insights gained

from studying POLG have shed light on the molecular mechanisms underlying mitochondrial diseases, many of which are associated with mutations in the *POLG* gene. As we continue to unravel the intricacies of POLG function, the knowledge will undoubtedly pave the way for the development of novel therapeutic strategies for the treatment of mitochondrial disorders.

1.3.2 Structure and Functions of POLG

1.3.2.1 Structure of POLG

POLG is a multi-subunit enzyme composed of a catalytic subunit (POLG) and two accessory subunits (POLG2). The catalytic subunit, encoded by the *POLG* gene, has a molecular weight of approximately 140 kDa and contains three functional domains: the N-terminal exonuclease domain, the linker region, and the C-terminal polymerase domain. contains three functional domains: the N-terminal exonuclease domain, the linker region, and the C-terminal polymerase domain (Figure 7). Exonuclease Domain is responsible for the proofreading activity of POLG. It enables the enzyme to remove mismatched nucleotides, ensuring high fidelity during mtDNA replication and repair. The linker region connects the exonuclease and polymerase domains. This flexible region facilitates the coordination between the two domains, allowing for efficient mtDNA replication and repair. The polymerase domain carries out the primary function of POLG, which is the incorporation of nucleotides during mtDNA replication and repair.

The accessory subunit, POLG2, is encoded by the *POLG2* gene and exists as a homodimer. Each subunit has a molecular weight of approximately 55 kDa. POLG2 interacts with the catalytic subunit to enhance its processivity, allowing the enzyme to synthesize long stretches of DNA without dissociating. The structure of POLG appears to vary depending on the species; in yeast, it exists as a single catalytic subunit while in *Drosophila*, it occurs as a homodimer (28). There are three distinct roles performed by the POLG's catalytic subunit: 3'-5' exonuclease, DNA polymerase, and 5'-deoxyribose phosphate (dRP) lyase.

The exonuclease domain (aa 171-440), which is found at the N-terminus of the catalytic subunit, has a 3'-5' proofreading activity. It comprises motifs I, II, and III, which are extremely conserved and necessary for the exonuclease function. The mtDNA synthesizing activity is carried out by the DNA polymerase domain, which is composed of the thumb (aa 441-475; aa 768-815), palm (aa 816-910; aa 1096-1239), and finger (aa 816-910; aa 789-1239) subdomains. (aa 911-1095). The polymerase domain also includes the conserved motifs A, B, and C. As they bind to both the nucleotide triphosphate of the substrate and the template mtDNA, they are essential for the polymerase's ability

to function. The palm subdomain, which houses the catalytic residues, is where the active site is located (28, 30).

The linker region in humans consists of approximately 482 amino acid residues that are connected via long helices to the exonuclease and polymerase domains (32). There are two subdomains within the linker region: the global intrinsic processivity (IP), which contains residues 475-510, and the extended accessory interacting determinant (AID), which contains residues 511-570. According to (30, 32), the linker domain of POLG's catalytic subunit physically interacts with only one accessory subunit (p55). This feature makes POLG unique from other DNA polymerases.

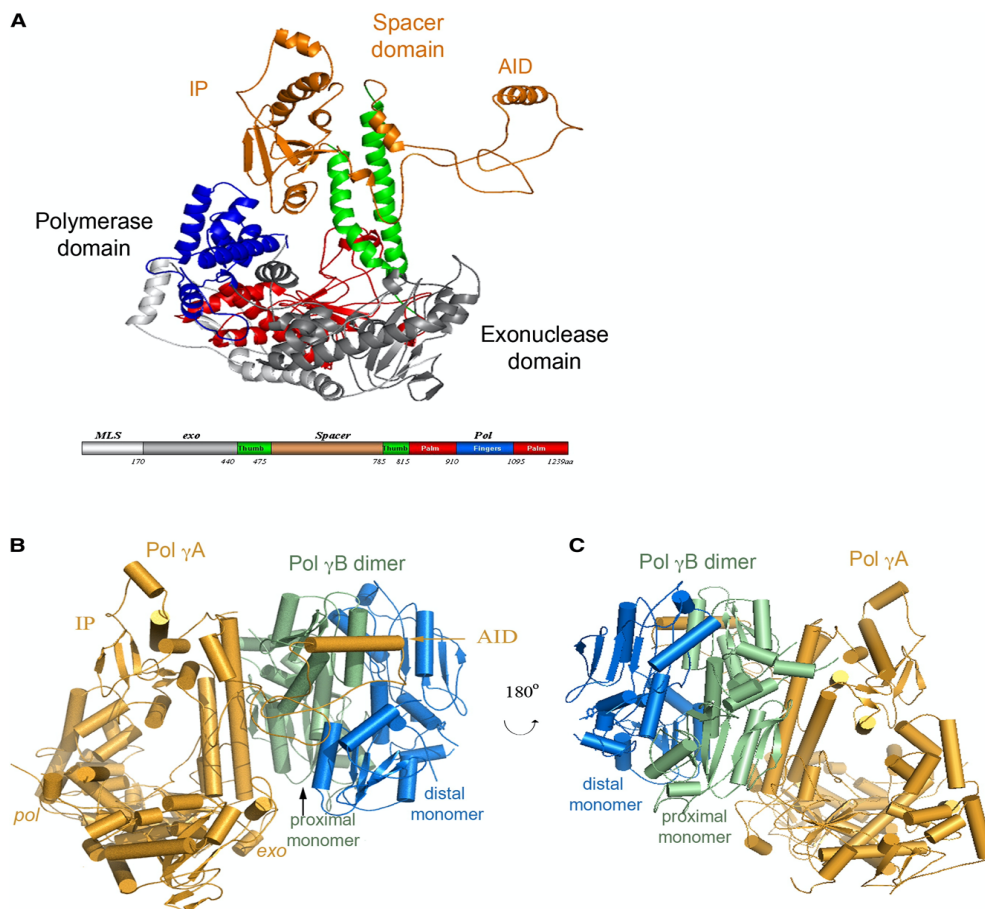


Figure 7: 3D structure of POLG catalytic subunits. (A) illustrating different domains: exonuclease(grey), Linker (orange) and polymerase (blue). (B) Heterotrimer POLG structure consisting of the Catalytic subunit p140 (orange) and the proximal (green) and distal (blue) (32).

1.3.2 Functions of POLG

POLG is responsible for the synthesis of the leading and lagging strands during mtDNA replication. It works in concert with other proteins, such as the mitochondrial helicase Twinkle and the mitochondrial single-stranded DNA-binding protein (mtSSB), to ensure accurate and efficient

replication of mtDNA. Furthermore, POLG also participates in the repair of damaged mtDNA through its involvement in base excision repair (BER) and other repair pathways. In BER, POLG removes and replaces damaged bases, ensuring the integrity of the mtDNA molecule. In addition, by replicating and repairing mtDNA, POLG plays a crucial role in maintaining mitochondrial function and energy production. Disruptions in POLG function can lead to mtDNA depletion or the accumulation of mtDNA mutations, which can result in mitochondrial dysfunction and various human diseases.

In conclusion, the structure and functions of POLG are essential for maintaining the integrity of mtDNA and, consequently, cellular energy production. The study of POLG has provided valuable insights into the molecular basis of mitochondrial disorders, and further research in this area promises to contribute to the development of innovative treatments for these debilitating diseases.

1.3.3 *POLG* Mutations

POLG mutations can occur in any of the functional domains of the enzyme, including the exonuclease, linker, and polymerase domains. Depending on the specific mutation, the resulting changes in enzyme function can lead to mtDNA instability, depletion, or an increased rate of mtDNA mutations. *POLG* mutations can impair the enzyme's ability to maintain the structural integrity of mtDNA. This can result in the formation of multiple mtDNA deletions, leading to a decrease in mitochondrial function and an increase in oxidative stress. Certain *POLG* mutations can lead to a reduced capacity for mtDNA replication, causing a decrease in the overall amount of mtDNA within a cell. This depletion can result in impaired energy production and mitochondrial dysfunction. Some *POLG* mutations can compromise the enzyme's proofreading ability, resulting in an increased rate of mtDNA mutations. These mutations can accumulate over time and contribute to the development of mitochondrial disorders.

POLG mutations can lead to a wide range of clinical manifestations, reflecting the diverse impact of these mutations on mitochondrial function. Common symptoms associated with *POLG*-related disorders include muscle weakness, ataxia, peripheral neuropathy, seizures, and gastrointestinal problems. Progressive external ophthalmoplegia (PEO) is often caused by dominant *POLG* mutations and is characterized by progressive weakness of the eye muscles, leading to drooping eyelids and difficulty moving the eyes. The other severe type is Alpers-Huttenlocher Syndrome. This severe autosomal recessive disorder is caused by biallelic *POLG* mutations and is characterized by early-onset progressive encephalopathy, seizures, and liver dysfunction. In addition, mitochondrial Neurogastrointestinal Encephalomyopathy (MNGIE) is an autosomal recessive disorder caused by

POLG mutations, presenting with gastrointestinal dysmotility, peripheral neuropathy, and leukoencephalopathy. Besides, Sensory Ataxic Neuropathy with Dysarthria and Ophthalmoplegia (SANDO) is a rare autosomal recessive disorder caused by *POLG* mutations, characterized by sensory ataxia, dysarthria, and ophthalmoplegia.

POLG mutations have a significant impact on mitochondrial function, leading to various mitochondrial disorders with diverse clinical manifestations. Understanding the molecular mechanisms underlying these disorders is essential for the development of targeted therapies and the improvement of patient outcomes. As research into *POLG* mutations and their effects on human health continues, novel treatment strategies may emerge, offering hope for those.

A major cause of mitochondrial disease in humans is a pathogenic mutation occurring in the catalytic subunit of *POLG*. There are over 300 *POLG* mutations known to date (33), which are associated with a spectrum of disorders that differ in age of onset, pattern of inheritance, and clinical presentation (discussed in the subsequent section). The Human DNA Polymerase Gamma Database (<https://tools.niehs.nih.gov/polg/>) contains a list of all *POLG* mutations identified (Figure 8).

It is essential to comprehend how *POLG* mutations affect the protein's various domains and activities since doing so could provide insight into the mechanisms underlying phenotypic variability.

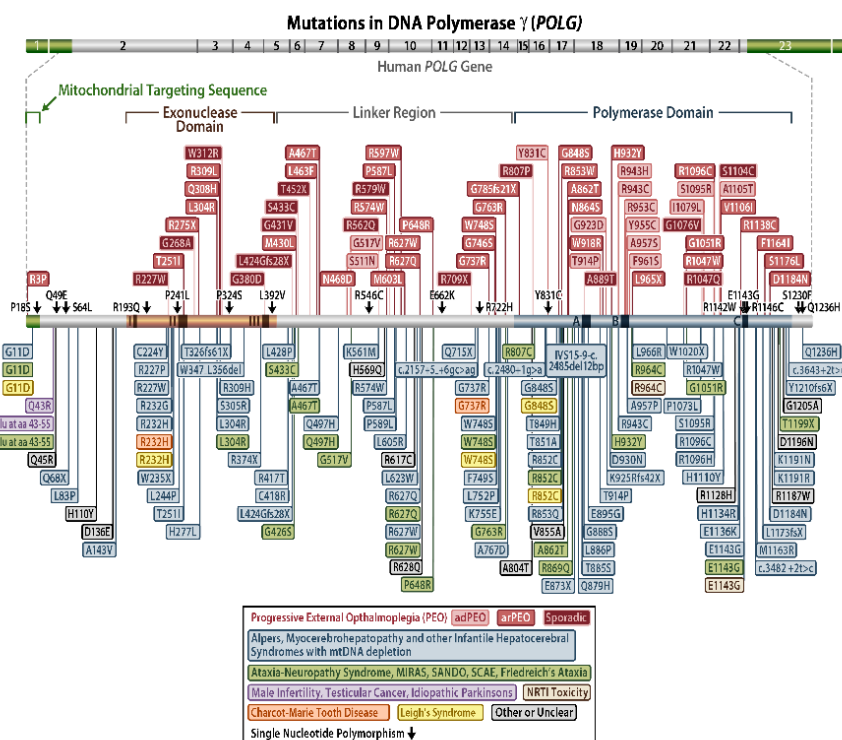


Figure 8. *POLG* mutations identified (<https://tools.niehs.nih.gov/polg/>).

There are two modes of inheritance of pathogenic mutations: autosomal recessive and autosomal dominant, with the former mode of inheritance occurring most frequently. Recessive mutations can be observed throughout the lifespan, whereas dominant mutations are associated with adult-onset disease (31).

Mutations were found in all POLG domains, but these three pathogenic variants were classified as the most common mutations, causing mild adult onset to severe early-onset disease. These mutations include p.(Ala467Thr), p.(Trp748Ser) and p.(Gly848Ser) (34). POLG's p.(Ala467Thr) mutation is located in the linker domain, disrupting the interaction with the proximal p55 subunit. POLG activity reduces by less than 4% in vitro when the p. (Ala467Thr) mutation is present compared with wild-type POLG (35) demonstrated that the p. (Ala467Thr) mutation results in poor p140-p55 interaction from co-immunoprecipitation and processivity analyses. DNA polymerase activity is dramatically reduced in people with the p. (Ala467Thr) mutation however, the exonuclease activity is only reduced by 2-fold.

The p. (Trp748Ser) (c.2243G > C, Exon 13) mutation is reported as the second most common and it is seen co-occurring with the p. (Glu1143Gly) mutation in 1:125 patients from Finland. The most frequent mutation identified in ataxia-neuropathy spectrum disorders and Alpers is the p.(Trp748Ser) mutation (34). This mutation was found on the linker domain affecting DNA-binding affinity. When the p. (Trp748Ser) mutation was characterized biochemically, it was shown to have poor DNA-binding properties, which in turn hindered the processivity of mtDNA synthesis and primer extension. It's interesting to note that although the p140/p55 interaction was unaffected, the catalytic defect was still present (35). The POLG with the p. (Glu1143Gly) mutation alone, on the other hand, had an activity that was 1.4 times higher than the wild type. When these two mutations are combined the effect becomes deleterious. It spikes the overall DNA binding, catalytic activity, and fidelity of the POLG (35).

The p. (Gly848Ser) is the third most common *POLG* mutation associated with Alpers, MELAS, CPEO and LS in a recessive state. It is found in the polymerase domain of the p140 catalytic subunit in the thumb region. In vitro, relative to the wild-type, it causes a 5-fold reduction in DNA-binding affinity. Data on the prevalence of this mutation is very little. Intriguingly, the holoenzyme only kept 0.03% of the wild-type polymerase activity (36), while POLG with mutations in the palm sub-domain kept 50 - 70% of the polymerase activity. The fidelity of the enzyme was unaffected, and the p140-p55 interaction was unaffected (36).

In conclusion, mutations in the *POLG* gene can lead to a wide range of mitochondrial disorders that are characterized by mitochondrial dysfunction, resulting in a variety of clinical manifestations, including muscle weakness, neurological deficits, and gastrointestinal problems. Understanding the structure and functions of *POLG* has been instrumental in elucidating the molecular mechanisms underlying these disorders. This knowledge has the potential to pave the way for the development of novel therapeutic strategies to treat mitochondrial diseases.

1.3.4 *POLG*-Related Disorders

POLG-related disorders are characterized as a continuum of heterogeneous but clinically overlapping phenotypes (37). *POLG*-related disorders can begin at any age, from infancy to adulthood. The severity of disease associated with infancy and childhood is greater than that associated with older age, though the reasons behind this observation remain uncertain.

Alpers, Myoclonic Epilepsy Sensory Ataxia (MEMSA), Ataxia Neuropathy Spectrum (ANS), Childhood Myocerebrohepatopathy Spectrum (MCHS), and autosomal dominant (adPEO) or autosomal recessive (arPEO) are some of the disorders associated with *POLG*. Among *POLG*-related disorders, Alpers is the most severe. The clinical paradigm of *POLG*-related Disorders is presented in Table 1.3.4.

Table 1.3.4: Clinical description of *POLG* mitochondrial disorders

Disorder	Onset	Clinical features
Alpers	Infancy/childhood or adolescence/early adulthood	Seizures/epilepsy, psychomotor regression, and liver dysfunction/failure.
MEMSA (myoclonic epilepsy myopathy sensory ataxia)	Early to teenage- onset	Epilepsy, myopathy, and ataxia.
MCHS (Childhood Myocerebrohepatopathy Spectrum)	First months of life	Developmental delay, early-onset dementia, lactic acidosis, and myopathy with failure to thrive.
ANS (ataxia neuropathy spectrum)	Early to late onset	Ataxia and neuropathy (seizures and ophthalmoplegia).
arPEO (autosomal recessive progressive external ophthalmoplegia)	Late-onset	Ophthalmoplegia and ptosis.

adPEO (autosomal dominant progressive external ophthalmoplegia)	Late-onset	Ophthalmoplegia, ptosis, generalised myopathy, depression, Parkinsonism, sensorineural hearing loss and ataxia.
---	------------	---

POLG-related disorders are linked to faulty mtDNA maintenance and expression. The exact mechanisms underlying *POLG* mutations remain unclear, but they lead to mtDNA depletion and/or multiple deletions in affected tissues, resulting in ATP depletion and OXPHOS dysfunction. As the mtDNA-encoded subunits become rate-limiting, mtDNA depletion ultimately causes a reduction in the amount of ETC complexes, which disrupts the ratio of complexes within the super complexes and lowers ATP synthesis (30).

In both adults and children, the biochemical assay may reveal mtDNA depletion and respiratory chain deficits affecting complexes I–V; however, biochemical assay in muscle may be normal, indicating that the effects of *POLG* mutations are tissue-specific. Therefore, proper respiratory chain function and mtDNA content in any particular tissue should not rule out the possibility of a *POLG*-related illness, and genetic confirmation of biallelic *POLG* mutations should be the gold standard for the diagnosis of *POLG*-related disorders (30, 37, 38)

Recessive *POLG* mutations are characterized in the form of homozygous or compound heterozygous. Despite the lack of a direct link between genotype and phenotype, Compound heterozygous mutations are linked to more severe early-onset symptoms (39). Contrarily, homozygous mutations are linked to milder, later-onset illness. Furthermore, compared to compound heterozygotes with the p. (Ala467Thr)/p. (Trp748Ser) mutations, homozygous p. (Ala467Thr) and p. (Trp748Ser) mutations have been associated with prolonged longevity (40). It is noteworthy that early-onset and late-onset *POLG*-related diseases might have homozygous or compound heterozygous mutations, making it challenging to establish genotype-to-phenotype relations. Uncertainty persists regarding the causes of such genotypic/phenotypic variance within single or multiple syndromes (31).

1.4 Stem Cell Models for NDs

1.4.1 Disease Model of NDs

Due to the immense complexity of the molecular mechanism, the disease mechanisms are not clearly understood in the field of NDs. Therefore, disease models are essential because they not only enhance our understanding of the disease mechanism but also serve as a model for developing therapies and testing novel drug targets that are difficult to treat.

To date, many animals model including mice, zebrafish, drosophila (*D. melanogaster*), and roundworms (*C. elegans*) – all of which have recapitulated only some aspects of human disease. Mitochondrial diseases are considered even more challenging to diagnose, treat and model because of their heterogeneous phenotype even among patients with the exact same mutation. Although there are numbers of advantages to using animal models such as they are reproduced in large numbers making them inexpensive and their small size allows easier to manage and manipulate them (41, 42). Also, in roundworms and drosophila, many of their genome sequences are complete, making genetic modification simple. More crucially, the in vivo setting enables the examination of both cell- and non-cell-autonomous contributions to a given disease (43).

Nevertheless, using animal models has some drawbacks. Many of the organisms used in the study is not a true representation of the disease. Even though models, like the mouse, and humans share a common ancestor, there are still considerable differences in their genetic makeup that frequently make it difficult to extrapolate results from them to humans. In human trials, numerous drugs that worked well in mouse models fell short (43). Mice lack genetic variation of the human population because they are inbred. In order to determine whether the effects observed are due to any other causes, a thorough understanding of the animal's genome employed in the study is also required (42). Animals may not always be the best study subjects for tracking the progression of internal problems, such as neuronal malfunction in neurodegenerative disorders, the study's focus. For example, the POLG mouse model does not mimic the epileptic phenotype seen in human patients (44).

1.4.2 Human Pluripotent Stem Cells (hPSCs)

To overcome such limitations, hPSC offers the best model for capturing the internal environment of human cells and observing development. For example, live-cell imaging can monitor disease progression over time (43). A variety of cell types can be developed from these undifferentiated and unspecialized cells in the laboratory without any significant ethical concerns. They can then be differentiated into specialized cells or tissues of interest. Hence, these cells hold great potential as disease models, for the development of tissue replacement therapies, and for screening novel drugs to determine their efficacy and toxicity (45). A large number of PSCs can be grown very quickly in large quantities, enabling large-scale genetic and chemical screens very quickly (43), hence results can be observed reasonably quickly. Additionally, in vitro models can be used to study genotype-phenotype correlations in a controlled environment.

There are two types of pluripotent stem cells: human embryonic stem cells (ESCs) and human induced pluripotent stem (iPSCs). Human ES cells are derived from blastocyst-stage human embryos and can develop and differentiate into all three germ layers and some extraembryonic tissues (46).

The first embryonic stem cells were described in 1981 from mouse blastocysts. Twenty years later, in 1998, human ES cells were isolated from pre-implantation embryos grown in culture for five days after oocyte fertilization (46). Most of the embryos used were spared from IVF clinics. However, generating embryos specifically for this purpose has been criticized (47). Since the process of deriving human ES cells entails the destruction of the embryo, which raises ethical issues. Using donated embryos for research also has quality concerns (47).

1.4.3 Induced Pluripotent Stem Cells (iPSCs)

Human iPSCs can help overcome the ethical challenge around ES cells. human iPSCs can be derived from adult somatic cells that are genetically reprogrammed under conditions that induce the cells to revert to their embryonic pluripotent state. This reprogramming strategy was first introduced in 2006 by Yamanaka employing fibroblasts of adult mouse and later from human skin fibroblasts (48). In this procedure, with the help of Four transcription factors Oct3/4, Sox2, c-Myc, and Klf4 also known as Yamanaka factors after the person's discovery are used to induce adult human dermal fibroblast and revert to an undifferentiated state of cells and their ability to self-renew. The morphology, physiology, gene expression capabilities, and epigenetic status of pluripotent cell-specific genes of iPSCs are very similar to those of ES cells. As a result of these iPSCs dedifferentiating into cells of the three germ layers in vitro and in teratomas (48), they can differentiate into all three germ layers in vitro. iPSCs are not limited to dermal fibroblasts; they can also be generated from neuronal cells, hematopoietic cells, adipose cells, and others. The first iPSC-based models of neuronal diseases were demonstrated in 2008 (49). In that study, fibroblasts from ALS patients were reprogrammed into iPSCs and differentiated into functional motor neurons.

The major advantage of iPSCs over ES cells is the ability to overcome ethical concerns since iPSCs are derived directly from somatic cells. In contrast to ES cells, iPSCs can be used to generate disease-specific and patient-specific cell models, which provide insights into the molecular mechanisms and progression of diseases. The use of disease-specific iPSC models can also improve drug screening efficiency and accuracy (50). Patient-derived iPSCs also offer the benefit of eliminating the risks of tissue rejection as they use the patient's own cells in therapy. In addition, healthy cells can also be reprogrammed to iPSCs and genetically modified using gene editing techniques to facilitate wider research.

However, iPSCs have several limitations, including a considerable degree of diversity in their propensities for differentiation, which prevents the observation of phenotypic consequences at the organism level. The existence of mutations in the parental cell line prior to reprogramming and the partial silencing of reprogramming factors may also have an impact on the characteristics of iPSCs (51). Ectopic expression of the c-Myc and Klf4 genes is harmful to tissue replacement treatment since it has the potential to cause cancer. To minimize these hazards, these oncogenes can be replaced by other elements such as Nanog and Lin28 (52), or they can be completely removed (53). Taking into account all of these aspects, iPSCs have unquestionably created new opportunities for disease modelling, therapeutic agent development, and medical research (50).

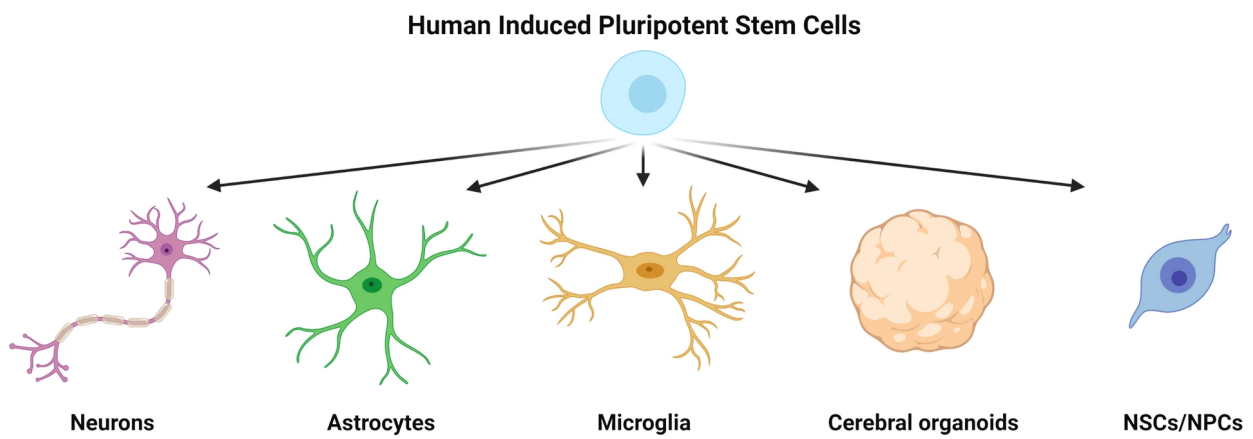


Figure 9: Represents a few of the many cell types that can be derived from the iPSCs (54).

1.4.4 Astrocyte Differentiation from iPSCs

Over the past decade, various techniques for converting iPSCs into astrocytes have been established (55, 56, 57). These iPSC-differentiated astrocytes have been shown to be functional *in vitro* and used in *in vivo* cell-based models of neurological disease. However, some methods are slow (up to 6 months) or require sorting to reduce heterogeneity (57). To address this issue, Tcw et al. (2017) developed a 30-day differentiation protocol suitable for experiments on neuroinflammation, phagocytosis, and spontaneous calcium activity (57). Using the inducible expression of NFIA or NFIA and SOX10 in iPSCs, the developed method can efficiently generate astrocytes within 4-7 weeks. By adapting a previously published protocol, our group established the generation of astrocytes from iPSC-derived neural stem cells (NSCs) using a cocktail of growth factors and small chemicals (Figure 10).

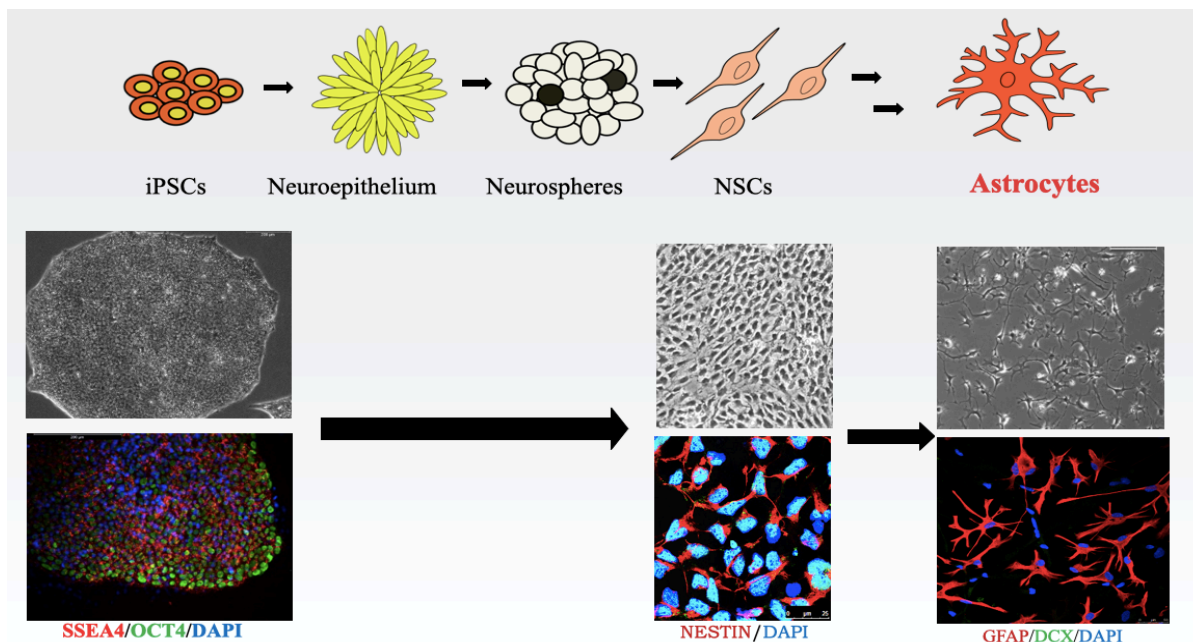


Figure 10: Derivation of astrocytes from iPSC (58).

Importantly, multiple studies on iPSC-derived astrocytes were performed to demonstrate their functionality and activity *in vivo*, making them suitable for ND models. Santos and colleagues assessed the response of iPSC-derived astrocytes to interleukin-1 (IL-1) and tumor necrosis factor- α (TNF- α), which primed the identical to human pro-inflammatory responses and altered gene expression in primary astrocytes (59). To study AD, researchers have generated astrocytes from iPSCs and found that these astrocytes responded to a neurotoxic A β fragment with state-dependent Ca $^{2+}$ alteration and multiphasic transmitter release, in association with a multiphasic release of signalling molecules and converted into reactive astrocytes (60).

1.4.5 Brain Organoids

Converting a 2D system into the 3D organoid culture will allow us to develop an *in vitro* system that faithfully recapitulates the complexity of the human brain, making it a better system for examining the complex cellular interactions that underlie disease development. Brain organoids are 3D cell aggregates derived from human PSCs, including ESCs and iPSCs. The 3D brain organoid resembles a developing human fetal brain and displays a variety of associated cell types that have undergone the inherent developmental patterns of the modelled organ (61). Furthermore, the ability of organoids to achieve specialized functions commonly found in model organs has proved to be a revolutionary tool for understanding the human brain. Notably, improvements in 3D cerebral organoid cultures have opened new avenues for studying human brain disorders *in vitro*, potentially bridging the gap between *in vitro* human cell-based systems and animal models. In fact, animal models often fail to replicate human-specific pathophysiology. 2D human cellular cultures cannot accurately represent the complex interaction of the *in vivo* ecosystems. Thus, the complex 3D arrangement of cerebral

organoids, especially when considering the extracellular deposition of pathogenic proteins in a wide range of neurodegenerative illnesses, opens new study avenues.

Currently, both guided (62) and unguided (63) methods are used to create human brain organoids from iPSCs. As opposed to guided organoid approaches, which add exogenous patterning stimuli to encourage iPSCs to differentiate towards desired lineages, unguided methods completely rely on spontaneous morphogenesis and inherent differentiation capacities within iPSCs aggregates.

These approaches rely on the inherent ability of stem cells to self-assemble and differentiate into region-specific brain organoids. Region-specific growth stimulators, differentiation factors, and specialized cytostatic agents direct these "guide" organoids. Thus, brain organoids from specific regions are more typical in mimicking the cellular composition, structural properties, and molecular activity of brain regions. Different region-specific organoids have been developed, such as cortical spheroids, cerebellar organoids, hippocampal organoids, and midbrain organoids, improving our understanding of differences in brain regions.

Another well-known benefit of brain organoids is their ability to create patient-derived models with key features of patient genetic data. However, despite recent advances in cellular biology, significant restrictions (e.g., heterogeneity, lack of vascularization, and ageing) must be overcome to match all major features of human brain function. Overall, brain organoids have the potential to provide new insights into ND modelling and drug screening research, thus opening new avenues in personalized treatment.

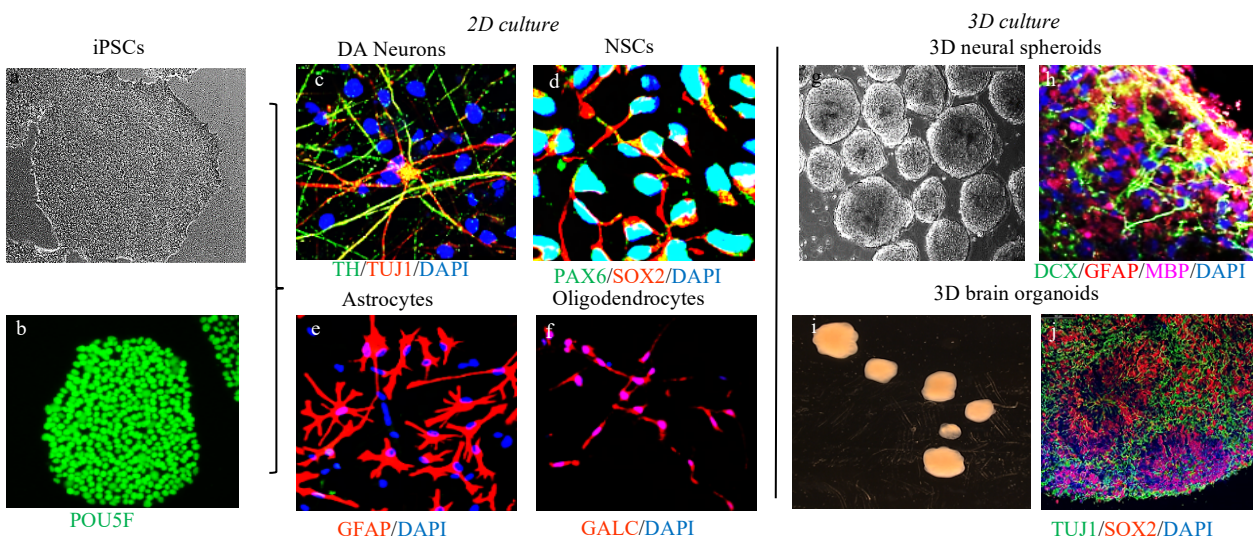


Figure 11: Developing astrocytes and co-culture systems to grow astrocytes and neurons together. This figure shows the derivation of iPSCs (a & b) to the monolayer of NSCs (d), glial cells including astrocytes (e) and oligodendrocytes (f), and DA neurons (c, 2D culture). We also develop two types of complexes, 3D culture

(g-j): one used an equal number of astrocytes, oligodendrocytes and neurons mixed in a hanging drop (spheroid, g & h), and the other method is iPSC-derived cortical organoids with a 3D structure (i & j). (Source: provided by Dr. Kristina Xiao Liang)

Previously, our group developed robust 2D and 3D model systems based on the iPSC system (Figure 11). These advanced iPSC systems allow us to generate 2D NSCs, functional dopaminergic (DA) neurons, glial astrocytes and oligodendrocytes and 3D culture systems including simple hanging drops (spheroid formation) that combine iPSCs derived neurons, astrocytes, and oligodendrocytes (Figure 11), and 3D cortical organoids (Figure 11).

1.5 Astrocytes in NDs

1.5.1 Astrocytes and Their Normal Function

Astrocytes are the most abundant glial cell type in the center neural system (CNS). They got their name from the radially arranged foot processes that give them their star-like appearance. Until decades back, astrocytes have been understood as passive support cells of the neuron. Recent research implicated that astrocytes play vital roles in various physiological functions, including trophic molecules secretion, modulation of brain microenvironment, regulates blood-brain barrier (BBB) and influence on synaptic function (Figure 11) (64, 65, 66). Astrocytes exhibit morphological heterogeneity, a wide spectrum of reactivity, and a wide range of molecular expression (67). The reactivity of astrocytes can be triggered by chemicals, toxins, oxidative stress, or pathogens (Figure 11) (66, 68). Additionally, astrocytes undergo morphological changes in response to epilepsy, mechanical lesions of the cerebrospinal parenchyma, and tumors (69, 70). Several molecular triggers can activate astrocytes, including transforming growth factor β 1 (TGF- β 1), leukemia inhibitory factor (LIF), and ciliary neurotrophic factor (71). After stimulation, astrocytes either release protective molecules like vascular endothelial growth factor (VEGF), brain-derived neurotrophic factor (BDNF), and nerve growth factor, or pro-inflammatory molecules like reactive oxygen species (ROS), interleukin-6 (IL-6), interleukin-1 (IL-1), and tumor necrosis factor (TNF- α), or molecules that promote inflammation (72). Consequently, chemokines like β -chemokine 2 (CCL2), β -chemokine 20 (CCL20), α -chemokine 10 (CXCL10), and α -chemokine 12 (CXCL12) are released by reactive astrocytes in addition to cell adhesion molecules like vascular cell adhesion molecule, the neural cell adhesion molecule, and intercellular adhesion molecule (73). In relation to this, it has been hypothesized that reactive astrocytes may exhibit different polarization in neurodegenerative disorders (74).

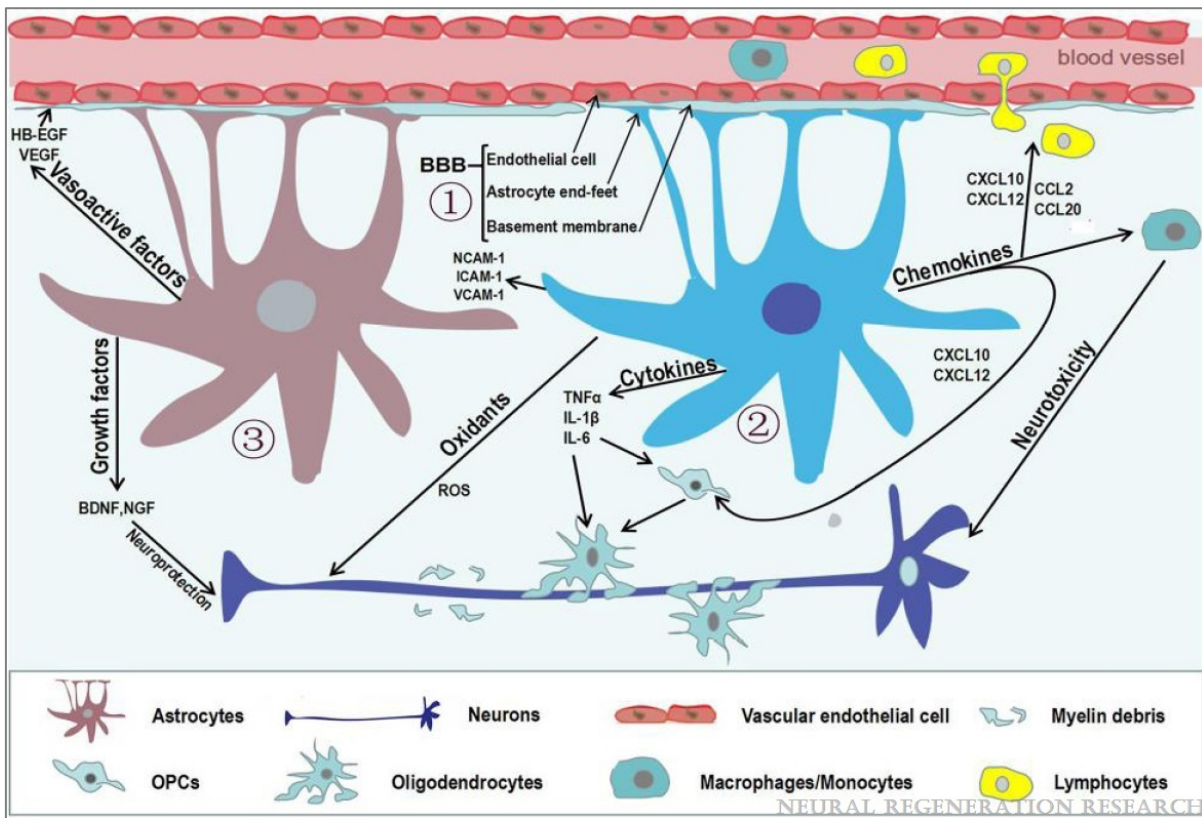


Figure 12: Reactive astrocytes in neurodegenerative diseases. Numerous stimuli, in particular cytokines released by several brain cell types, can activate astrocytes. Additionally, activated astrocytes can have an array of effects, positive as well as negative. 1) The BBB, which is created by the capillary endothelial cells, basement membrane, and end feet of astrocytes, preserves the homeostasis of the central nervous system. 2) BBB leaks occur when astrocyte end-feet are dysfunctional via a specific BMP signaling mechanism. The release of oxidants, cytokines, chemokines, and cell adhesion molecules is accelerated by reactive astrocytes, which can harm neurons, oligodendrocyte precursor cells, and oligodendrocytes directly or indirectly. (3) By controlling junction-related proteins, vasoactive substances released by activated astrocytes influence healthy endothelial cells, maintaining the BBB's integrity. Additionally, by secreting several growth factors, reactive astrocytes can encourage remyelination and neural regeneration (66).

More recent research reported that reactive astrocytes play a dual role in the pathophysiological processes that underlie neurodegenerative disorders (75, 76). Nevertheless, strategies to assess this potential are still lacking.

1.5.2 Progression of resting (A0) astrocytes to reactive (A1 and A2) astrocytes

Numerous studies have shed light on astrocyte polarization as well as the functions of transcription factors in regulating astrocyte activity in *in vitro* and animal models of NDs (66, 77, 78). Depending on their reactivity, reactive astrocytes may result in either negative or positive implications (Figure 13). Resting (A0) astrocytes are transformed into reactive forms by upregulating or downregulating

certain genes in the lipopolysaccharide-induced and middle cerebral artery blockage mice models of infection and stroke, respectively (79). Reactive astrocytes can be classified as A1 (neurotoxic) or A2 (neuroprotective) based on gene expression profiles (74).

Activated neuroinflammatory microglia are known to traditionally induce A1 astrocytes (74). According to studies, reactive microglia release C1q, TNF- α , and IL-1 α , contributing to the astrocytes' transition to an A1 phenotype (74). Numerous classical complement cascade genes significantly upregulate A1 astrocytes, which causes them to secrete well-known neurotoxins that cause neurotoxicity. In addition, A1 astrocytes can impair synaptogenesis, stimulate oligodendrocytes, and result in neuronal death (74).

A2 reactive astrocytes are called neuroprotective exhibiting neuroprotective astrocytic phenotype after the activation of microglia through traumatic brain injury (66). In the engrafted adult mouse brain, nuclear factor IA (NFIA), a molecular switch that produces human glial competency, enables astrocytes to change their activity towards neuroprotection (A2) (80). As a result, A2 astrocytes upregulate several neuroprotective factors that support synaptic repair, development, and survival of neurons (81); on the contrary, A1 astrocytes upregulate inflammatory markers (ROS, IL-1, TNF- α) (77). Protein prokineticin-2 (PK2), chitin-like 3, Frizzled class receptor 1, arginase 1, NF-E2-related factor 2 (Nrf2), pentraxin 3, sphingosine kinase 1, and transmembrane 4 L6 family member 1 are examples of protective mediators that are upregulated in A2 astrocytes (74).

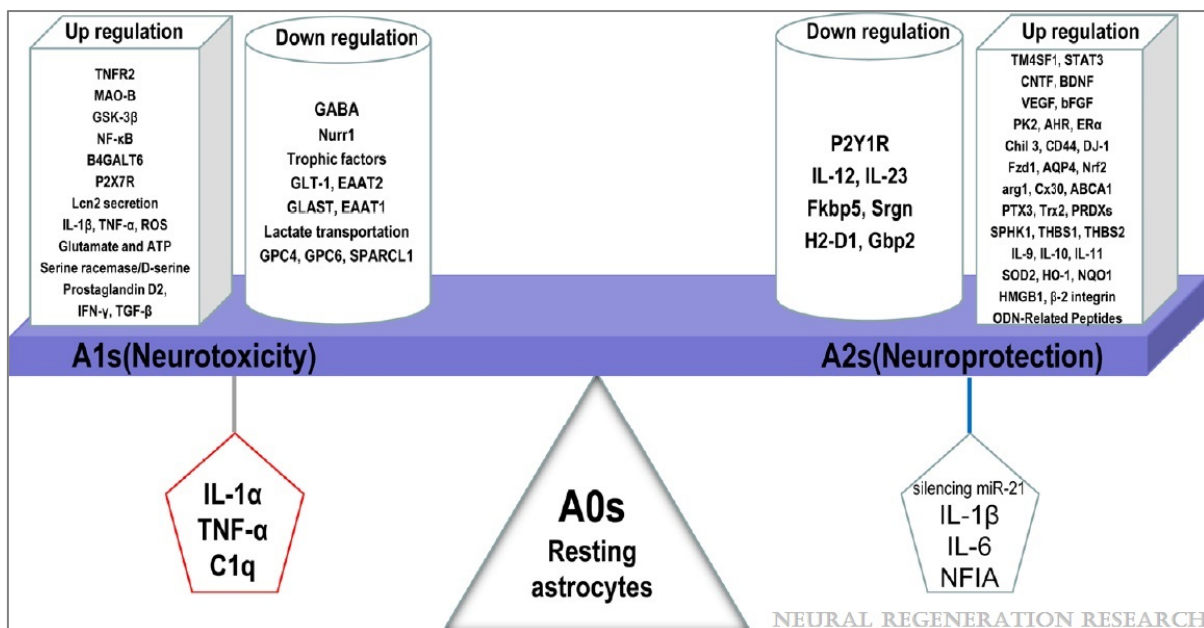


Figure 13: Neurotoxic and neuroprotective effect of reactive astrocytes stimulated through various mediators or upregulation and downregulation of different genes (66).

To date, the two polarization states of reactive astrocytes and their features are characterized. It has been suggested, however, that reactive astrocyte may also exist in forms other than A1 and A2, which are activated by other substances and undergo up- or down-regulation of other genes in response to disease. Additional study is required to verify and support the astrocyte switching notion (66).

1.5.3 Reactive astrocytes in NDs

In NDs, astrocytes can undergo significant changes in morphology, gene expression, function and then become a reactive state. For example, they can become hypertrophic, meaning they increase in size and complexity, and can form dense scar-like structures around the site of injury or disease. They can also upregulate the expression of a range of genes, including cytokines, chemokines, and growth factors, that contribute to neuroinflammation and neurodegeneration. It has been shown that astrocytes modulate neurotransmitter synthesis, ultimately regulating their release from the glial (82). Reactive astrocytes also control the release fates of metabolites (81), cytokines, chemokines, and neurotrophic factors (66). Moreover, reactive astrocytes can increase the rate of phagocytosis and produce or remove ROS in disease models (83). Activation of astrocytes can change the cellular functions (70).

Reactive astrocytes are a complex and dynamic cell type that plays a critical role in the pathogenesis of NDs. While they can contribute to neuronal damage and neuroinflammation, they also possess neuroprotective functions that may be harnessed for therapeutic intervention. Future research will likely focus on elucidating the precise mechanisms underlying reactive astrocyte activation in neurodegenerative diseases and developing novel therapies that target these cells for the treatment of these conditions.

Reactive astrocytes in this context release pro-inflammatory cytokines, such as interleukin-1 β and tumor necrosis factor-alpha, which can activate microglia and induce neuronal damage. Reactive astrocytes in Parkinson's disease are thought to play a role in the aggregation of alpha-synuclein protein, which forms toxic clumps called Lewy bodies that are found in affected brain regions.

Despite their negative effects on the CNS, reactive astrocytes can also play a protective role in neurodegenerative diseases. For example, they can release neurotrophic factors, such as glial-derived neurotrophic factor (GDNF) and brain-derived neurotrophic factor (BDNF), that promote neuronal survival and regeneration. Reactive astrocytes can also phagocytose and clear cellular debris and toxic proteins, such as beta-amyloid and alpha-synuclein.

Targeting reactive astrocytes for therapeutic intervention in neurodegenerative diseases is a complex and challenging task. Some researchers propose that targeting the pro-inflammatory cytokines produced by reactive astrocytes may reduce neuroinflammation and subsequent neuronal damage. Other researchers suggest that promoting the neuroprotective functions of reactive astrocytes, such as their ability to release neurotrophic factors, may be a more effective therapeutic approach.

1.5.3.1 Reactive Astrocytes in AD

In AD, reactive astrocytes play a critical role in the pathogenesis of the disease by contributing to neuroinflammation, neuronal damage, and the accumulation of beta-amyloid protein, a hallmark of the disease. Reactive astrocytes in AD become hypertrophic and form dense scar-like structures around the site of beta-amyloid deposition. They also upregulate the expression of a range of genes, including cytokines, chemokines, and growth factors, that contribute to neuroinflammation and neurodegeneration. In addition to promoting neuroinflammation, reactive astrocytes in AD also contribute to the accumulation of beta-amyloid protein. They can release proteins that increase the production of beta-amyloid and decrease its clearance, such as apolipoprotein E and insulin-like growth factor-1. Reactive astrocytes can also phagocytose beta-amyloid, but their capacity to clear it is limited, and they can contribute to its aggregation and toxicity.

During the progression of AD, astrocytes acquire toxic properties and lose their neuroprotective properties (22). Another report suggested that reactive astrocytes exhibit biphasic reactions (beneficial or detrimental) in AD. A1 astrocytes produce pro-inflammatory cytokines (TNF- α , IL-1, and IL-6) and surround amyloid plaques, causing AD pathogenesis and development (84). By controlling the expression of genes encoding extracellular matrix proteins that surround neurons, astrocytes have an impact on cognitive performance (85).

1.5.3.2 Reactive Astrocytes in PD

Reactive astrocytes were observed in animal models of PD, where they have a dual function in the onset of the disease (72). In PD mouse models, A1 reactive astrocytes release harmful substances that cause dopaminergic neuronal death. In mice that overexpress α -synuclein, the buildup of α -synuclein causes astrocytes to emit pro-inflammatory cytokines (TNF- α , IL-1, and IL-6) and chemokines (CCL2, CCL20, CXCL1, and CX3CL1).

Reactive astrocytes in PD respond to the accumulation of α -synuclein by becoming hypertrophic and releasing pro-inflammatory cytokines and chemokines. This results in neuroinflammation, which exacerbates neuronal damage and death. In addition, reactive astrocytes can release proteins, such as

apolipoprotein E and insulin-like growth factor-1, which increase the production of α -synuclein and decrease its clearance, thereby contributing to its accumulation.

Reactive astrocytes can also phagocytose and clear α -synuclein protein. However, their capacity to clear it is limited, and they can contribute to its aggregation and toxicity. Moreover, reactive astrocytes can release neurotrophic factors, such as GDNF and BDNF, which can promote neuronal survival and function. However, the capacity of reactive astrocytes to release neurotrophic factors is reduced in PD, likely due to the toxic effects of α -synuclein.

Overall, reactive astrocytes play a critical role in the pathogenesis of PD by contributing to neuroinflammation and neuronal damage through the accumulation of α -synuclein protein. Although reactive astrocytes can phagocytose and clear α -synuclein, their capacity to do so is limited, and they can contribute to its aggregation and toxicity.

1.5.3 Reactive Astrocytes in POLG-Related Disorders

Using our iPSC system, we showed recently that astrocytes from patients with mitochondrial disease caused by *POLG* mutations manifested clear cellular phenotypes (Figure 14) (86). These included: 1), loss of mitochondrial volume and membrane potential; 2), loss of both complex I and IV; 3) mtDNA depletion; 4) defective NAD⁺ metabolism. Interestingly, we found these astrocytes were toxic to the neurons in both in-direct co-culture systems and 3D spheroids (Figure 15).

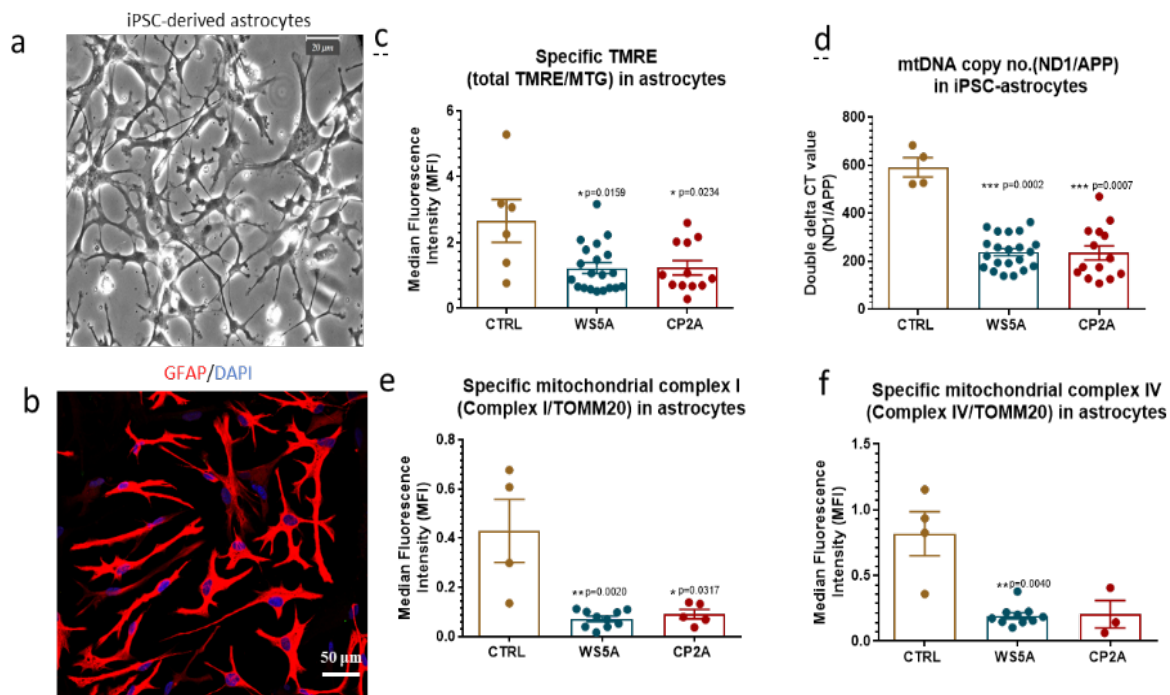


Figure 14: Mitochondrial dysfunction and mtDNA depletion in POLG-astrocytes derived from iPSCs. *a*, Phase-contrast images for iPSC-derived astrocytes; *b*, GFAP and DAPI staining in confocal microscopy; *c*, Lower specific mitochondrial membrane potential (MMP); *d*, mtDNA depletion; *e*, complex I deficiency; *e*, complex IV deficiency in POLG-astrocytes (ref. doi: <https://doi.org/10.1101/2020.12.20.423652>).

More interestingly, POLG-astrocytes displayed an abnormal reactivated-like phenotype with 1), increased cell proliferation and migration; 2), upregulated A1 reactive astrocyte-related gene expression; 3) C3 and GFAP double stained subtype; 4) neurotoxicity in DA neuron/astrocyte co-culture system. POLG-astrocytes also showed upregulation of the reactive marker alpha-SMA, GFAP and NESTIN (Figure 15), and lower A2-type related gene expressions (86). Interestingly, there was no change in *C1q* expression (Figure 15), a marker that defines microglial A1-astrocyte activation, suggesting the possibility of other pathways for activation and the possibility that there were more reactive subtypes (other than A1 and A2) induced by mitochondrial dysfunction.

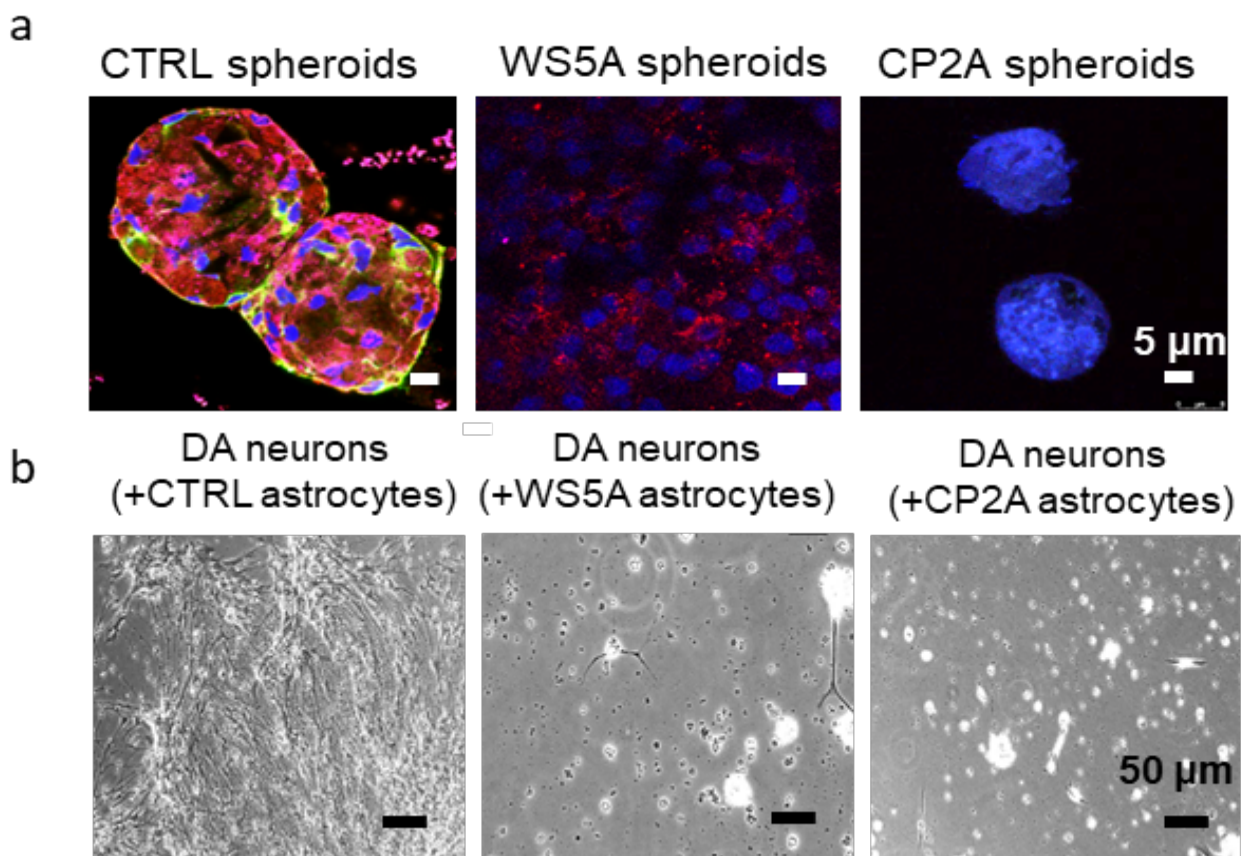


Figure 15: Neurotoxicity in in-vitro POLG samples. *a*, confocal images for staining of astrocyte marker GFAP (red), oligodendrocyte marker Galactosylceramidase/GALC (Pink) and neuron marker doublecortin/DCX (green) for one-month iPSC-derived spheroids, which is composed of neurons, astrocytes, and oligodendrocytes. Loss of both neurons and oligodendrocytes was observed in WS5A and CP2A organoids compared to control. *b*, phase-contrast images of the normal DA neurons after co-cultured with astrocytes for

15 days. Neural death was observed in WS5A and CP2A co-culture systems (Source from: Kristina Xiao Liang).

When we studied the changes in astrocytes *in vivo*, i.e., in the postmortem brain, we found an accumulation of GFAP⁺ reactive astrocytes in acute cortical lesions in POLG patients (Figure 16 c and d). However, we do not know which subtype of reactive astrocytes are found in POLG-related diseases and whether A1 reactive astrocytes result in a neural death/loss in POLG-related diseases.

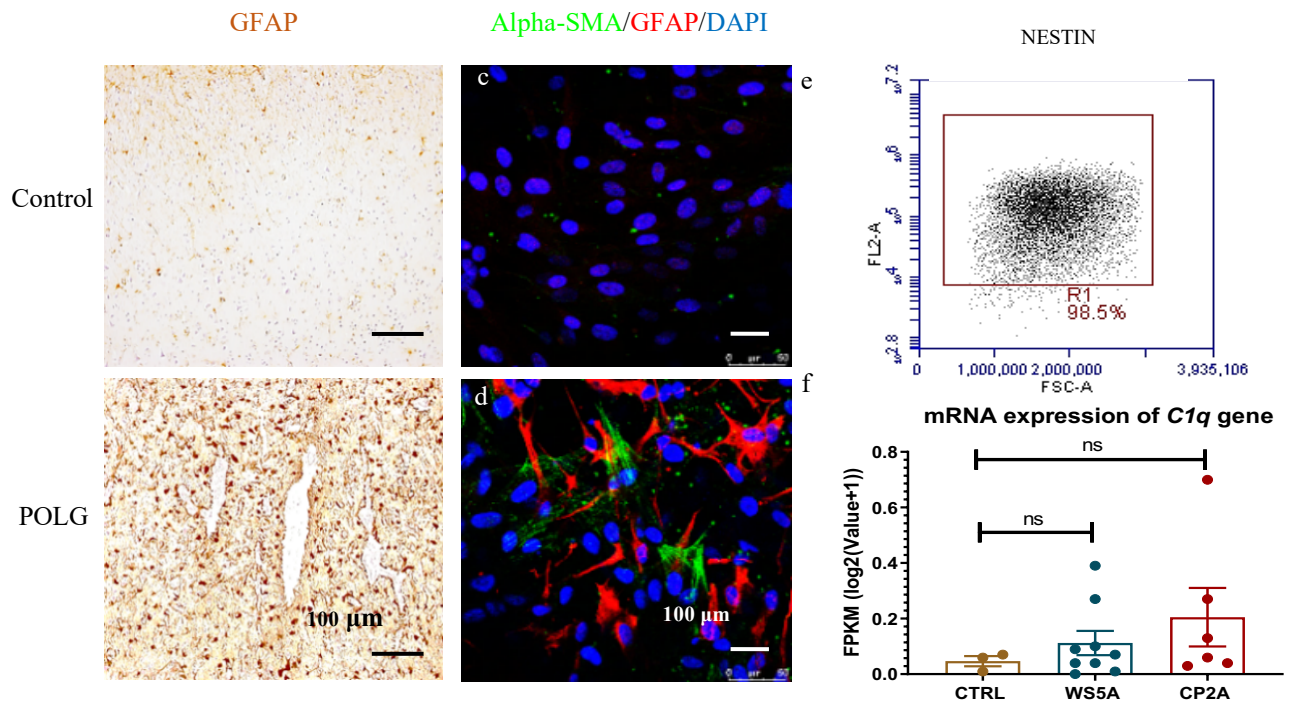


Figure 16: Reactive astrocyte markers in POLG samples. a & b. Immunostaining of GFAP in postmortem brain samples shows an accumulation of GFAP (brown) expression in the patient (b) than in healthy control (a). e & f. Confocal images of iPSC-derived astrocytes demonstrate an increased expression in reactive markers alpha-smooth muscle actin (alpha-SMA, green) and GFAP (red) in POLG astrocytes (d) compared to control lines (c). The nuclear is stained with DAPI (blue). e. Flow cytometry shows a positive expression of reactive astrocyte marker NESTIN in POLG astrocytes. f. The mRNA expression of A1-type gene C1q shows a trend of increased levels in POLG astrocytes, however, no statistical difference was detected (Source from: Kristina Xiao Liang).

CHAPTER 2: RATIONAL AND AIMS

2.1 Rational

While we (86, 87) and others (21) have shown that mitochondrial dysfunction is associated with astrocyte reactivation and neurotoxicity, several important research questions remain to be explored here, including 1), how many subtypes of reactive astrocytes induced by mitochondrial defect? Can they be identified and labelled? 2) What are the neurotoxic factors produced by these reactive astrocytes? How do they attack neurons? 3) Are there any compounds that can be used to reverse mitochondrial dysfunction to drive neuronal toxicity of reactive astrocytes?

The broader rationale can be stated as follows: *POLG* mutations induced mitochondrial dysfunction similar to that observed in other NDs such as PD. which lack accurately reflecting the pathogenesis of the disease in humans. Thus, we can use our mitochondrial models as a paradigm to interrogate the system to elucidate underlying disease mechanisms and further develop the potential therapies that will be useful both for mitochondrial disease and other ND such as PD.

2.2 Aim

The main aim of this study is to dissect the mechanism by which mitochondrial stress activates astrocytes to acquire neuron killing. We ask the following question – can we be sure? If so, which types of reactive astrocytes are involved in the neurodegenerative processes in *POLG*-associated diseases, and can we target these processes to enhance neuronal health/survival and thereby improve neurodegenerative processes in the patients?

The specific aims include:

Specific Aim 1

Use our in vitro iPSC system to define markers for reactive astrocyte subtypes induced by mitochondrial dysfunction.

Specific Aim 2

To identify neurotoxic factors produced by these mitochondrial stress-induced reactive astrocytes.

CHAPTER 3: MATERIALS AND METHOD

3.1 Equipment and Consumables

Table 3.1.1: Equipment

Name	Supplier
Centrifuge 5702	Eppendorf
Heracell™ VIOS 160i CO2 Incubator	Thermo Scientific™
Centrifuge 5810 R	Eppendorf
Pipette	Thermo Fisher Scientific
Pipette Controller	Thermo Fisher Scientific
Countess II	Invitrogen
ChemiDoc™ XRS+ System with Image Lab™	Bio-Rad
Rocking platform shaker	VWR
Vortex mixer	Thermo Fisher Scientific
My Spin 12 mini centrifuge	Thermo Fisher Scientific
Mars Pro biological safety cabinet	Labogene
Light Microscope	Leica
SP8 Confocal Microscope	Leica
BD LSRFortessa™ flow cytometer	BD Bioscience

Table 3.1.2: Software

Name	Suppliers
ImageJ Processing and Analysis	National Institute of Health (NIH)

The ChemiDoc XRS+ Imaging Software.	Bitplane
Flowjo software	BD Bioscience
LAS X microscope software	Leica
GraphPad Prism (version 8.0)	GraphPad

Table 3.1.3: Consumables

Name	Supplier
Nunc™ Cell-Culture Multidishes	Thermo Fisher Scientific
Microscope Slides	Thermo Fisher Scientific
Cryotube Vials	Thermo Fisher Scientific
Falcon tube (15ml and 50ml)	Globe Scientific
Pipette Tips (10ul,20ul,200ul,1000ul, 5ml)	Thermo Fisher Scientific
Countess™ cell counting chamber slides	Thermo Fisher Scientific
Pipette (5ml,10ml,25ml)	Thermo Fisher Scientific
Aspirator	Thermo Fisher Scientific
ProLong™ Gold Antifade Mountant	Invitrogen
FACS Tube	Thermo Fisher Scientific
Eppendorf (1.5ml, 2ml)	Thermo Fisher Scientific
Parafilm	Thermo Fisher Scientific
Human Cytokines array kit	R&D system
PAP Pen Liquid Blocker-Super	Fisher Scientific
Triton X-100	Sigma Aldrich

Normal Goat serum	Invitrogen
Bovine Serum Albumin (BSA)	Sigma Aldrich (A7906)

3.2 Chemical Reagent

Table 3.2.1: Cell culture reagents

Cell Culture Reagent	Supplier	Catalogue number
AGM™ Astrocyte Growth Medium BulletKit™	Lonza	CC-3186
Fetal Bovine Serum	Gibco	10439024
Penicillin/streptomycin	Sigma Aldrich	P4333
BDNF	PeptoTech	450-02
GDNF	PeptoTech	450-10
Essential 8 media	ThermoFisher	A1517001
Geltrex, LDEV-Free Reduced Growth Factor Basement Membrane Matrix	Invitrogen	A1413302
Y-27632 dihydrochloride Rock Inhibitor	Tocris Bioscience	1254
Essential 8 Basal Medium (DMEM/F12 (HAM) (1:1)	Thermo Fisher Scientific	A151669-01
Dulbecco's Phosphate Buffered Saline (DPBS - /- 1x)	Thermo Fisher Scientific	14190-144
Advanced DMEM / F12 (1x) Reduced Serum Medium	Thermo Fisher Scientific	12634-010
TrypLE™	Gibco	12604
16% Formaldehyde	Thermo Fisher Scientific	28908
Dimethyl Sulfoxide (DMSO)	Thermo Fisher Scientific	D12345

Table 3.2.2: Neural stem cell medium

Reagent	Supplier	Catalogue number
Knockout DMEM/F12	Invitrogen	12634-010
StemPro neural supplement	Thermo Fisher Scientific	A1050801
bEGF	R&D system	236-EG
bFGF	R&D system	423-F8
GlutaMax	Thermo Fisher Scientific	10565018

Table 3.2.3: DA neuron differentiation reagents

Reagent	Supplier	Catalogue number
IMDM	Invitrogen	21980-32
F12	Invitrogen	31765-027
BSA fraction V	Europa bioproducts ITD	62-1000
Lipid 100X	Invitrogen	11905-031
Monothioglycerol	Sigma Aldrich	M6145
Insulin 10mg/ml	Roche	1376497
Transferrin	Roche	652202
Purmorphine (PM)	PM	483367-10-8
Brain-derived neurotrophic factor (BDNF)	PeproTech	450-02
Glial cell derived neurotrophic factor (GDNF)	PeproTech	450-10
FGF	R&D system	423-F8
Poly-L-Ornithine	Sigma Aldrich	P4957
Laminin	Sigma Aldrich	L2020

3.3 iPSC Cell Culture and Differentiation

3.3.1 Ethical Consideration

The project was approved by the Western Norway Committee for Ethics in Health Research (REK nr. 2012/919). Tissues were acquired with written informed consent from all patients, and the experiments conformed to the principles set out in the WMA Declaration of Helsinki and the Department of Health and Human Services Belmont Report.

3.3.2 Generation of iPSCs

The iPSC lines were generated from the fibroblasts of the POLG patients carrying the homozygous mutation c.2243 G > C, p.W748S/W748S (WS5A). The iPSCs generated from human normal fibroblasts Detroit 551 (ATCC® CCL 110™), CCD-1079Sk (ATCC® CRL-2097™), and AG05836 (RRID: CVCL2B58) were used as controls.

All the iPSC cell lines used in this study were generated by Dr. Gareth Sullivan's group at the University of Oslo. The Detroit 551, CCD-1079Sk iPSCs, and patient iPSCs were reprogrammed using retroviral vectors encoding POU5F1, SOX2, Klf4, and c Myc and AG05836 control fibroblasts were reprogrammed by Sendai virus vectors.

Normal karyotype and expression of pluripotent stem cell lineage markers were confirmed for all iPSC lines as previously described (58). All cells were routinely monitored for mycoplasma contamination using the MycoAlert™ Mycoplasma Detection Kit.

3.3.3 Maintenance of iPSCs

They were maintained at 37 °C and 5% CO² in a humidified incubator. All iPSCs were cultured in feeder-free condition on a 6-well plate coated with Geltrex solution and kept with 3 ml E8 medium. The medium was changed daily. When the cells reached 70% confluency, the cells were split with a split ratio of 1:2. For passaging, the medium was aspirated and washed once with DPBS -/- (without calcium and magnesium). Then, 1 ml of 50 mM EDTA solution was added and incubated for 5-9 min. The EDTA was further removed and the fresh E8 medium was added into the wells. The cell suspensions were then transferred to a new Geltrex-coated well. The plate was gently Shaked horizontally and vertically to evenly distribute the cell colonies, and then placed in the incubator. All the cell culture procedures were carried out in a laminar flow hood under sterile conditions. All the materials are listed in Tables 1, 3.

3.3.4 Thawing and Freezing of iPSCs.

Thawing medium was prepared using E8 medium and 10uM Rock inhibitor (Y-27632), which enhances cell survival by preventing dissociation-induced apoptosis). Once the frozen cells were partially thawed in a 37 °C water bath with a small piece of ice remaining, 1ml of the prepared medium was gently added dropwise. A total of 6ml of the thawing medium was added into each Geltrex-coated well and the thawed cells from vials were then transferred to the well while stirring carefully. The plate was placed in the incubator and the medium was changed into E8 complete medium without ROCK inhibitor the next day.

For freezing iPSCs, the freezing medium was priorly prepared using E8 medium, 10% DMSO and 2%(v/v) ROCK inhibitor and kept at 4 °C. The cells were detached following the same steps for passaging as previously above. A total of 1ml of cell suspension in the freezing medium was gently transferred to a cryovial and placed in a cool cell freezing container (which lowers the temperature by 1 °C per min) overnight at -80 °C and then transferred to liquid nitrogen for long storage.

Table 3.3.4: Recipe for thawing and freezing medium

Geltrex medium	Coating	Culture Medium	Thawing Medium	Freezing Medium
Geltrex solution, 1:100 in DMEM (1% final concentration)	Advanced (1% final concentration)	E8 complete medium. Dissociation agent (1 ml EDTA solution (0.5 mM EDTA in DPBS -/-)	For one vial, 6 ml of E8 medium with 12 µl of Y-27632 ROCK inhibitor (10 µM Final concentration)	E8 medium + 10% DMSO + 2% 10µM of Y-27632 ROCK inhibitor.

3.3.5 Astrocyte Differentiation

Our lab had previously differentiated the astrocytes from iPSCs-derived neural stem cells (NSCs). NSC was generated via neural induction from iPSCs as described in the previous paper (88). To generate the astrocytes, the NSCs were plated on poly-d-lysine (PDL) - coated coverslip in a neural stem cell culture medium. Next day, the cells were then washed with DPBS -/- and culture in an astrocyte differentiation medium composed of DMEM/F12 supplemented with GlutaMAX, 1XN2, 1XB27, 200 ng/ml insulin-like growth factor I (IGF-I), 10 ng/ml heregulin 1β. For the first week, the medium was switched every other day, every two days for the second week, and every three days for the third and fourth weeks.

Following a 28-day differentiation period, the cells were cultured for one month more in maturation medium AGM™ Astrocyte Growth Medium BulletKit™ (Lonza, cat. # CC3186), which contains Astrocyte Basal Medium supplemented with ascorbic acid, rhEGF, Gentamicin Sulfate/Amphotericin (GA1000), insulin, l-glutamine, and FBS. After passage 4, the differentiated astrocytes were frozen down for further investigation.

3.3.6 Culturing and Passaging of Astrocytes

Astrocytes are cultured using AGM™ Astrocyte Growth Medium. The medium was changed every two days. At approximately 80% confluency, the cells were split 1:2 into new six well plates. The old medium was aspirated from the cells and washed once with DPBS -/- (without calcium and magnesium). Cells are then detached using TrypLE™ (1 ml/well) for 5-9 min in the incubator at 37°C. The neutralization medium was then added to the wells and the cell suspensions were transferred into a 15 ml falcon tube. The cells were centrifuged at 300 x g for 5 min at RT. The supernatant was aspirated, and cell pellets were resuspended gently to form a single-cell suspension. The cells were then plated into a new 6 wells plate with 3 ml of the culture medium per well. The plates were then gently shaken horizontally and vertically to evenly distribute the cells and placed in the incubator.

3.3.7 Thawing and freezing

For thawing the astrocyte cells, the astrocyte growth medium was warmed to RT. The frozen vial of cells was partially thawed at 37 °C water bath until a small piece of ice remained. 2 ml of DPBS -/- was added to a 15 ml falcon tube and then thawed cells are transferred into it. The tube was spun at 300 x g for 5 min at RT. The supernatant was discarded, and cell pellets are resuspended and seeded in a 6-well plate with 3 ml of astrocyte medium per well in the incubator.

For freezing and storage, the astrocyte freezing medium was prepared using an ice-cold astrocyte culture medium supplemented with 10% DMSO. The cell pellets were collected as described above and then resuspended in 1ml of ice-cold freezing medium and then transferred into a cryotube. The cryotube was placed at 20°C overnight and then transferred to -80°C overnight before kept in liquid nitrogen.

Table 3.3.7: Recipe for thawing and freezing medium

Astrocyte Culture Medium	Neutralization medium	Freezing Medium
AGM™ Astrocyte Growth Medium which contains Astrocyte Basal Medium supplemented with ascorbic acid, rhEGF, Gentamicin Sulfate/Amphotericin (GA-1000), insulin, l-glutamine, and FBS	AGM™ Astrocyte Growth Medium, 10% FBS	AGM™ Astrocyte Growth Medium, 10% DMSO

3.3.8 Differentiation of DA Neurons from iPSCs

Since DA neurons cannot be stored and propagated like astrocytes due to their post-mitotic phase. DA neurons were differentiated from the iPSC stage. when the iPSCs culture plate reached 60% confluency with good size and colonies in full 6-well plates. The E8 medium was aspirated and washed with DPBS -/- before the addition of 3 ml of Neural Induction Medium (NIM) to each well. NIM was changed on day 1, day 3, and day 4. On day 5, neural rosettes were detached into suspension culture. The induction medium was aspirated, and the cells were washed once with DPBS -/-. 1 ml collagenase IV (Invitrogen, cat. # 17104-019) was added per well and incubated for 1 min, then aspirated and washed carefully with DPBS -/-. followed by the addition of 2 ml NSC medium per well. To generate neural spheres, an even grid pattern was made by manually scraping using a 10 µl pipette tip. The cells were collected with the 12 ml NSC medium and then transferred to suspension dishes. The cells were kept on an orbital shaker at 65 rpm. On days 6 and 8, the medium was changed into fresh NSC medium. The medium was changed by transferring the cell suspensions into falcon tubes, and after 10-15 min when the spheres had precipitated at the bottom of the tube the medium up to 1 cm above the spheres was aspirated. 12 ml NSC medium was added to new suspension dishes, in which the spheres were transferred. On day 9, the medium was changed to CDM supplemented with 100 ng/ml FGF-8b (R&D systems, cat. # 423-F8). This was repeated the day after and then every other day until day 16. Whenever the spheres increased in size above 200 µm in diameter, they were triturated by repeated pipetting (about 10-15 times depending on the size), at the step before transferring them into new dishes when changing the medium. On day 17, the medium was changed, and the medium was changed into the CDM supplemented with 1 µM purmorphamine (PM) and 100

ng/ml FGF-8b. The medium was then changed next day and every other day for 7 days. At day 25, the spheres were terminated as described below.

Table 3.3.8: Recipe for DA differentiation medium

Medium	Composition
NSC (500ml)	485 ml Knockout DMEM, 10ml stempro neural supplement (2%), 20 ng/ml bFGF, 20 ng/ml bEGF, 5ml Glutamax (1%)
CDM (500ml)	250ml IMDM (50%), 250ml F12 (50%), 2.5g BSA fraction V (5 mg/ml), 5ml lipid 100X (1%), 20ul monothioglycerol (450 µM), 350µl Insulin (7 ug/ml), 258, 3µl Transferin (15 mg/ml).

Seeding of DA Precursors

Termination of the neurospheres was performed by dissociating the spheres into single cells and plating them in a monolayer. Falcon tubes (15 ml) were used to collect the spheres from the suspension dishes, and the spheres were precipitated for 10-15 min at RT. The suspensions were carefully aspirated, and 2 ml TrypLE™ was added to each tube and kept in a 37 °C water bath for 10 min. After 10 min, the spheres were carefully pipetted a few times to make a single-cell suspension. Pre-warmed neutralisation medium (DMEM + 10% FBS) was added and centrifugated at 400 x g for 5 min. The supernatant was aspirated, and the cells were seeded into DA medium (CDM supplemented with 10 ng/ml BDNF and 10 ng/ml GDNF) in the 6-well plate coated with Poly-L-Ornithine and laminin.

Maintenance of DA Neurons

DA neurons were fed with DA medium on the third day after seeding and then refreshed every 2-7 days depending on the density of the cells when the medium turns yellow. hat attached to the plate, most commonly every 5th day. As a rule, the medium was changed when it started to turn yellow, but never less often than every 10 days even if the medium did not turn yellow. The medium was changed carefully by leaving a small amount of medium and then gently adding the new medium to prevent the neurons from detaching. The neurons were split using TrypLE™ and re-seeded into new coated plates at a lower density. After 3 weeks of maturation, the DA neurons were collected and used for co-culture.

3.3.9 Cortical Organoid Generation

Cortical organoids were generated from iPSCs using the previously described protocol (89). Briefly, the iPSCs were fed daily with E8 medium for at least 3 days before differentiation. The iPSCs were dissociated using Accutase (Life Technologies) for 10 min at 37 °C and centrifuged for 3 min at 300 × g. The single cells were diluted in neural induction medium, and then a total of 9,000 viable cells were seeded into 150 µl NIM in 96-well ultra-low attachment tissue culture plates (Thermo Fisher Scientific) and kept in suspension for 24 h under rotation (85 rpm). The 50 µM ROCK inhibitor was added to form embryoid bodies (EBs). On day 2, half of the media was replaced by human neural induction media in the presence of 50 µM ROCK inhibitor to each well. On days 4, 6, and 8, 100 µl medium was placed with 150 µl neural induction without ROCK inhibitor. After 10 days, the organoids were transferred into a 6-well ultra-low attachment tissue culture plate (Life Sciences) in neural differentiation media minus vitamin A and brain organoids were induced for the next 8 days using an orbital shaker. At day 18, organoids were then matured in neural differentiation medium (NDM) containing vitamin A, with medium changes every 3-4 days. BDNF and ascorbic acid were supplemented to facilitate long-term neural maturation.

3.4 Nicotinamide Riboside (NR) Treatment

NR was kindly provided by Evandro Fei Fang, University of Oslo, Norway. One-month-old organoids were treated with 1 mM NR. NR was added to the medium and replaced every day for one month.

3.5 Immunofluorescence

Immunostaining

To stain the astrocytes and neurons, the cells were seeded on 12 mm glass sterile coverslips placed into 6 well plates. The coverslips and well were coated with Poly-L-Ornithine and laminin as previously described (58, 90). When the cell reached the confluence of 70%, the coverslips were transferred to 12 wells plates. The cells were then washed with DPBS -/- and fixed in 4% (v/v) paraformaldehyde (PFA) in phosphate-buffered saline (PBS) for 10 min at RT. PFA was then aspirated and cells are gently washed 3 times with PBS. Fixed cells were incubated with blocking buffer (10% (v/v) normal goat serum, 0.3% (v/v) Triton X-100, in PBS) for 1hr at RT before incubation at 4°C with primary antibodies (Table X) diluted in blocking buffer. Following overnight incubation, cells are rinsed with PBS three times. Secondary antibodies solution was then added to the coverslip for 1hr at RT in the humid and dark chamber. Antibodies are aspirated and quickly

rinsed with PBS the next day. Subsequently, the coverslips were mounted on a microscope slide using a 10-15 μ l ProLong diamond antifade mounting medium (Life Technologies).

For cortical organoids, the organoids were collected from the medium using a 1000 μ L pipette to place gently on a medium with the minimal medium on a standard microscope slide and allowed to dry completely at RT. The organoids were then fixed with 4% PFA for 30 min at RT and then incubated in 30% sucrose solution to slide overnight at 4 °C. The organoids were then blocked and permeabilized with a blocking buffer containing PBS, 0.3% Triton X-100, and 10% normal goat serum for 2 h at room temperature. Then the primary antibody in the blocking buffer was added overnight at 4 °C following the washing of PBS for 3 hours with two to three buffer changes on a gentle rocking platform. The samples were then incubated in the secondary antibody (1:800 in blocking buffer) solution overnight at 4 °C. Hoechst 33342 (1:5000) nuclear stains were added at the same time. Next, the organoids were rinsed quickly with PBS, then incubated in PBS containing 0.01% NaAzide for 1-2 days at 4°C to prevent contamination. After aspirating PBS and removing the excess, the organoids were mounted using a ProLong diamond antifade mounting medium (Life Technologies). The details of the antibodies used were listed in *Table 3.5.1. and Table 3.5.2.*

Table 3.5.1: The primary antibodies used for both 2D astrocyte and 3D brain organoid staining

Primary antibody	Host	Dilution (μ l)	Catalog number
GFAP	Chicken	1:500	AB4674
C3	Rat	1:100	AB181147
SERPING1/ anti C1	Rabbit	1:100	12259-1-AP
S100A10 (Conjugated)	Mouse	1:100	CL488-66227
SCG2	Rabbit	1:100	20357-1-AP
GFAP	Mouse	1:100	AB279289

Table 3.5.2: The secondary antibodies used for both 2D astrocyte and 3D brain organoid staining

Secondary antibody	Dilution (μl)	Catalog number
Alexa Fluor goat anti-chicken IgG 594	1:800	A211449
Alexa Fluor goat anti-rabbit IgG 647	1:800	A11037
Alexa Fluor goat anti-mouse IgG 488	1:800	A11032
Alexa Fluor goat anti-rat IgG 488	1:800	A11034
Nuclear Staining (Hoechst)	1:5000	62249

Imaging Acquisition and Analysis

The images were acquired using the Leica TCS SP8 confocal microscope (Leica Microsystems) or Dragonfly Confocal Microscope (Andor). The system is equipped with an inverted and automated microscope with a motorized XY-stage, four spectrally unmixed lasers (405 nm, 488 nm, 561 nm and 647 nm), six objectives (air and oil) and the Leica LAS AX version 3.5.5 software. Astrocyte and DA neurons were detected using a water 40x objective. Microscope and laser settings were kept constant throughout each experiment. The resonant scanning mode was selected as this enabled fast scanning at high resolution (512x512 frames).

Image analysis and fluorescent signal quantification were performed with ImageJ software. For all the staining, the mean fluorescent intensity of each representative field was calculated and compared between groups. For each sample, more than 5 random areas were recorded for quantification.

3.6 Flow cytometry

Cell Preparation for Fixation

The cells were detached with TrypLE™ for 5 min incubation at 37°C. The neutralization medium was then added, and then cells were collected into a 15 ml falcon tube and centrifuged at 400 x g for 5 min. The supernatant was aspirated, and the cells are washed again with 10ml of DPBS -/- and centrifuged at 400 x g for 5 min. To fix the cells, 1.5 ml of 1.6 % PFA was then added to the cell pellet and incubated in RT for 10 min. Following the incubation, cells are washed with DPBS -/- and

centrifuged. The cells were resuspended in 1 ml of flow buffer containing 1X PBS and 0.2% BSA. Then fixed cells were stored at 4 °C before staining.

Staining

The fixed cells were then permeabilized with -20 °C methanol (90%). 1 ml of ice-cold methanol was gently added dropwise to the cells and resuspended to the single cells at -20 °C for 20 min, followed by adding 10 ml of flow buffer (PBS with 1% (v/v) BSA) and centrifugation at 400 x g for 5 min. After the supernatant was removed, the cells were resuspended in 1 ml of blocking buffer (10% (v/v) normal goat serum, 0.3% (v/v) Triton X-100, in PBS) and incubated in RT for 30 min. cells are washed with flow buffer and centrifuged again. The antibodies solution was added and incubated for 30 min at 4°C in the dark. After incubation, the cells were washed once with flow buffer and centrifuged. The unstained sample was used for negative control and the bead with single staining was set up for compensation control. The supernatants were aspirated, and the cell pellets were resuspended in 200 µl flow buffer. The samples were kept in the dark until acquisition at a flow cytometer, which was performed the same day.

Table 3.6: Antibodies used for flow cytometry

Antibody	Dilution (µl)	Filter	Catalog number
GFAP conjugated with Alexa 594	1:50	PE-Texas Red	SC-33673 AF594
S100A10 conjugated with Alexa 647	1:50	APC	SC-81153 AF 647
TFAM conjugated with Alexa 488	1:200	FITC	AB119684
NDUFB10(complex1) conjugated with Alexa 405	1:100	BV421	NBP2-72915 AF405
VDAC conjugated with Alexa 647	1:50	APC	SC-390996 AF647
COX1V PE	1:50	PE	SC-376731 PE

Gating Strategy and Data Analysis

BD LSRFortessa™ flow cytometer equipped with Fours lasers: 407 nm, 488 nm, 561nm, and 640 nm was used to acquire the flow cytometry measurements. The voltage gating for samples was optimized and kept the same throughout the experiment. Flow cytometry data were analyzed using FlowJo V10.8.1. The first step was identifying and gating the main population of cells. The main population was located and gated as shown in (Figure 16a). Within the main population gate, FSC-A versus FSC-H and SSC-A versus SSC-H plots were viewed to exclude as doublets (Figures 16b and 16c). The gating of the main population was created based on the unstained negative control while viewing SSC-A and Chanel (BV421, FITC, PE, PE-Texas Red and APC). The gating strategy was applied to the stained cell samples. More than 10 000 cells were then recorded. For quantification, the median fluorescent intensity (MFI) was then calculated, and the MFI of the negative control populations was subtracted.

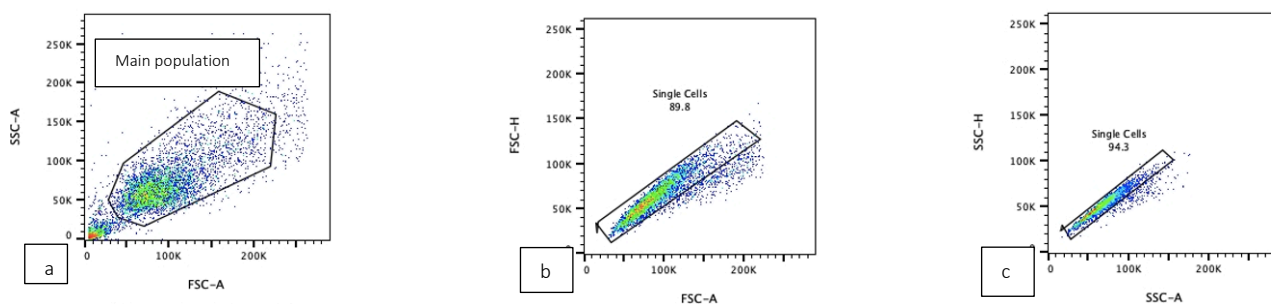


Figure 17: Flow cytometry gating strategy: Plot a) shows the gating of the main population in the cell. b) and c) show the gating of single cells for FSC-H versus FCS-A and SSC-H versus SCS-A.

3.7 Indirect Astrocyte Neuron Co-Culture System

Astrocytes (normal or diseased) and DA neurons (normal or diseased) were co-cultured in separate compartments of use trans well plates (Figure 17) with 24 mm inserts and polyester membrane with 0.4 um pore size and the astrocytes and neurons were indirect co-culture plates and communicate only through paracrine signals from membrane pores. DA neurons and astrocytes were collected as previously described methods and the cell viability was examined before co-culture. A total of 50,000 astrocytes were then seeded in the insert of the transwell with 1 ml astrocyte growth medium. DA neurons were seeded in poly-L-ornithine and laminin-coated wells (bottom chambers) in 2 ml of CDM medium supplemented with BDNF and GDNF. The co-culture medium was changed every two days, and the medium from the indirect co-culture was harvested on day 10 for human proteome cytokine array analysis. Both astrocytes and DA neuronal cells were harvested and fixed for flow cytometry analysis.

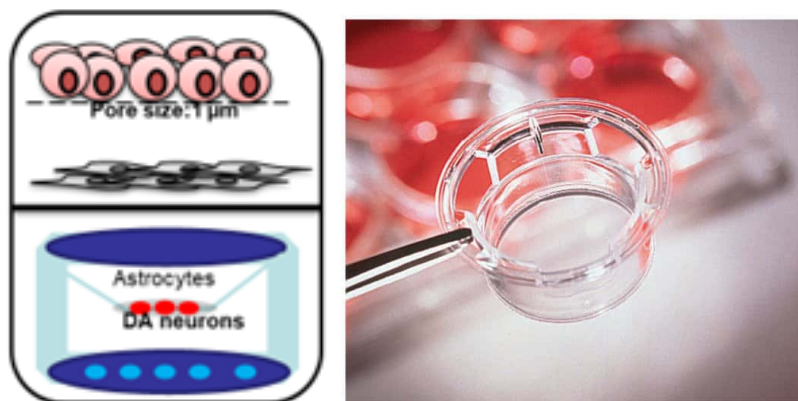


Figure 18: Illustration of the transwell plates.

3.8 Human Cytokines Array

The human cytokines productions were measured using human cytokine proteome profiler arrays (ARY005; R&D System) following the manufacturer's instructions. Supernatants were taken from the collected medium from the indirect coculture. The membranes were blocked with the blocking buffer for 1 h at RT) on a shaker. After removing the blocking buffer, the sample buffer containing the sample lysate in the membranes was added and incubated for 2 h at RT on a shaker. The sample buffer was then removed, and the membranes were washed three times with wash buffer. The detection antibody cocktail with samples was then incubated for 1 h at RT on a shaker. The detection antibody cocktail was then removed, and the membranes were washed three times with a wash buffer. The Streptavidin-HRP was added to membranes and incubated for 30 min at RT on a shaker. Once the Streptavidin-HRP was removed, the membranes were washed thrice with wash buffer. Chemiluminescent detection reagents were added, and the membranes were exposed to Chemi Doc XRS+ Gel Imaging System to visualize the signals. Image Lab™ Software was used for data analysis.

3.9 Statistical analysis

Data were presented as mean \pm standard deviation (SD) for the number of samples ($n \geq 3$). Distributions were tested for normality using the Shapiro-Wilk test. Outliers were detected using the ROUT method. The Mann-Whitney U-test was used to assess statistical significance for variables with non-normal distribution, while a two-sided Student's t-test was applied for normally distributed variables. Data were analyzed and figures were produced with GraphPad Prism 8.0.2 software (GraphPad Software, Inc). $P \leq 0.05$ was considered significant.

CHAPTER 4: RESULT

4.1 POLG Patient Astrocytes Exhibited Lower Levels of A2 markers compared to Controls.

Our previous study showed the astrocytes derived from POLG patient iPSCs were toxic to neurons which may be caused by the reactive phenotype (87) with increased reactive marker glial fibrillary acidic protein (GFAP) and nestin (91). In this project, we aimed to further identify the subtypes of the reactive astrocytes induced by mitochondrial stress. We performed the immunofluorescence staining approach with staining of the known A1 marker, complement component 3 (C3) which is known to be upregulated in the course of NDs and expressed by microglial cells and Plasma protease C1 inhibitor (SERPING1) which interferes with C3 and CFB by physical binding, influencing the alternate complement activation (92). Two known A2 markers were also included: one is S100 Calcium Binding Protein A10 (S100A10) which has the physiological function of modulating cell proliferation, membrane repair, and inhibition of cell apoptosis and another one was Secretogranin II (SCG2) that involves packaging and sorting of neuropeptide into secretory vesicles (93).

We used 3 individual clones from WS5A iPSCs (homozygous c2243G>C, p.W748S) compared to 4 controls (Detroit 551: fetal female fibroblast; AG05836: 44 yr. old female fibroblast). By using immunostaining, we observed higher expressions of C3, but a lower level of C1 in the patient astrocytes as compared to the controls, although the data is not statistically significant this may partly be due to the small sample size (Figure 19). Regarding the A2 markers, we identified the significantly lower expression of S100A10, however, the level of SCG2 was similar in patient astrocytes compared to the control (Figure 20). In addition, we used GFAP as a classical marker for astrocytes in the central nervous system, to confirm the astrocyte lineage and stander reactive astrocyte maker. We found an increased GFAP expression in patient astrocytes compared to controls. although the difference did not reach significance (Figure 20).

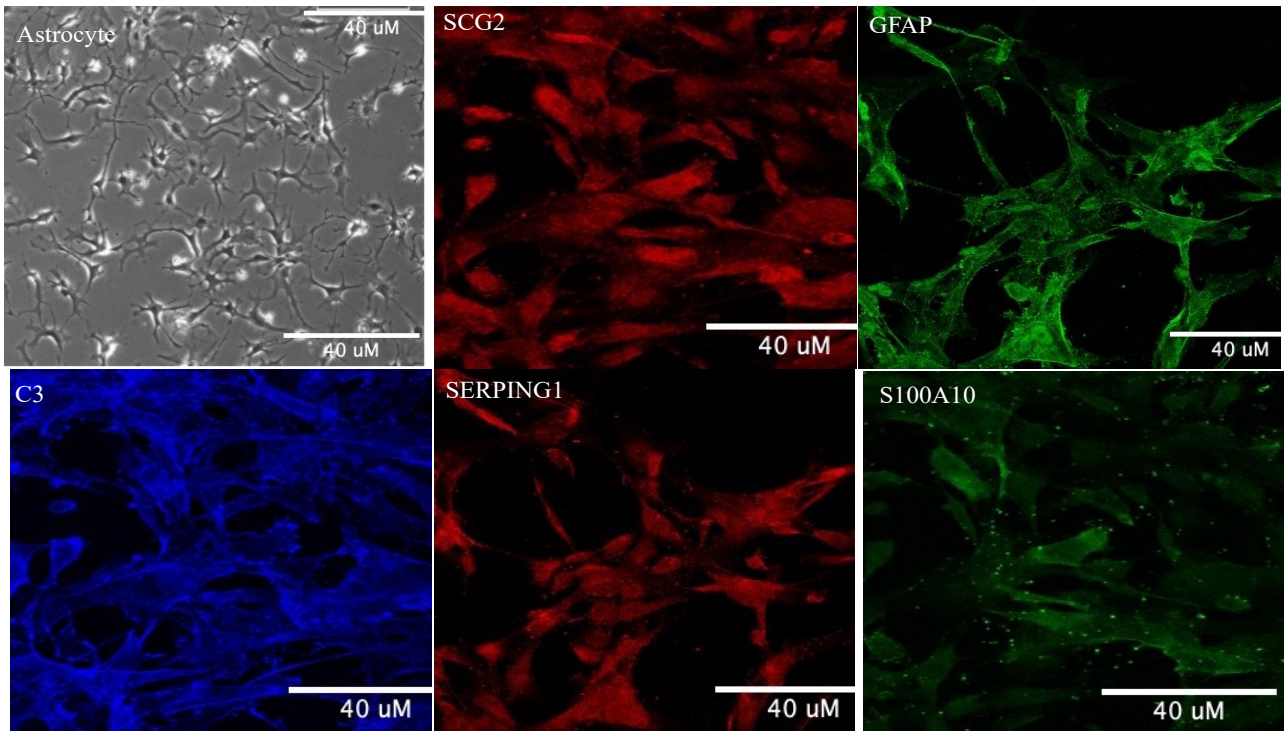


Figure 19: Panel of reactive astrocyte markers expression in 2D astrocyte: representative images for the expression of GFAP, A1 marker: C3 and SERPING1 and A2 markers: S100A10 and SCG2 in astrocytes derived from iPSCs. The scale bar is 40 μm.

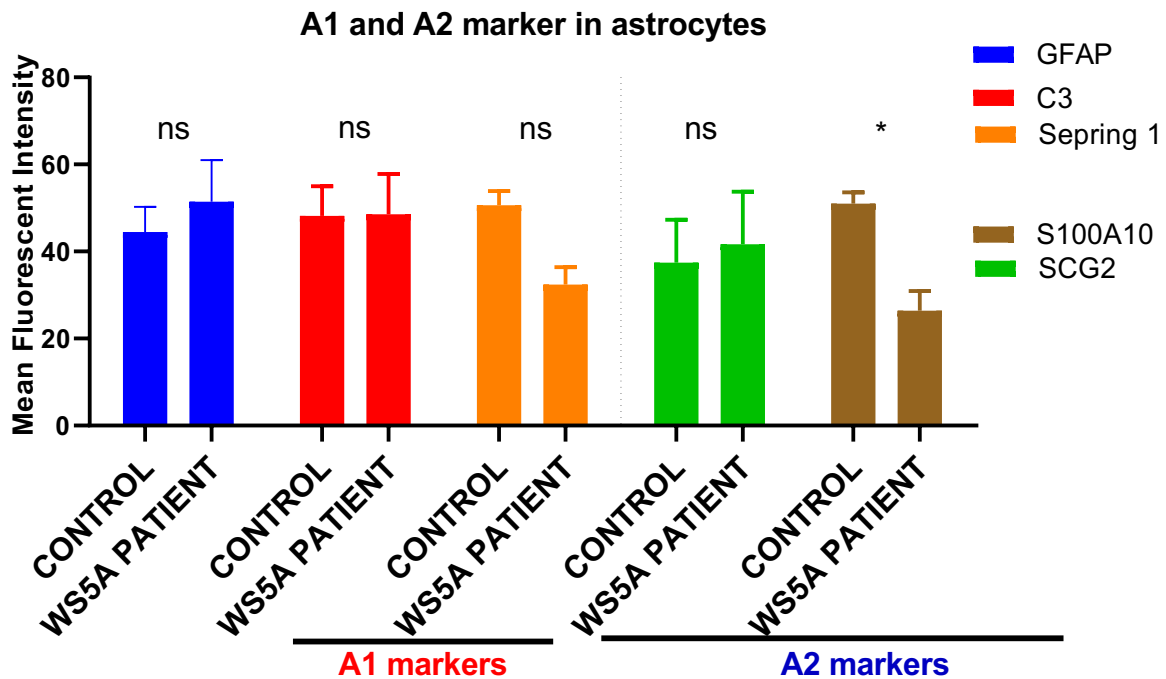


Figure 20: Mean fluorescence intensity (MFI) of A1 and A2 markers: The MFI of GFAP, A1 markers and A2 markers in the WS5A patient line was compared to the control line. Significance is denoted by * $p < 0.05$.

4.2 Patient Astrocytes Showed a Loss of Complex 1, Complex IV and TFAM Compared to Controls.

To further validate the finding above and investigate the mitochondrial-related features, we applied flow cytometry, which is more sensitive for detecting antigens/epitopes present in low (94) and measurement expressions per cell. Previous findings showed that respiratory chain complex I and mtDNA copy number measured by the level of mitochondrial transcription factor A (TFAM) was lost in iPSC- NSCs (58) and subsequently confirmed in POLG-affected cerebellar and frontal neuron (23, 38) in patient post-mortem brain samples and iPSC-derived dopaminergic (DA) neurons (58). Therefore, we investigated the level of mitochondrial respiratory chain complex I, IV and mtDNA copy number using TFAM level as an indirect measurement in the POLG astrocytes.

In agreement with previous findings (86), we observed a loss of complex I, complex IV (COX IV) and TFAM in patient astrocytes (Figure 21). Co-staining with S100A10 showed a decrease in POLG astrocytes compared to controls (Figure 21), which was consistent with the finding of immunostaining. Since this data is based on one experiment, more replicate experiments are required to determine the result.

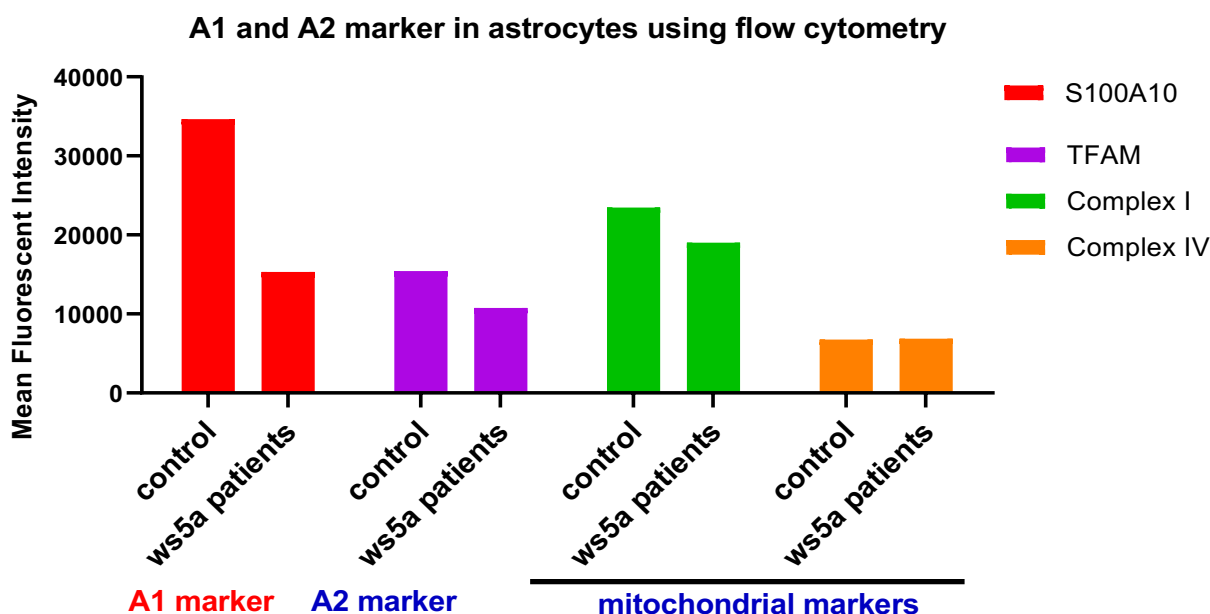
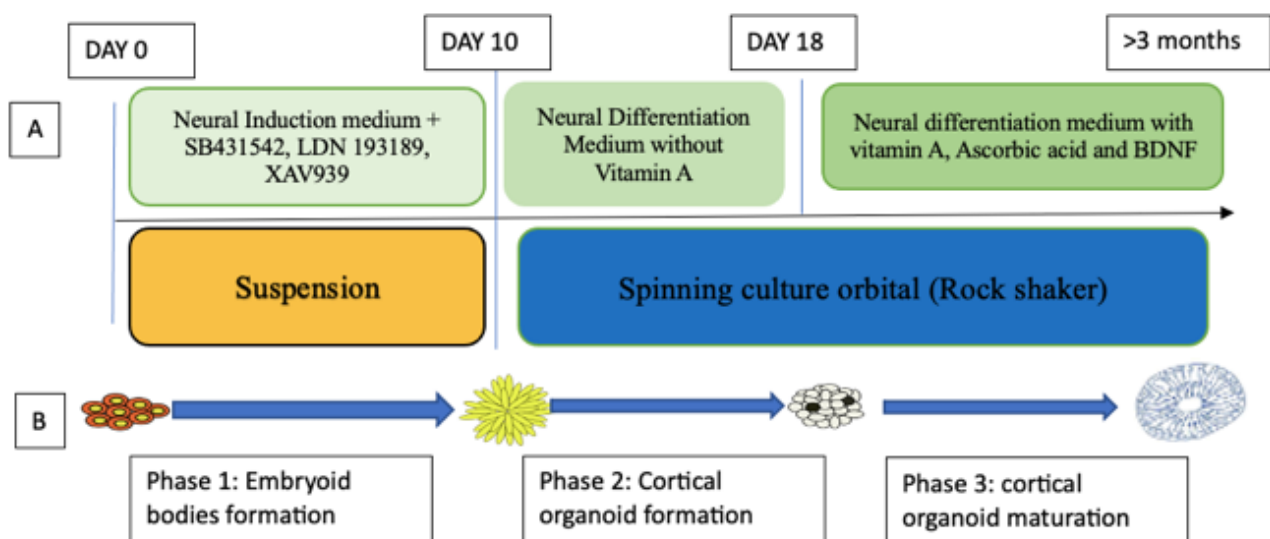


Figure 21: The median fluorescence intensity of S100A10 and GFAP is shown in this graph. Where S100A10 is considerably lower in patients than in controls. The MFI of mitochondrial functional markers such as TFAM, Complex I and Complex IV is lower in the patient sample.

4.3 Differentiation and Characterization of Cortical Organoid from Patient and Control iPSCs.

Cortical organoids were differentiated from iPSCs using a previously reported method (89). First, neural induction was initiated by generating EBs in suspension 3D culture via dual SMAD and Wnt inhibition (Figure 22 A). On day 10, EBs were formed and transferred into spin culture using an orbital shaker and the NIM was replaced by an NDM without vitamin A to allow differentiation into the cortical organization (Figure 22 C). On day 18, the cortical organoids were subjected to long-term culture and neural maturation using the NDM with vitamin A. BDNF and ascorbic acid were added to the medium to aid in the long-term neural maturation process. This process resulted in the formation of a brain tissue-like structure called cortical organoid (Figure 22 C). On day 20, the organoids began to assemble into little rosette-like neuroepithelia, and on day 30, this became even more apparent (Figure 22 C, d). Brain organoids began to develop complex heterogeneous tissues and big in size which could last in a rotating rotator for up to 4 months.

We characterized cell identity during the differentiation using immunofluorescence staining. In Figure 22 D, immunostaining confirmed that the iPSC-derived cortical organoids expressed the specific neural progenitor marker SOX2, mature neuron marker MAP2 and astrocyte marker GFAP. These findings collectively show that we succeed in generating human cortical organoids in the composite of neural tubes, neurons and astrocytes.



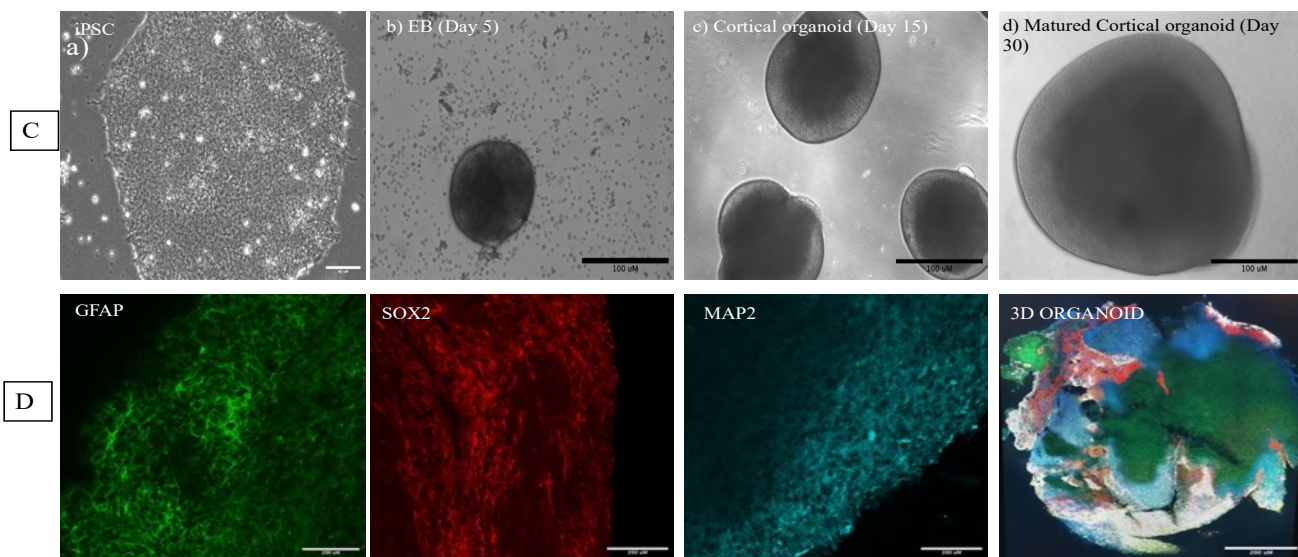


Figure 22: Differentiation of the cortical organoids from iPSCs. (A & B) Schematic representation of iPSCs differentiation to organoids. (C) Different stages during differentiation: iPSC, EB, cortical organoid and matured cortical organoid. (D) A panel of marker expression in our 3D organoid: stained with SOX2 (Red), GFAP(Green), MAP2 (sky blue) and full view of 3D organoids. The scale bar is 100 μ m.

4.4 Patient Cortical Organoids Showed Higher Expression of the A1 Marker and Lower Level of A2 Marker than Control Organoids.

Next, we aimed to investigate the astrocyte markers in the 3D cortical organoids to mimic the human brain more closely. Employing the cortical organoid to quantify the expression of various reactive astrocyte markers gives a more accurate representation of the diseases. Previous studies showed that the behaviour of reactive astrocytes is also influenced by their surrounding cells such as neurons, oligodendrocytes, other glial cells, and the fluidic environment in our brain (61). Therefore, we applied cortical organoids to validate the results generated from 2D astrocytes in order to reflect more closely to the patient's brain.

The iPSC-derived cortical organoids were stained with reactive astrocytes marker glial fibrillary acidic protein (GFAP), A1 marker C3 and SERPING1, as well as A2 marker S100A10 and SCG2. We found that GFAP and A1 reactive astrocyte markers were expressed more in patient cortical organoids as compared to control organoids (Figure 24). The A2 reactive astrocyte marker S100A10 was decreased in patient organoids versus control organoids (Fig 24). These findings further confirm the findings in 2D astrocytes described in *Section 4.1*.

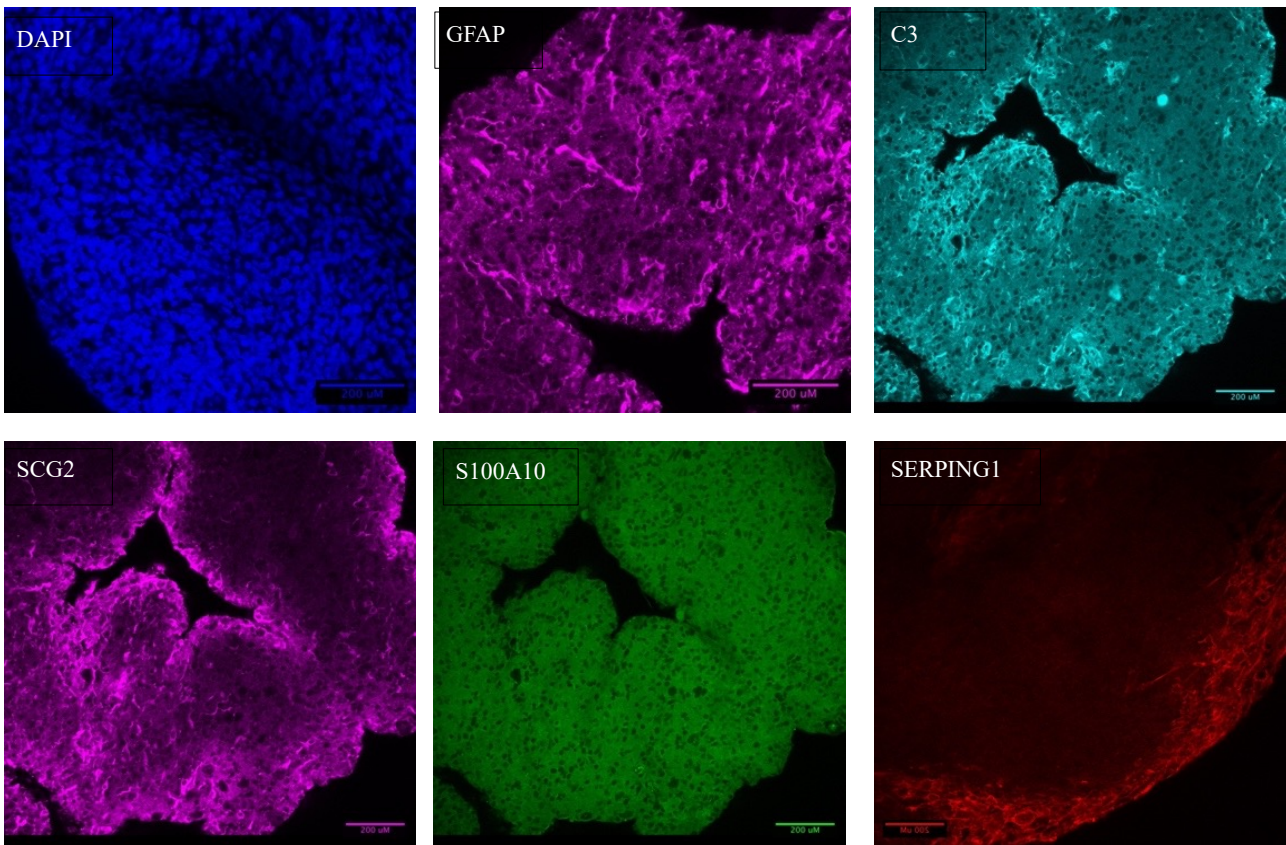


Figure 23: The Panel of reactive astrocyte markers expression in 3D organoid: Images of the cortical organoids stained with various astrocytes markers including GFAP, A1 marker (C3 and SERPING1) and A2 markers (S100A10 and SCG2). The nuclei are stained with DAPI. The scale bar is 200 μm

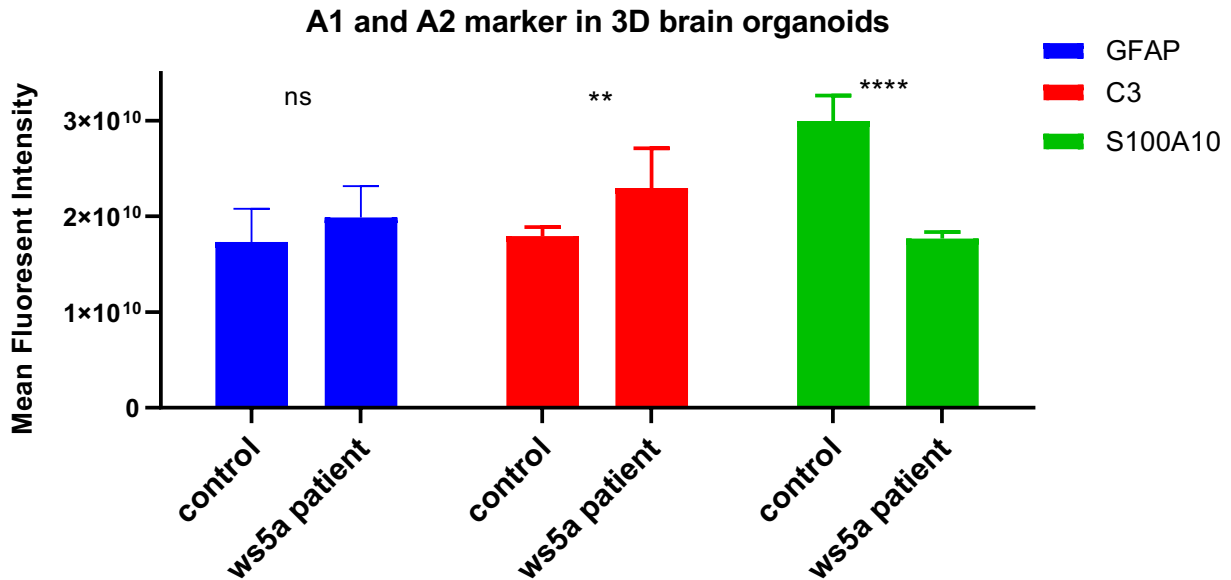


Figure 24: Graphical representation of the quantification of MFI for astrocytes marker in the 3D organoid. The level of expression of reactive markers GFAP and A1 marker C3 are higher while the A2 marker S100a10 in patient organoids as compared to control organoids after the treatment of NR, the reactive marker GFAP and C3 are decreased while the A2 marker S100A10 is increased in patient organoids. Significance is denoted for ** $P < 0.01$; **** $P < 0.0000$; ns, not significant.

4.5 POLG Astrocytes Secreted High Levels of Pro-inflammatory Cytokines and Chemokines.

Previous studies reported the loss of DA neurons in post-mortem POLG patients (90) similar to PD patients (72). Our previous study also demonstrated that the POLG astrocytes were toxic to the DA neurons (90). Here we further investigated how POLG-reactive astrocytes induce neurotoxicity. To address this, astrocytes (POLG or control) and DA neurons (POLG or control) were co-cultured indirectly in separate compartments (Figure 17), allowing the exchanging of the medium. After 20 days of co-culture with control DA neurons, we found a loss of DA neurons grown with POLG astrocytes as compared to those co-cultured with control astrocytes (Figure 25). Furthermore, a more severe neuronal loss was observed when POLG DA neurons were co-cultured with POLG astrocytes (Figure 25C).

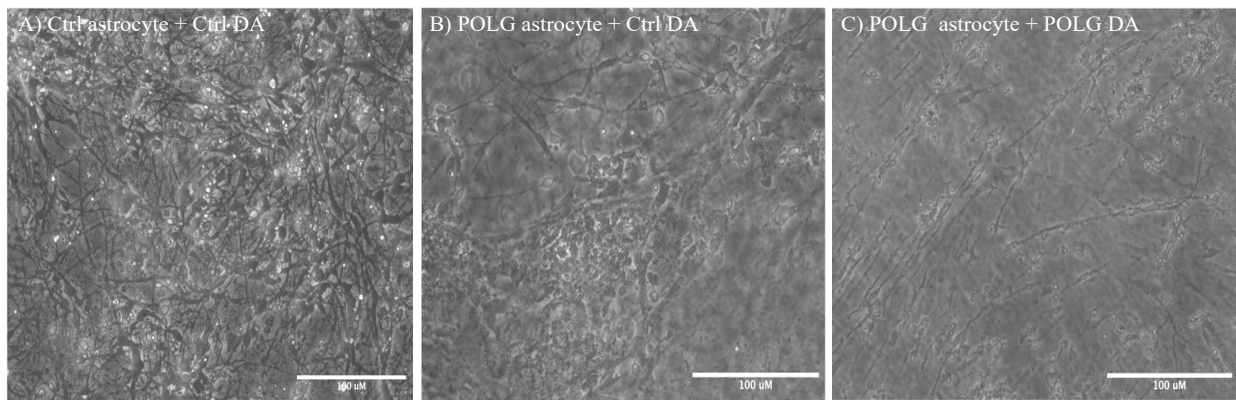


Figure 25: Illustration of the condition of the culture plate of DA neurons on day 10. Control (*ctrl*) DA neurons co-cultured with POLG astrocytes (B) exhibited huge neuronal death as compared to control DA neurons incubated with control astrocytes (A). Patient DA and patient astrocytes (C) had the worst neuronal loss. The scale bar is 100 μm .

Next, we further investigated the cytokine and chemokine expression in the medium of indirect co-culture conditions involving different combinations of astrocytes and DA neurons. We compared the expression profiles in different co-culture conditions: a. control DA+ control astrocytes; b. control DA + POLG astrocytes; c. POLG DA + control astrocytes; d. POLG DA + POLG astrocytes; e. POLG DA + control astrocytes; and f. POLG DA + POLG astrocytes + NR. The cytokine array showed that the control astrocyte and control DA neuron co-culture group expressed six cytokines and chemokines, including IL-6, IL-8, MCP-1 (CCL2), GRO α (CXCL1), MIF, and serpin E1 (Figure 26 a). On the other hand, POLG astrocytes co-cultured with control DA neurons expressed eight cytokines and chemokines, including IL-6, IL-8, MCP-1 (CCL2), GRO α (CXCL1), MIF, serpin E1,

MIP-1 α (CCL3), and RANTES (CCL5) (Figure 26 b). We observed substantially elevated levels of proinflammatory cytokines and chemokines, such as IL-6, GRO α , MCP-1 (CCL2), IL-8, and MIF, in POLG astrocytes co-cultured with control DA neurons compared to control astrocytes and control DA neurons co-culture (Figure 26). This finding is consistent with previous studies on PD, which showed that A1 reactive astrocytes induced the death of DA neurons by releasing pro-inflammatory cytokines (TNF- α , IL-1, and IL-6) and chemokines (CCL2, CCL20, CXCL1, and CX3CL1) (66).

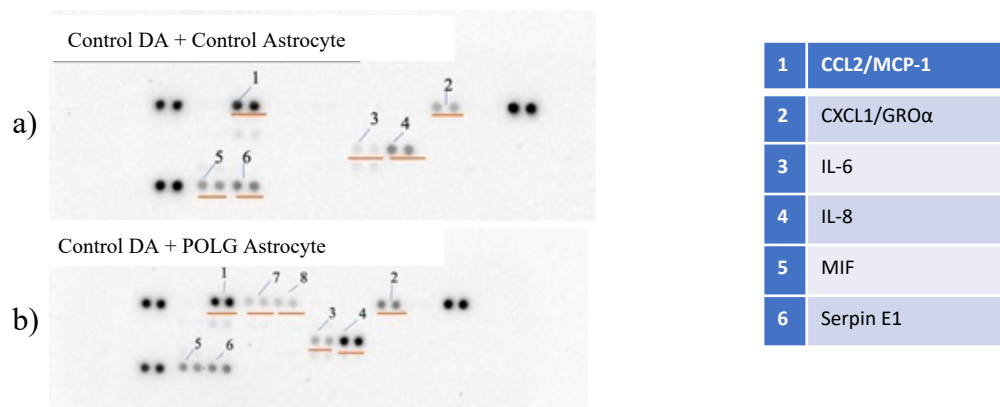


Figure 26: Detection of cytokines on membrane antibody array by chemiluminescence: a) Control DA + Control astrocytes and b) Control DA + POLG astrocytes.

Interestingly, when POLG DA neurons were grown with control astrocytes, we did not observe the secretion of IL-6 and GRO α (CXCL1) (Figure 27 B and C), suggesting that these pro-inflammatory cytokines were specifically secreted by POLG astrocytes rather than DA neurons. These observations were based on one experiment, and further replication is necessary to validate these findings and establish their consistency.

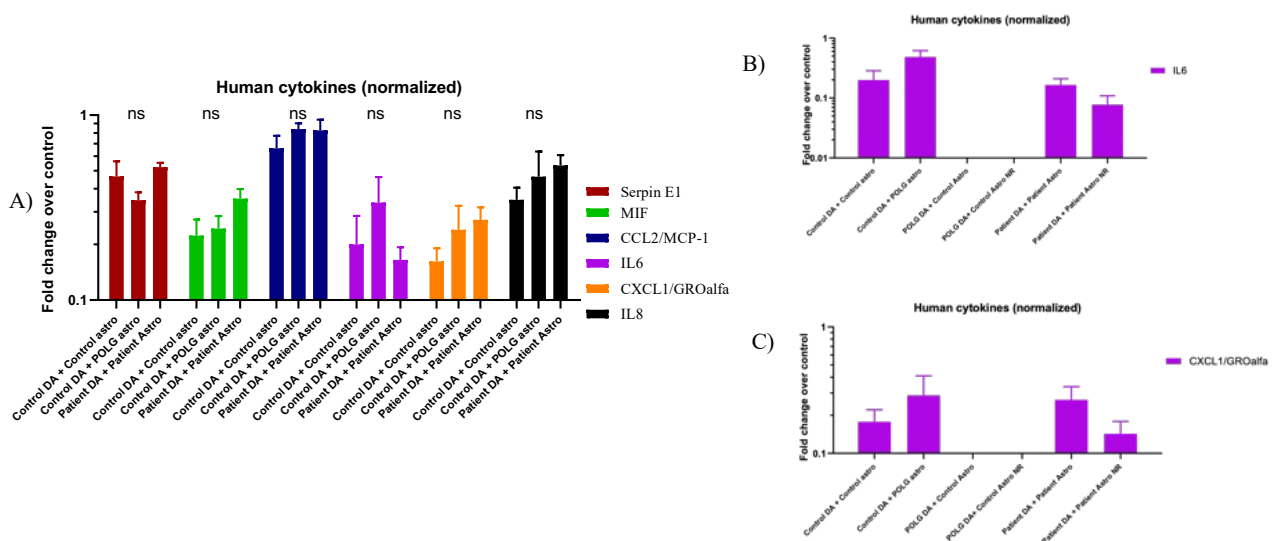


Figure 27: Cytokines profiles of the in-direct co-culture medium. A) Arrays of cytokines expressed in all three conditions: Control POLG + Control DA neuron, POLG astrocyte + Control DA neuron and POLG astrocyte + POLG DA. B) IL-6 expression in all three conditions C) GRO α (CXCL1) expression in all three conditions.

These findings shed light on the neuroinflammatory response mediated by POLG astrocytes and its potential role in contributing to the neurotoxic effects observed in co-culture experiments. The dysregulated cytokine and chemokine expression highlights the complex interplay between astrocytes and neurons in POLG-related disorders. Further investigations are warranted to elucidate the underlying mechanisms and explore potential therapeutic interventions targeting neuroinflammation in these conditions.

4.6 DA Neurons Displayed Morphological and Mitochondrial Damage When Cultured with POLG Astrocyte.

Next, we examined DA neurons in different co-culture conditions for their expression of DA neuronal marker tyrosine hydroxylase (TH) neuronal marker MAP2 and mitochondria mass marker voltage-dependent anion channel (VDAC). We observed that the control DA neurons co-cultured with patient astrocytes have much less expression of mitochondrial marker VDAC and both neuronal markers TH and MAP2 compared to control DA neurons co-cultured with control astrocytes (Figure 28). In addition, control DA neurons exhibited morphological damage when co-cultured with POLG astrocytes (Fig 28 b and d) in contrast to those co-cultured with control astrocytes (Figure 28 a and c). These findings further confirm the neurotoxicity of POLG astrocytes as previously reported (87, 90).

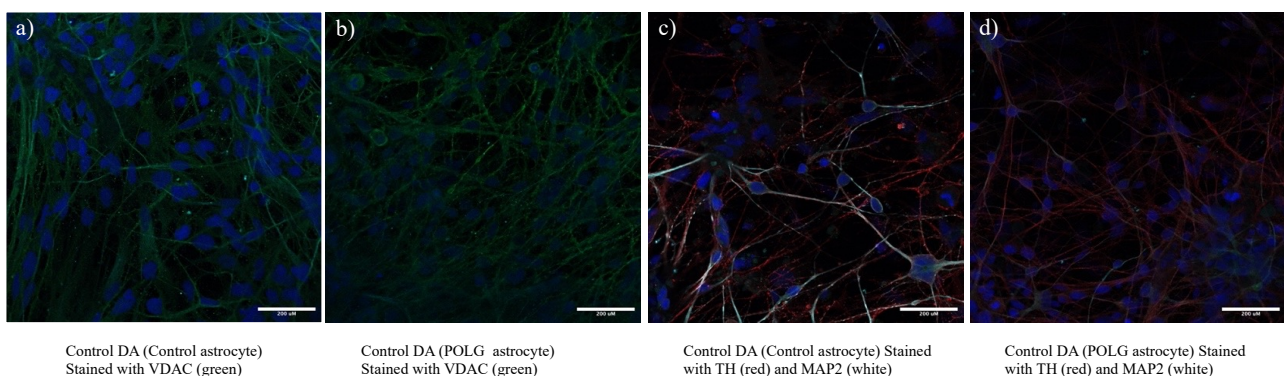


Figure 28: Confocal images of DA neuron: a and b) stained with marker VDAC (green), c and d) TH (red) and MAP2 (white). The scale bar is 200 μ m.

4.7 NR Rescues POLG Astrocyte Reactivity and Cytokines

The potential benefits of NAD⁺ progenitor nicotinamide riboside (NR) have been shown in improving mitochondrial dysfunction (95, 96, 97), here we treated the patient cortical organoids with 1 mM NR for one month and then investigated whether it can reverse the astrocyte reactivity. Here, we used the same antibodies for standard reactive marker GFAP, A1 marker C3 and A2 marker S100A10 to investigate whether NR can rescue their expressions in POLG patient cortical brain organoids. The quantification of the fluorescent intensity showed that patient cortical organoids had decreased the GFAP expression and A1 marker C3 and increased the expression of A2 marker S100A10 after the NR treatment (Figure 29).

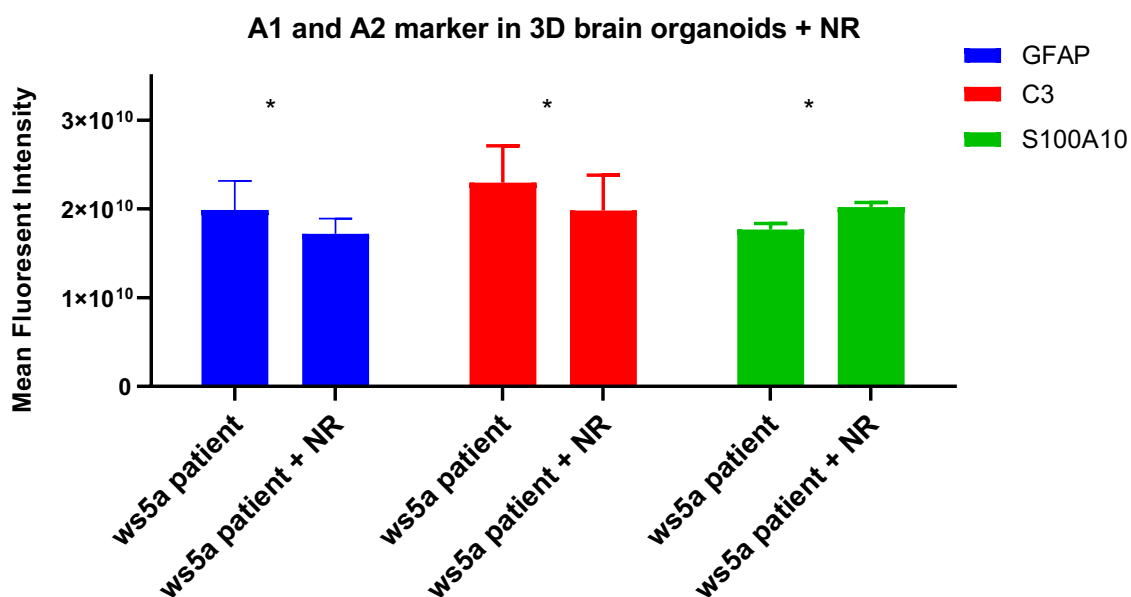


Figure 29: Analysis of reactive marker expressions in POLG patient cortical brain organoids treated with NR. When treated with NR, ws5a (POLG) patients showed significant downregulation of reactive astrocyte marker GFAP and A1 marker; C3 and upregulation of A2 marker; S100A10. Significance is denoted by * $p < 0.05$.

In the co-culture condition plates, the impact of NR was examined across all our co-culture conditions. Notably, the culture plates treated with NR exhibited a greater presence of cells with well-defined morphologies when observed under the microscope (Figure 30). We then investigated whether NR could mitigate the toxic cytokine secretion observed in our previous findings in **Section 4.5**. In order to assess this, we employed the same human cytokine array and compared the levels of proinflammatory cytokines and chemokines in the culture medium from two experimental conditions: POLG astrocytes co-cultured with POLG DA neurons with and without NR treatment. Remarkably,

our analysis revealed a significant reduction in the secretion of proinflammatory cytokine IL-6, and chemokines including GRO α , MCP-1 (CCL2), and MIF in the presence of NR treatment in co-cultured (Figure 31). These findings indicate that the addition of NR effectively attenuated the release of these toxic cytokines by the astrocytes.

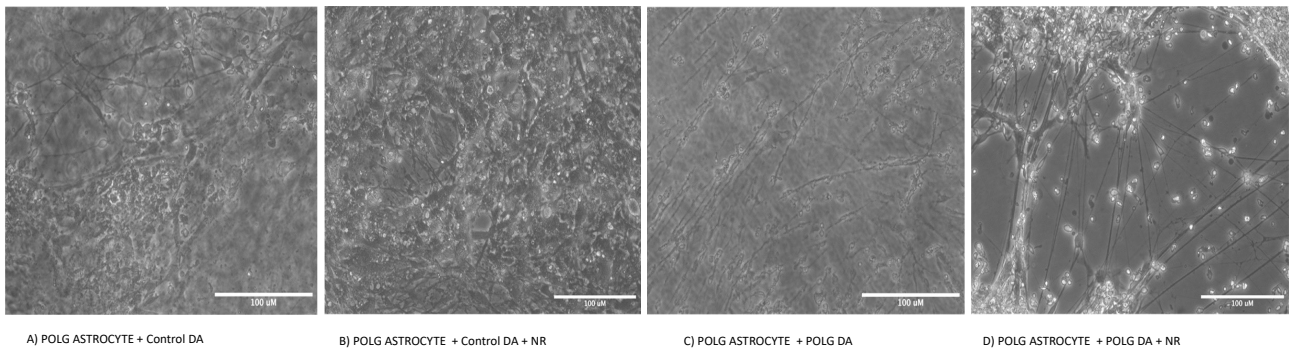


Figure 30: Microscopic images of the DA culture plate on day 10. A) displays POLG astrocytes co-cultured with control DA neurons in the absence of NR. B) shows the co-culture of POLG astrocytes with control DA neurons in the presence of NR. C) illustrates the culture condition of POLG astrocytes with POLG DA neurons without NR and D) the culture condition of POLG astrocytes with DA neurons in the presence of NR.

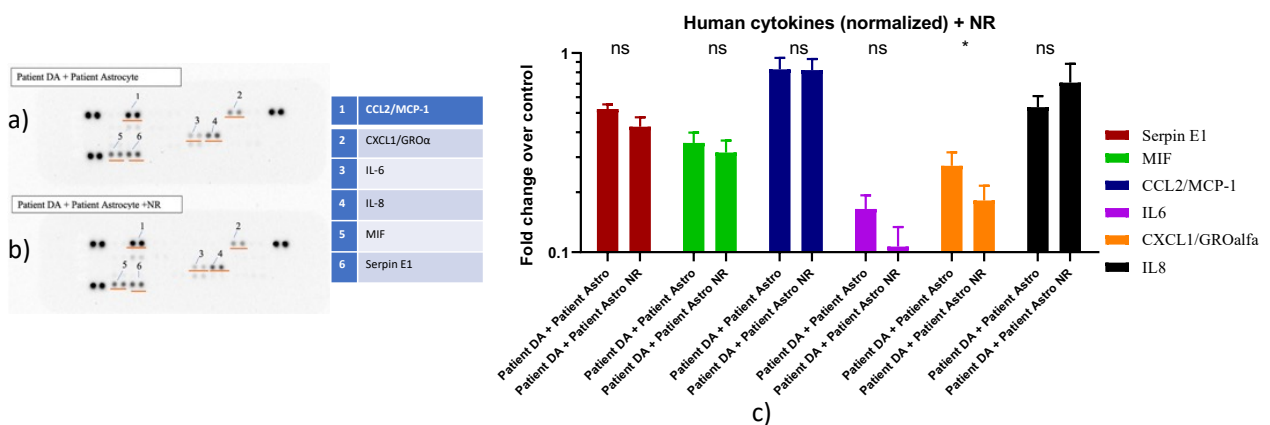


Figure 31: Results from cytokines array analysis: Detection of cytokines on membrane antibody array by chemiluminescence in a) POLG DA + POLG astrocyte, b) POLG DA neuron + POLG astrocytes treated with NR and c) Graph illustrating the level of cytokines and chemokines in the above two conditions. Significance is denoted by * $p < 0.05$

The observed reduction in the levels of IL-6, CCL2, MIF, and CXCL1 suggests a potential therapeutic role for NR in mitigating neuroinflammatory responses associated with POLG-related disorders. By targeting the dysregulated cytokine profile, NR may help alleviate the detrimental effects of neuroinflammation on neuronal health and survival.

CHAPTER 5: DISCUSSION

Reactive astrocytes have been implicated in the pathogenesis of NDs, including those associated with *POLG* mutations. When the POLG enzyme is defective, mitochondrial dysfunction and oxidative stress occur, leading to neuronal damage and death. Reactive astrocytes are thought to facilitate this process by becoming activated and releasing inflammatory cytokines, chemokines, and other toxic molecules that can exacerbate neuronal damage (66, 76). In addition, reactive astrocytes form glial scars that can impede neuronal regeneration and repair.

Studies have shown that reactive astrocytes are present in the brains of patients with POLG-related diseases, including Alpers syndrome and MNGIE (87). These reactive astrocytes are thought to contribute to the pathogenesis of these diseases by promoting inflammation and inhibiting neuronal repair mechanisms. Therefore, studying POLG astrocytes can help to better understand the mechanisms of neuronal death in these diseases.

Currently, there are no established markers that specifically identify POLG astrocytes. We, therefore, aimed to identify potential markers that could be used to detect reactive astrocytes in general. One approach we used was to look for changes in the expression of genes known to be involved in astrocyte activation, which has been reported in other studies (74, 86). Our study employed reactive markers such as GFAP, C3, SERPING1, SCG2, and S100A10 for our POLG astrocytes.

Secondly, our research focused on understanding the mechanism by which toxic-reactive astrocytes lead to neuronal death in POLG diseases. Previous studies have shown that A1 reactive astrocytes secrete harmful substances that lead to the death of DA neuronal in mouse models of PD (3, 72). In this model, accumulation of α -synuclein triggers the release of chemokines (CCL2, CCL20, CXCL1, and CX3CL1) and proinflammatory cytokines (TNF- α , IL-1, IL-6) from reactive astrocytes, indicating their deleterious effects. We aimed to explore the way in which POLG astrocytes cause neuronal death. To achieve this, we used indirect co-culture of astrocytes and DA neurons and analyzed the cytokines present in the medium collected from the co-culture. Our findings showing

the presence of CCL2, CXCL1, IL-6, and IL-8 suggest that these molecules might be responsible for the death of DA neurons.

Lastly, we investigated the potential of NR to reverse astrocyte reactivity. Previous studies have already demonstrated the beneficial effects of NR in improving mitochondrial dysfunction, particularly in conditions like PD and AD. (95, 97). To assess the effects of NR treatment in POLG astrocytes, we measured and compared the expression levels of reactive markers GFAP, C3 and S100A10 in NR-treated and untreated 3D organoids. We observed a decrease in GFAP and C3 marker expression, indicating a reduction in astrocyte reactivity. Conversely, the expression of the S100A10 marker increased, suggesting a positive response to NR treatment. We also examined the effects of NR in an indirect co-culture system. The findings showed that the co-culture medium treated with NR exhibited a reduction in proinflammatory cytokines such as IL-6, CCL2, MIF, and CXCL1 compared to the untreated medium. This indicates a positive effect of NR in reducing the secretion of these harmful cytokines in the co-culture system.

6.1 Differentiation of 3D Cortical Organoid

The use of brain organoids is a powerful tool in the field of neuroscience research because it provides a 3D *in vitro* structure of the developing human brain. To date, the organization and development of the midbrain, hippocampus, hypothalamus, and cerebellum have been recapitulated (54, 61, 63). In our study, we have demonstrated both POLG patients (WS5A) and control iPSCs can be successfully differentiated into cortical organoids using a previously established protocol (89). It is crucial to maintain the quality and pluripotency of iPSCs throughout the culture period. This can be achieved by regularly monitoring cell morphology and changing medium regularly. One of the critical factors in the successful differentiation of cortical organoids is the formation of stable neural rosette structures, which are the precursors for cortical neurons. We found that obtaining iPSC colonies with good quality as well as the neural induction medium is important for forming a neural rosette. The findings of this study also form the basis for further research using cortical organoids to study POLG and other NDs.

However, several limitations to generating and using cortical organoids must be considered. The reproducibility and quality of organoids may vary from batch to batch, which may affect the accuracy and reliability of experimental results. The size and longevity of cortical organoids are also limited by the lack of vascularization. When organoids lack proper vascularization, they cannot get enough oxygen and nutrients, resulting in necrosis and cell death. Due to this limitation, it is challenging in

using organoids that cannot be used for drug screening or long-term studies of neuronal development. It is important to note that cortical organoids have several advantages over traditional two-dimensional cell culture systems, despite their limitations. These models enable the study of cell-cell interactions as well as the development of complex tissue structures in a physiologically relevant environment. Despite their limitations, cortical organoids present an exciting opportunity to study the development and function of the human brain. As differentiation protocols improve and characterization techniques become standardized, cortical organoids are expected to become more useful tools for neuroscience research.

6.2 Identification of Reactive Astrocyte Markers

In our POLG samples, the reactive astrocyte marker GFAP, and A1 marker C3 showed consistently higher expression than control astrocytes and cortical organoids. Likewise, our findings also showed that the A2 marker S100A10 was significantly upregulated in patient samples compared to the patient. The overexpression of GFAP and C3 and the downregulation of the A2 marker S100A10 coincide with previous studies (74) that have shown an increase in reactive astrocytes in a variety of NDs such as PD, MS and AD.

GFAP is an intermediate filament protein that is heavily expressed in astrocytes, and increased levels are often associated with reactive astrogliosis, a common response to CNS injury. Therefore, GFAP overexpression could be indicative of astrocyte activation in POLG-related disease. C) is part of the immune system's complement system and is known to be involved in inflammatory processes in the CNS. Its overexpression in our study might be suggestive of an ongoing inflammatory response. On the other hand, S100A10, also known as p11, is a protein expressed in various cell types including astrocytes and has been implicated in several physiological and pathological processes. Downregulation of S100A10 could be indicative of altered astrocytic functions, though its exact implications in POLG disease may warrant further investigation.

However, to validate our findings, more patient samples need to be studied. Future research should also consider *in vitro* and *in vivo* studies to explore the mechanisms underlying these changes in protein expression and their consequent impact on astrocyte function. Furthermore, given the involvement of these proteins in various pathways, proteomic and genomic analyses might provide insights into pathway regulation. In-depth investigations into the role of these potential markers could help in the early diagnosis and intervention of POLG disease, as well as contribute to the understanding of astrocyte dysfunction in neurodegenerative diseases.

However, further validation of these markers is needed to ensure their specificity in identifying POLG astrocytes. It is imperative to acknowledge that there is significant heterogeneity in astrocyte response to a variety of insults. Different markers may be more appropriate for different diseases such as in AD, reactive astrocytes are identified by increased expression of GFAP, S100 β , and vimentin (98). PD exhibits an increased expression of GFAP, S100 β , and clusterin (99). ALS involves markers such as GFAP, S100 β , and AQP4 (81). MS shows increased expression of GFAP, vimentin, and nestin in the reactive astrocytes (66). Therefore, future studies should investigate additional markers and determine their specificity for POLG astrocytes by comparing their expression profiles across disease models.

Overall, our study provides evidence that the overexpression of GFAP and C3 and the downregulation of S100A10 may be possible markers for reactive astrocytes in POLG diseases. However, to validate our findings, more patient samples need to be studied. Future research should also consider *in vitro* and *in vivo* studies to explore the mechanisms underlying these changes in protein expression and their consequent impact on astrocyte function. Furthermore, given the involvement of these proteins in various pathways, proteomic and genomic analyses might provide insights into pathway regulation. In-depth investigations into the role of these potential markers could help in the early diagnosis and intervention of POLG disease, as well as contribute to the understanding of astrocyte dysfunction in neurodegenerative diseases.

6.3 Indirect Co-culture of POLG Astrocytes and DA Neurons

Our study seems to add an important dimension to our understanding of the role of astrocyte-neuron interactions in POLG diseases and for other NDs like PD.

The increased production of proinflammatory cytokines (IL-6, IL-8) and chemokines (CCL2 and CXCL1) in DA neurons co-cultured with POLG astrocytes, as compared to control DA neurons co-cultured with control astrocytes, suggests an inflammatory response. These inflammatory response result in reactive astrocytes further lead to the toxic to the DA neurons. Studies in other NDs including PD, showed that these proinflammatory cytokines and chemokines induce reactive astrocytes that have been shown to contribute to neurodegenerative diseases (3, 72). As these molecules can promote the development of reactive astrocytes, it could indeed contribute to neuronal toxicity and cell death, exacerbating neurodegeneration in POLG diseases for other NDs like PD.

The mitochondrial function of both cell types was also assessed in the co-culture system, in addition to the secretome. The percentage of mitochondrial respiratory chain complex one subunits

(COMPLEX I/VDAC) was lower in co-cultures of POLG astrocytes and DA neurons, suggesting mitochondrial dysfunction. The results of this study are consistent with previous studies demonstrating a link between mitochondrial dysfunction and POLG (58, 87).

Further, the evidence of mitochondrial dysfunction observed in POLG astrocytes and DA neurons co-cultures adds another layer to the mechanism of how POLG astrocytes might be inducing neuronal toxicity. Given the essential role of mitochondria in energy production, a reduction in mitochondrial respiratory chain complex one subunits could negatively impact neuronal survival and function.

Our findings not only support the existing literature linking mitochondrial dysfunction with POLG, but they also extend it by highlighting the role of inflammatory responses in astrocyte-mediated neurotoxicity. This line of research could have significant implications for the development of new therapeutic strategies for POLG disease and other NDs.

Investigating astrocyte-neuron interactions through co-culture systems indeed seems to be a promising approach for future studies. It would be interesting to see if these findings could be replicated *in vivo*, and if manipulating astrocyte activity could have a protective effect on DA neurons.

In conclusion, our work adds valuable knowledge to the field and underscores the potential of astrocytes as a target for interventions in POLG diseases. Future studies could explore the possibility of modulating astrocyte function to reduce neuroinflammation and mitochondrial dysfunction in the context of POLG and other NDs.

6.4 Limitations of the Study

Sample Size

The limitations we have identified are important to consider and show a thoughtful approach to our research. The use of a small number of iPSC clones from WS5A cells and controls certainly could limit the generalizability of our findings, given the broad range of diseases and varied age of onset associated with *POLG* mutations. Further, since these mutations are autosomal recessive, the disease phenotype can vary even in individuals with the same mutation, depending on their other allele.

The use of patient-specific iPSCs differentiated into cerebral organoids, which contain cortical regions and astrocytes, is indeed an advanced method in studying POLG diseases and NDs. However, without the use of isogenic controls, the influence of patient-specific genetic background cannot be entirely ruled out. Isogenic controls involve the correction of the pathogenic mutation in patient-

derived iPSCs, which allows for a comparison between cells with and without the mutation in an otherwise identical genetic background.

Despite these limitations, our study still offers valuable insights into the role of *POLG* mutations in astrocyte-neuron interactions and neurodegenerative diseases. Future research could address these limitations by including a larger and more diverse set of samples, and if possible, the use of isogenic controls. Studies with larger cohorts are needed to validate our findings and to explore the complex phenotypic variability seen in *POLG*-related diseases.

Regardless, our current work still contributes significantly to the understanding of *POLG* diseases and NDs, particularly those associated with mitochondrial dysfunction, and may help pave the way for future research in this field.

The Challenge in Immunostaining and Quantification in 3D Brain Organoid.

There are several limitations when immunostaining of 3d cortical organoids. The densely packed interior of organoids can pose significant obstacles for antibody penetration. Antibody penetration is a common problem faced in many tissue-based studies, especially for larger and more complex 3D structures. In our study, the decision to use organoids without cryosectioning might have made this issue more prominent. Future studies, when resources allow, should consider implementing cryosectioning or other methods to improve antibody penetration.

Autofluorescence can be a significant issue, especially in long-term cultures where increased metabolic activity can lead to the accumulation of auto fluorescent metabolites. Careful selection of fluorophores that have emission spectra distinct from the autofluorescence of the organoid tissue, as well as image analysis strategies that can subtract autofluorescence, can help mitigate this issue.

The intrinsic heterogeneity of brain organoids, due to differences in cellular composition and maturation, indeed adds another layer of complexity. This can make it challenging to make direct comparisons between different organoids or even different regions within the same organoid. Careful experimental design and statistical analysis can help account for this variability.

The potential for artifacts is indeed a concern in the immunostaining process. Over-fixation or incorrect permeabilization can not only lead to loss of structures but may also result in false-positive or false-negative staining. Thus, it's critical to validate and optimize staining protocols, and to include appropriate controls in all experiments.

Despite these challenges, 3D brain organoid offer an unparalleled opportunity to model and understand human brain development and disease. The ability to generate complex, three-dimensional tissues from patient-derived cells opens the door to personalized medicine approaches that were previously unimaginable. Technical difficulties are obstacles to be overcome rather than insurmountable barriers.

CHAPTER 6: CONCLUSIONS AND FUTURE PERSPECTIVES

6.1 Conclusions

The main aim of this project was to use our *in vitro* iPSC-based model (2D astrocyte, 3D brain organoid and neuron co-culture system) to study the markers/subtype of reactive astrocytes induced by the mitochondrial defect and explore the mechanism of neurotoxic effects that involved in the POLG neurodegeneration process. The findings of our research offer valuable insights into the role of reactive astrocytes in POLG-related neurodegeneration and expand our understanding of astrocyte biology in NDs. The main conclusions from this study were highlighted below:

1. Our observations of a shift in astrocytes towards a reactive phenotype, reflected in the reduced expression of A2 markers and increased expression of A1 markers, are particularly compelling. These changes, in conjunction with evidence of mitochondrial dysfunction, suggest a link between astrocyte reactivity and mitochondrial deficits. This association is further strengthened by our co-culture experiments demonstrating neuronal damage when control DA neurons are cultured with patient astrocytes, highlighting the toxic impact of reactive astrocytes on neuronal health.
2. The higher secretion levels of pro-inflammatory cytokines and chemokines by POLG astrocytes underscores the role of neuroinflammation in neuronal dysfunction, which is characteristic of many NDs. This insight may be of particular significance given the rising interest in the role of glial cells and inflammation in neurodegeneration.
3. Additionally, our experiments using the NAD⁺ precursor NR to ameliorate astrocyte reactivity and reduce toxic cytokine secretion in patient samples could represent a promising therapeutic strategy to modulate astrocyte function and mitigate neuronal damage in POLG-related disorders.
4. The use of 3D brain organoids to model the complex cellular composition of the human brain, and the recapitulation of the astrocyte reactivity seen in patient astrocytes in these organoids, demonstrates the power of these models in studying disease mechanisms in a context that closely mirrors *in vivo* conditions.

While these findings are crucial, the necessity for additional investigations with larger sample sizes is needed to validate and build upon these results. Moreover, expanding this work to other NDs could clarify whether these mechanisms are unique to POLG-related disorders or are more broadly applicable.

In summary, our study offers considerable insights into the pathogenic role of reactive astrocytes in POLG disease and NDs that are relevant to mitochondrial defects, further emphasizing the need to consider these cells in our understanding of, and therapeutic strategies for, these conditions.

6.2 Future Perspectives

Our study provides a promising avenue for future research in the field of NDs, particularly those related to mitochondrial dysfunction. Here are several directions for future research that stem from our work:

1. **Further Characterization of Astrocyte Phenotypes:** Although our study provides evidence for a shift towards a reactive phenotype in POLG patient-derived astrocytes, additional work could provide a more detailed characterization of these changes. This could involve assessing changes in gene expression profiles using techniques like RNA sequencing or examining the functional consequences of these changes on astrocyte physiology.
2. **Larger Cohorts and Diverse *POLG* Mutations:** To validate our findings and improve their generalizability, it will be crucial to conduct studies on larger cohorts and diverse *POLG* mutations. This could help clarify whether the observed phenomena are common to all *POLG* mutations or are specific to certain variants.
3. **Longitudinal Studies:** Given the progressive nature of NDs, it would be interesting to conduct longitudinal studies that monitor changes in astrocyte phenotype and function over time.
4. **Therapeutic Interventions:** Our preliminary findings with the NAD⁺ precursor NR suggest a potential therapeutic strategy. Future studies could explore this further and test additional interventions that could mitigate the harmful effects of reactive astrocytes.
5. **Study of Other NDs:** Given the evidence for the role of astrocytes in other neurodegenerative diseases, it would be interesting to examine whether similar mechanisms are at play in other contexts.

Overall, our research opens up several promising avenues for future investigation. The insights gained from these studies could significantly enhance our understanding of neurodegenerative diseases and could eventually lead to the development of new therapeutic strategies.

CHAPTER 7: REFERENCES

1. Klothe Pathways, Myelination Disorders, Neurodegenerative Diseases, and Epigenetic Drugs. *BioResearch Open Access*. 2020;9(1):94-105.
2. Hou Y, Dan X, Babbar M, Wei Y, Hasselbalch SG, Croteau DL, et al. Ageing as a risk factor for neurodegenerative disease. *Nature Reviews Neurology*. 2019;15(10):565-81.
3. Li W, Fu Y, Halliday GM, Sue CM. PARK Genes Link Mitochondrial Dysfunction and Alpha-Synuclein Pathology in Sporadic Parkinson's Disease. *Frontiers in Cell and Developmental Biology*. 2021;9.
4. Guzman-Martinez L, Maccioni RB, Andrade V, Navarrete LP, Pastor MG, Ramos-Escobar N. Neuroinflammation as a Common Feature of Neurodegenerative Disorders. *Front Pharmacol*. 2019;10:1008.
5. Bell SM, Barnes K, De Marco M, Shaw PJ, Ferraiuolo L, Blackburn DJ, et al. Mitochondrial Dysfunction in Alzheimer's Disease: A Biomarker of the Future? *Biomedicines*. 2021;9(1).
6. Halliwell B. Role of free radicals in the neurodegenerative diseases: therapeutic implications for antioxidant treatment. *Drugs Aging*. 2001;18(9):685-716.
7. Kowalczyk P, Sulejczak D, Kleczkowska P, Bukowska-Ośko I, Kucia M, Popiel M, et al. Mitochondrial Oxidative Stress-A Causative Factor and Therapeutic Target in Many Diseases. *Int J Mol Sci*. 2021;22(24).
8. Brakedal B, Toker L, Haugarvoll K, Tzoulis C. A nationwide study of the incidence, prevalence and mortality of Parkinson's disease in the Norwegian population. *NPJ Parkinsons Dis*. 2022;8(1):19.
9. Fernández-Ruiz J. The biomedical challenge of neurodegenerative disorders: an opportunity for cannabinoid-based therapies to improve on the poor current therapeutic outcomes. *Br J Pharmacol*. 2019;176(10):1370-83.
10. Cahoolessur DK, Rajkumarsingh B. Fall Detection System using XGBoost and IoT. *R&D Journal*. 2020;36:8-18.
11. Programme EJ. Neurodegenerative Disease Research. (2019). Why Choose Neurodegenerative Diseases? 2019 [Available from: <https://www.neurodegenerationresearch.eu/about/why/>].
12. Prof Simon Iain Hay IfHMaE, Seattle, WA 98121, US. Global, regional, and national disability-adjusted life-years (DALYs) for 333 diseases and injuries and healthy life expectancy (HALE) for 195 countries and territories, 1990–2016: a systematic analysis for the Global Burden of Disease Study 2016. *The Lancet*. 2017;390(10100):1260-344.
13. Evaluation IfHMa. Global burden disease (GBD): Global Health Data Exchange; 2022 [cited 2019. neurological disorders both sexes, all ages, 2019, DALYs per 100,000]. Available from: <https://vizhub.healthdata.org/gbd-compare/>.
14. Andersson SGE, Zomorodipour A, Andersson JO, Sicheritz-Pontén T, Alsmark UCM, Podowski RM, et al. The genome sequence of *Rickettsia prowazekii* and the origin of mitochondria. *Nature*. 1998;396(6707):133-40.
15. Martijn J, Vosseberg J, Guy L, Offre P, Ettema TJG. Deep mitochondrial origin outside the sampled alphaproteobacteria. *Nature*. 2018;557(7703):101-5.
16. Baker N, Patel J, Khacho M. Linking mitochondrial dynamics, cristae remodeling and supercomplex formation: How mitochondrial structure can regulate bioenergetics. *Mitochondrion*. 2019;49:259-68.
17. Noguchi M, Kasahara A. Mitochondrial dynamics coordinate cell differentiation. *Biochem Biophys Res Commun*. 2018;500(1):59-64.
18. Seo BJ, Yoon SH, Do JT. Mitochondrial Dynamics in Stem Cells and Differentiation. *Int J Mol Sci*. 2018;19(12).

19. Kukat C, Davies K, Wurm C, Spähr H, Bonekamp N, Kühl I, et al. Cross-strand binding of TFAM to a single mtDNA molecule forms the mitochondrial nucleoid. *Proceedings of the National Academy of Sciences*. 2015;112.
20. Singh T, Jiao Y, Ferrando LM, Yablonska S, Li F, Horoszko EC, et al. Neuronal mitochondrial dysfunction in sporadic amyotrophic lateral sclerosis is developmentally regulated. *Scientific Reports*. 2021;11(1):18916.
21. Bantle CM, Hirst WD, Weihofen A, Shlevkov E. Mitochondrial Dysfunction in Astrocytes: A Role in Parkinson's Disease? *Frontiers in Cell and Developmental Biology*. 2021;8.
22. Acosta C, Anderson HD, Anderson CM. Astrocyte dysfunction in Alzheimer disease. *J Neurosci Res*. 2017;95(12):2430-47.
23. Tzoulis C, Tran GT, Coxhead J, Bertelsen B, Lilleng PK, Balafkan N, et al. Molecular pathogenesis of polymerase γ -related neurodegeneration. *Ann Neurol*. 2014;76(1):66-81.
24. Ignatenko O, Chilov D, Paetau I, de Miguel E, Jackson CB, Capin G, et al. Loss of mtDNA activates astrocytes and leads to spongiform encephalopathy. *Nature Communications*. 2018;9(1):70.
25. Lestienne P. Evidence for a direct role of the DNA polymerase gamma in the replication of the human mitochondrial DNA in vitro. *Biochemical and Biophysical Research Communications*. 1987;146(3):1146-53.
26. Hance N, Ekstrand MI, Trifunovic A. Mitochondrial DNA polymerase gamma is essential for mammalian embryogenesis. *Hum Mol Genet*. 2005;14(13):1775-83.
27. Walker RL, Anziano P, Meltzer PS. A PAC Containing the Human Mitochondrial DNA Polymerase Gamma Gene (POLG) Maps to Chromosome 15q25. *Genomics*. 1997;40(2):376-8.
28. Yakubovskaya E, Lukin M, Chen Z, Berriman J, Wall JS, Kobayashi R, et al. The EM structure of human DNA polymerase gamma reveals a localized contact between the catalytic and accessory subunits. *Embo j*. 2007;26(19):4283-91.
29. Ropp PA, Copeland WC. Cloning and characterization of the human mitochondrial DNA polymerase, DNA polymerase gamma. *Genomics*. 1996;36(3):449-58.
30. Saneto R, Naviaux R. Polymerase gamma disease through the ages. *Developmental disabilities research reviews*. 2010;16:163-74.
31. Stumpf JD, Saneto RP, Copeland WC. Clinical and molecular features of POLG-related mitochondrial disease. *Cold Spring Harb Perspect Biol*. 2013;5(4):a011395.
32. Lee YS, Kennedy WD, Yin YW. Structural insight into processive human mitochondrial DNA synthesis and disease-related polymerase mutations. *Cell*. 2009;139(2):312-24.
33. Rahman S, Copeland WC. POLG-related disorders and their neurological manifestations. *Nature Reviews Neurology*. 2019;15(1):40-52.
34. Hakonen AH, Isohanni P, Paetau A, Herva R, Suomalainen A, Lönnqvist T. Recessive Twinkle mutations in early onset encephalopathy with mtDNA depletion. *Brain*. 2007;130(11):3032-40.
35. Chan SS, Longley MJ, Copeland WC. The common A467T mutation in the human mitochondrial DNA polymerase (POLG) compromises catalytic efficiency and interaction with the accessory subunit. *J Biol Chem*. 2005;280(36):31341-6.
36. Kasiviswanathan R, Longley MJ, Chan SS, Copeland WC. Disease mutations in the human mitochondrial DNA polymerase thumb subdomain impart severe defects in mitochondrial DNA replication. *J Biol Chem*. 2009;284(29):19501-10.
37. Cheldi A, Ronchi D, Bordoni A, Bordo B, Lanfranconi S, Bellotti MG, et al. POLG1 mutations and stroke like episodes: a distinct clinical entity rather than an atypical MELAS syndrome. *BMC Neurol*. 2013;13:8.

38. Anagnostou ME, Ng YS, Taylor RW, McFarland R. Epilepsy due to mutations in the mitochondrial polymerase gamma (POLG) gene: A clinical and molecular genetic review. *Epilepsia*. 2016;57(10):1531-45.
39. Graziewicz MA, Longley MJ, Copeland WC. DNA Polymerase γ in Mitochondrial DNA Replication and Repair. *Chemical Reviews*. 2006;106(2):383-405.
40. Tzoulis C, Engelsen BA, Telstad W, Aasly J, Zeviani M, Winterthun S, et al. The spectrum of clinical disease caused by the A467T and W748S POLG mutations: a study of 26 cases. *Brain*. 2006;129(Pt 7):1685-92.
41. Barut BA, Zon LI. Realizing the potential of zebrafish as a model for human disease. *Physiol Genomics*. 2000;2(2):49-51.
42. Benavides F, Guénet JL. [Murine models for human diseases]. *Medicina (B Aires)*. 2001;61(2):215-31.
43. Merkle FT, Eggan K. Modeling human disease with pluripotent stem cells: from genome association to function. *Cell Stem Cell*. 2013;12(6):656-68.
44. Trifunovic A, Wredenberg A, Falkenberg M, Spelbrink JN, Rovio AT, Bruder CE, et al. Premature ageing in mice expressing defective mitochondrial DNA polymerase. *Nature*. 2004;429(6990):417-23.
45. Ebert AM, Lamont RE, Childs SJ, McFarlane S. Neuronal expression of class 6 semaphorins in zebrafish. *Gene Expr Patterns*. 2012;12(3-4):117-22.
46. Thomson JA, Itskovitz-Eldor J, Shapiro SS, Waknitz MA, Swiergiel JJ, Marshall VS, et al. Embryonic stem cell lines derived from human blastocysts. *Science*. 1998;282(5391):1145-7.
47. de Wert G, Mummery C. Human embryonic stem cells: research, ethics and policy. *Hum Reprod*. 2003;18(4):672-82.
48. Takahashi K, Tanabe K, Ohnuki M, Narita M, Ichisaka T, Tomoda K, et al. Induction of pluripotent stem cells from adult human fibroblasts by defined factors. *Cell*. 2007;131(5):861-72.
49. Dimos JT, Rodolfa KT, Niakan KK, Weisenthal LM, Mitsumoto H, Chung W, et al. Induced pluripotent stem cells generated from patients with ALS can be differentiated into motor neurons. *Science*. 2008;321(5893):1218-21.
50. Ebert AD, Liang P, Wu JC. Induced pluripotent stem cells as a disease modeling and drug screening platform. *J Cardiovasc Pharmacol*. 2012;60(4):408-16.
51. Young MA, Larson DE, Sun C-W, George DR, Ding L, Miller CA, et al. Background mutations in parental cells account for most of the genetic heterogeneity of induced pluripotent stem cells. *Cell stem cell*. 2012;10(5):570-82.
52. Medvedev S, Shevchenko A, Zakian S. Induced pluripotent stem cells: problems and advantages when applying them in regenerative medicine. *Acta Naturae (англоязычная версия)*. 2010;2(2 (5)):18-27.
53. Huangfu D, Maehr R, Guo W, Eijkelenboom A, Snitow M, Chen AE, et al. Induction of pluripotent stem cells by defined factors is greatly improved by small-molecule compounds. *Nature biotechnology*. 2008;26(7):795-7.
54. Barak M, Fedorova V, Pospisilova V, Raska J, Vochyanova S, Sedmik J, et al. Human iPSC-Derived Neural Models for Studying Alzheimer's Disease: from Neural Stem Cells to Cerebral Organoids. *Stem Cell Reviews and Reports*. 2022;18(2):792-820.
55. Kumar M, Nguyen NTP, Milanese M, Bonanno G. Insights into Human-Induced Pluripotent Stem Cell-Derived Astrocytes in Neurodegenerative Disorders. *Biomolecules*. 2022;12(3).
56. Perriot S, Canales M, Mathias A, Du Pasquier R. Differentiation of functional astrocytes from human-induced pluripotent stem cells in chemically defined media. *STAR Protoc*. 2021;2(4):100902.

57. Tcw J, Wang M, Pimenova AA, Bowles KR, Hartley BJ, Lacin E, et al. An Efficient Platform for Astrocyte Differentiation from Human Induced Pluripotent Stem Cells. *Stem Cell Reports*. 2017;9(2):600-14.
58. Liang KX, Kristiansen CK, Mostafavi S, Vatne GH, Zantingh GA, Kianian A, et al. Disease-specific phenotypes in iPSC-derived neural stem cells with POLG mutations. *EMBO Mol Med*. 2020;12(10):e12146.
59. Santos R, Vadodaria KC, Jaeger BN, Mei A, Lefcochilos-Fogelquist S, Mendes APD, et al. Differentiation of Inflammation-Responsive Astrocytes from Glial Progenitors Generated from Human Induced Pluripotent Stem Cells. *Stem Cell Reports*. 2017;8(6):1757-69.
60. Pham C, Hérault K, Oheim M, Maldera S, Vialou V, Cauli B, et al. Astrocytes respond to a neurotoxic A β fragment with state-dependent Ca(2+) alteration and multiphasic transmitter release. *Acta Neuropathol Commun*. 2021;9(1):44.
61. Lancaster MA, Renner M, Martin CA, Wenzel D, Bicknell LS, Hurles ME, et al. Cerebral organoids model human brain development and microcephaly. *Nature*. 2013;501(7467):373-9.
62. Sasai Y. Next-generation regenerative medicine: organogenesis from stem cells in 3D culture. *Cell Stem Cell*. 2013;12(5):520-30.
63. Qian X, Song H, Ming GL. Brain organoids: advances, applications and challenges. *Development*. 2019;146(8).
64. Farhy-Tselnicker I, Allen NJ. Astrocytes, neurons, synapses: a tripartite view on cortical circuit development. *Neural Development*. 2018;13(1):7.
65. Verkhratsky A, Nedergaard M. Physiology of Astroglia. *Physiol Rev*. 2018;98(1):239-389.
66. Ding Z-B, Song L-J, Wang Q, Kumar G, Yan Y-Q, Ma C-G. Astrocytes: a double-edged sword in neurodegenerative diseases. *Neural Regeneration Research*. 2021;16(9):1702-10.
67. Escartin C, Guillemaud O, Carrillo-de Sauvage MA. Questions and (some) answers on reactive astrocytes. *Glia*. 2019;67(12):2221-47.
68. Angelova PR, Abramov AY. Functional role of mitochondrial reactive oxygen species in physiology. *Free Radic Biol Med*. 2016;100:81-5.
69. Henneberger C. Does rapid and physiological astrocyte-neuron signalling amplify epileptic activity? *J Physiol*. 2017;595(6):1917-27.
70. Cheng X, Wang J, Sun X, Shao L, Guo Z, Li Y. Morphological and functional alterations of astrocytes responding to traumatic brain injury. *J Integr Neurosci*. 2019;18(2):203-15.
71. Liu LR, Liu JC, Bao JS, Bai QQ, Wang GQ. Interaction of Microglia and Astrocytes in the Neurovascular Unit. *Front Immunol*. 2020;11:1024.
72. Rizer A, Pajarillo E, Johnson J, Aschner M, Lee E. Astrocytic Oxidative/Nitrosative Stress Contributes to Parkinson's Disease Pathogenesis: The Dual Role of Reactive Astrocytes. *Antioxidants (Basel)*. 2019;8(8).
73. Liddelow S, Hoyer D. Astrocytes: Adhesion Molecules and Immunomodulation. *Curr Drug Targets*. 2016;17(16):1871-81.
74. Liddelow SA, Guttenplan KA, Clarke LE, Bennett FC, Bohlen CJ, Schirmer L, et al. Neurotoxic reactive astrocytes are induced by activated microglia. *Nature*. 2017;541(7638):481-7.
75. Oksanen M, Lehtonen S, Jaronen M, Goldsteins G, Hämäläinen RH, Koistinaho J. Astrocyte alterations in neurodegenerative pathologies and their modeling in human induced pluripotent stem cell platforms. *Cellular and Molecular Life Sciences*. 2019;76(14):2739-60.
76. Cragolini AB, Lampitella G, Virtuoso A, Viscovo I, Panetsos F, Papa M, et al. Regional brain susceptibility to neurodegeneration: what is the role of glial cells? *Neural Regen Res*. 2020;15(5):838-42.
77. Guillamón-Vivancos T, Gómez-Pinedo U, Matías-Guiu J. Astrocytes in neurodegenerative diseases (I): function and molecular description. *Neurologia*. 2015;30(2):119-29.

78. Barkhuizen M, Renggli K, Gubian S, Peitsch MC, Mathis C, Talikka M. Causal biological network models for reactive astrogliosis: a systems approach to neuroinflammation. *Scientific Reports*. 2022;12(1):4205.
79. Zamanian JL, Xu L, Foo LC, Nouri N, Zhou L, Giffard RG, et al. Genomic analysis of reactive astrogliosis. *J Neurosci*. 2012;32(18):6391-410.
80. Tchieu J, Calder EL, Guttikonda SR, Gutzwiller EM, Aromolaran KA, Steinbeck JA, et al. NFIA is a gliogenic switch enabling rapid derivation of functional human astrocytes from pluripotent stem cells. *Nat Biotechnol*. 2019;37(3):267-75.
81. Li K, Li J, Zheng J, Qin S. Reactive Astrocytes in Neurodegenerative Diseases. *Aging Dis*. 2019;10(3):664-75.
82. Chung WS, Allen NJ, Eroglu C. Astrocytes Control Synapse Formation, Function, and Elimination. *Cold Spring Harb Perspect Biol*. 2015;7(9):a020370.
83. Lazic A, Balint V, Stanisavljevic Ninkovic D, Peric M, Stevanovic M. Reactive and Senescent Astroglial Phenotypes as Hallmarks of Brain Pathologies. *Int J Mol Sci*. 2022;23(9).
84. Kaur D, Sharma V, Deshmukh R. Activation of microglia and astrocytes: a roadway to neuroinflammation and Alzheimer's disease. *Inflammopharmacology*. 2019;27(4):663-77.
85. Dallérac G, Rouach N. Astrocytes as new targets to improve cognitive functions. *Prog Neurobiol*. 2016;144:48-67.
86. Liang KX, Kianian A, Chen A, Kristiansen CK, Hong Y, Furriol J, et al. Stem cell derived astrocytes with *POLG* mutations and mitochondrial dysfunction including abnormal NAD⁺ metabolism is toxic for neurons. *bioRxiv*. 2020:2020.12.20.423652.
87. Liang K, Kianian A, Chen A, Kristiansen C, Hong Y, Furriol-Palmer J, et al. Stem cell derived astrocytes with *POLG* mutations and mitochondrial dysfunction including abnormal NAD⁺ metabolism is toxic for neurons2020.
88. Liang KX, Chen A, Kristiansen CK, Bindoff LA. Flow Cytometric Analysis of Multiple Mitochondrial Parameters in Human Induced Pluripotent Stem Cells and Their Neural and Glial Derivatives. *J Vis Exp*. 2021(177).
89. Xiang Y, Yoshiaki T, Patterson B, Cakir B, Kim KY, Cho YS, et al. Generation and Fusion of Human Cortical and Medial Ganglionic Eminence Brain Organoids. *Curr Protoc Stem Cell Biol*. 2018;47(1).
90. Liang KX, Vatne GH, Kristiansen CK, Ievglevskiy O, Kondratskaya E, Glover JC, et al. N-acetylcysteine amide ameliorates mitochondrial dysfunction and reduces oxidative stress in hiPSC-derived dopaminergic neurons with *POLG* mutation. *Experimental Neurology*. 2021;337:113536.
91. Tamagno I, Schiffer D. Nestin expression in reactive astrocytes of human pathology. *J Neurooncol*. 2006;80(3):227-33.
92. Jurga AM, Paleczna M, Kadluczka J, Kuter KZ. Beyond the GFAP-Astrocyte Protein Markers in the Brain. *Biomolecules*. 2021;11(9).
93. Escartin C, Galea E, Lakatos A, O'Callaghan JP, Petzold GC, Serrano-Pozo A, et al. Reactive astrocyte nomenclature, definitions, and future directions. *Nat Neurosci*. 2021;24(3):312-25.
94. Diederichsen AC, Hansen TP, Nielsen O, Fenger C, Jensenius JC, Christensen PB, et al. A comparison of flow cytometry and immunohistochemistry in human colorectal cancers. *Apmis*. 1998;106(5):562-70.
95. Hou Y, Lautrup S, Cordonnier S, Wang Y, Croteau DL, Zavala E, et al. NAD(+) supplementation normalizes key Alzheimer's features and DNA damage responses in a new AD mouse model with introduced DNA repair deficiency. *Proc Natl Acad Sci U S A*. 2018;115(8):E1876-e85.
96. Lapatto HAK, Kuusela M, Heikkinen A, Muniandy M, van der Kolk BW, Gopalakrishnan S, et al. Nicotinamide riboside improves muscle mitochondrial biogenesis, satellite cell differentiation, and gut microbiota in a twin study. *Science Advances*. 2023;9(2):eadd5163.

97. Schöndorf DC, Ivanyuk D, Baden P, Sanchez-Martinez A, De Cicco S, Yu C, et al. The NAD⁺ Precursor Nicotinamide Riboside Rescues Mitochondrial Defects and Neuronal Loss in iPSC and Fly Models of Parkinson's Disease. *Cell Rep.* 2018;23(10):2976-88.
98. Carter SF, Herholz K, Rosa-Neto P, Pellerin L, Nordberg A, Zimmer ER. Astrocyte Biomarkers in Alzheimer's Disease. *Trends Mol Med.* 2019;25(2):77-95.
99. Hindeya Gebreyesus H, Gebrehiwot Gebremichael T. The Potential Role of Astrocytes in Parkinson's Disease (PD). *Med Sci (Basel).* 2020;8(1).

CHAPTER 8: APPENDICES

Appendix 1: Quantification of Cytokine Expression in Control DA Neurons and Control Astrocytes across Three Repetitions.

CYTOKINES	1st time	2nd time	3rd time	
	final adj volume	final adj volume	final adj volume	final adj volume
Serpin E1	0.80	0.30	0.31	
Serpin E1	0.71	0.45	0.23	
MIF	0.23	0.44	0.12	
MIF	0.17	0.26	0.12	
CCL2/MCP-1	0.68	1.00	0.38	
CCL2/MCP-1	0.66	0.92	0.33	
CXCL1/GROalfa	0.09	0.23	0.13	
CXCL1/GROalfa	0.12	0.27	0.13	
control	1.44	1.00	1.13	
control	1.42	1.11	1.12	
IL6	0.38	0.04		
IL6	0.31	0.07		
IL8	0.29	0.52	0.28	
IL8	0.22	0.53	0.25	
control	0.85	1.37	0.79	
control	0.82	1.13	0.71	
control	0.85	1.13	1.15	
control	0.62	1.26	1.10	

Appendix 2: Quantification of Cytokine Expression in Control DA Neurons and POLG Astrocytes across Three Repetitions.

CYTOKINES	1st time	2nd time	3rd time	
	final adj volume	final adj volume	final adj volume	final adj volume
SerpinE1	0.36	0.40	0.21	
SerpinE1	0.34	0.47	0.30	
MIF	0.12	0.38	0.26	
MIF	0.13	0.28	0.29	
CCL2/MCP-1	0.61	0.87	0.86	
CCL2/MCP-1	0.75	1.08	0.87	

CXCL1	0.07	0.50	0.14
CXCL1	0.08	0.50	0.15
Ref	1.20	0.96	1.01
Ref	1.20	0.99	0.82
IL-6	0.62	0.29	0.03
IL-6	0.79	0.24	0.05
IL-8	0.07	0.93	0.27
IL-8	0.10	1.03	0.39
Ref	0.94	1.20	1.11
Ref	0.91	1.14	0.96
Ref	0.94	0.81	1.08
Ref	0.81	0.91	1.02
MIP-1ALPHA		1.00	
MIP-1ALPHA		0.18	
CCL5		0.16	
CCL5		0.18	

Appendix 3: Quantification of Cytokine Expression in Patient DA + Patient Astrocyte across Three Repetitions.

CYTOKINES	1st time	2nd time	3rd time
	final adj volume	final adj volume	final adj volume
SerpinE1	0.58	0.53	0.46
SerpinE1	0.46	0.63	0.48
MIF	0.21	0.46	0.37
MIF	0.23	0.47	0.38
CCL2/MCP-1	0.53	1.16	0.73
CCL2/MCP-1	0.58	1.20	0.77
CXCL1	0.10	0.38	0.28
CXCL1	0.19	0.39	0.29
Ref	1.24	1.11	1.06
Ref	1.24	1.14	1.06
IL-6	0.23	0.07	0.16
IL-6	0.25	0.11	0.17
IL-8	0.75	0.37	0.40
IL-8	0.77	0.48	0.44
Ref	0.82	1.38	0.94
Ref	1.01	1.29	0.94
Ref	0.64	0.97	0.99

Ref	1.06	1.12	1.01
CXCL12/SDF-1	0.02		
CXCL12/SDF-1	0.03		

Appendix 4: Quantification of Cytokine Expression in Patient DA + Patient Astrocyte + NR across Three Repetitions.

CYTOKINES	1st time final adj volume	2nd time final adj volume	3rd time final adj volume
SerpinE1	0.48	0.57	0.41
SerpinE1	0.21	0.44	0.45
MIF	0.14	0.29	0.37
MIF	0.25	0.47	0.38
CCL2/MCP-1	0.46	1.22	0.83
CCL2/MCP-1	0.59	0.97	0.86
CXCL1	0.08	0.20	0.24
CXCL1	0.08	0.21	0.28
Ref	0.95	0.96	1.03
Ref	0.60	1.23	1.00
IL-6	0.08	0.01	0.17
IL-6	0.16	0.06	0.16
IL-8	1.29	0.54	0.41
IL-8	1.21	0.39	0.42
Ref	1.16	1.37	0.95
Ref	0.99	1.32	1.00
Ref	1.02	1.22	0.99
Ref	1.28	0.90	1.02
CXCL12/SDF-1	0.02		
CXCL12/SDF-1	0.03		